TESI DI DOTTORATO DI RICERCA IN CO-TUTELA

UNIVERSITÀ DEGLI STUDI DI MILANO
SCIENZE PER I SISTEMI ALIMENTARI
Agri-environment - XXXVI CICLO

KU LEUVEN
BIOMEDICAL SCIENCES

Dipartimento di Scienze per gli Alimenti, la Nutrizione e l'Ambiente
(DeFENS)

FUSARIUM MUSAE, A NEW POTENTIAL TRANSKINGDOM PATHOGEN

AGR/12

NOME DEL DOTTORANDO:
Valeria Tava
Matr. R13096 – u0161907

NOME E COGNOME DEL TUTOR ITALIANO:
Prof. Matias Pasquali

NOME E COGNOME DEL TUTOR ESTERO:
Prof. Greetje Vande Velde

NOME E COGNOME DEL COORDINATORE DEL DOTTORATO:
Prof. Diego Mora

A.A.
2023/2024

INDEX

Abstract

In recent years, the number of reported fungal infections has increased significantly, prompting experts to recognize invasive fungal diseases as a major public health concern.

The rising threat of fungal infections has roots across the full One Health spectrum, including climate change, population growth, globalization, deforestation, and intensive farming. These factors alter the interactions between humans, animals, and the environment, enabling pathogens to evolve new survival strategies. In particular, the excessive application of fungicides both in agricultural and clinical settings not only contributes to the increase of fungal resistance but also complicates the treatment landscape for immunocompromised patients, thus increasing the at-risk population.

A consistent number of clinically relevant pathogens recently have been identifies as already known pathogens in agricultural field. This ability of certain pathogens to cause infection in hosts across different kingdoms is known as transkingdom pathogenicity. In this context, plant pathogens, once primarily an agriculture concern due to their role in food contamination (e.g., mycotoxins) and significant crop losses, have now emerged as direct threats to human health through their ability to cross kingdoms and infect humans.

In response to fungal infection emergence, the fungal priority pathogens list (FPPL) was established in 2022, highlighting species of global concern that pose serious risks of morbidity and mortality due to limited therapeutic options and diagnostic challenges that often result in late detection.

Fusarium spp. are included in the “high priority group” of FPPL due to their demonstrated inherent resistance to many antifungal agents and yet global incidence rates of fusariosis remain unclear due to insufficient studies. Many *Fusarium* species are recognized for their transkingdom pathogenicity. Among the most recently identified is *F. musae*, a causative agent of crown rot disease in bananas that has also been implicated in superficial infections in immunocompromised human patients.

This thesis aims to investigate *F. musae* as a model organism for studying transkingdom pathogens, integrating methodologies from various fields to understand

its behavior across different hosts. Using a global collection of *F. musae* strains isolated from both bananas and human patients, we characterized the species' genetic diversity and clarified its phylogenetic relationship to *F. verticillioides* through multilocus phylogenetic analyses. Chromosome-level genome sequencing provided an initial comprehensive view of *F. musae* genomics, while mitochondrial haplotype comparisons revealed potential cross-host transmission events. *In vitro* sensitivity tests revealed that *F. musae* is less susceptible to azole treatments than *F. verticillioides*, potentially offering it adaptive advantages. Finally, infection models with banana fruits and *Galleria mellonella* larvae confirmed *F. musae*'s transkingdom pathogenicity, providing the first experimental evidence of its transkingdom infectious capacity and the first bioluminescence readout to quantify *F. musae* fungal burden and to track disease progression in different hosts. The contemporary threat of this species was confirmed by isolating *F. musae* from symptomatic bananas in Milan (Italy) markets.

Indeed, our research encompassed a comprehensive study on transkingdom pathogens, integrating diverse fields such as morphology, phenotypic analysis, genetics, taxonomy, molecular biology, infection biology, and evolutionary fitness.

Our findings highlight the importance of interdisciplinary collaboration in tackling this priority threat. By enhancing our understanding of fungal transkingdom pathogens, this work aims to inform food safety strategies and address the emerging risks posed by *F. musae* to consumer health. Ultimately, this research aligns with the One Health initiative, emphasizing the need for interdisciplinary collaboration in tackling this complex and emerging category of fungi.

We established a set of protocols for investigating fungal infections and outlined strategies to address emerging fungal species. This research contributes to the development of new food safety standards and raises awareness in medical and agricultural fields about the significance of fungal infections within the One Health framework, emphasizing the risks posed by transkingdom pathogens.

Chapter 1

Introduction

Chapter 1

Introduction

1.1 One world, One Health, two kingdoms

One Health is an integrated, unifying approach that aims to sustainably balance and optimize the health of people, animals, and ecosystems. It recognizes that the health of humans, animals and their shared environment are strictly connected and interdepend.

The concept of One Health was firstly introduced in 2004 after the global outbreak of Severe Acute Respiratory Syndrome caused by the coronavirus SARS-CoV-1. It is believed that this virus originated first in bats and only afterword crossed over to human, highlighted the interconnection between human and animal diseases (Mackenzie and Jeggo, 2019; “The Manhattan Principles,” 2005). Zoonoses diseases are currently considered 60% of the new emerging infectious diseases. Since then, this approach has become a priority, mobilizing collaborations across multiple sectors, discipline and communities (“One Health - European Commission,” 2023; “One Health - WHO,” 2024; “One Health - WOAH,” 2024; Pitt and Gunn, 2024).

Climate change, population growth, globalization, deforestation and intensive farming have been altering the balance between interactions among animal, humans and their shared environment. Access to sufficient amounts of safe and nutritious food is essential for sustaining life and promoting good health. The use of crop treatments has increased to improve food production and protect crops; consequently, also antimicrobial resistance has risen. Pathogens constantly adapt and the extensive use of treatments in plants can induce them to evolve resistance and new survival strategies. An increasing number of human pathogenic species isolated from hospitalized patients are being identified as originally known as plant pathogens. This suggests these new strategies can lead to invasion of different hosts, even those belonging to different kingdom. The ability of pathogen to cause infection in hosts from different kingdom is known as transkingdom pathogen or cross-kingdom pathogenicity. In this context, plant pathogens, that were once a concern primarily for agriculture and

indirectly a threat the human health by generating food contamination (as mycotoxins) and important food losses, have now become a direct threat to human health together with the rising of transkingdom pathogens (Berg et al., 2015; Gauthier and Keller, 2013; Van Baarlen et al., 2007). In this comprehensive context, food plays a crucial role, as access to sufficient amounts of safe and nutritious food is key to sustaining life and promoting good health.

The growing interest in transkingdom pathogens within the pathology community, along with their significant impact on food safety and overall health, motivated our investigation into these organisms.

1.2 Towards investigation of the emerging threat of fungal transkingdom pathogens

1.2.1 Abstract:

Numerous microbial species have already been associated with the ability to cause infection in different hosts, even hosts belonging to different kingdoms, known as transkingdom or cross-kingdom pathogens. Fungal plant pathogens have a remarkable capacity to adapt and evolve, acquiring the ability to thrive in novel environments and hosts. Additionally, antifungal resistance caused by the massive application of fungicides in agriculture and the increased number of patients with immunodeficiency disorders facilitate the success of transkingdom pathogenic fungi, making these fungi a threat to public health. Here, we collected the current knowledge about fungal transkingdom pathogens. We focus specifically on those which moved from the agricultural sector to the clinical environment. Thereby, we identify the challenges that scientists must overcome when studying this type of pathogens towards harnessing the emerging threats transkingdom pathogens pose to public health as well as to agriculture. Our results indicate that the field of transkingdom pathogens is still in its infancy. There is no common experimental strategy to investigate species considered as or newly defined as transkingdom pathogens. The biggest gap found in the literature is the lack of experimental proofs of transmission in models from different kingdoms. Fungal transkingdom pathogens represent a dynamic and evolving field of study that profits from interdisciplinary collaboration. Studying

transkingdom pathogens is a methodological challenge which requires the integration of diverse, traditionally separated, scientific disciplines.

1.2.2 Transkingdom pathogens

Several pathogenic microorganisms can infect a broad range of organisms, including different species, genera, families, or even kingdoms. In recent years a conspicuous number of bacterial and fungal pathogens of clinical interest have been isolated, characterised and identified that were already known to act as plant pathogens (Kim et al., 2020). It is well known that pathogens occupying spaces close to potential new hosts can evolve and develop the ability to overcome the host's defence systems. Through generations, these pathogens adapt to the new host environment, increasing their infectious potential and competitiveness. The contact between humans and different microbial species has significantly risen in recent decades due to factors such as encroachment into wildlife habitats, deforestation, live animal transportation, long-distance product transport, modern agricultural practices, changes in food preparation, and international travel (Sharma et al., 2014). Additionally, the population boom has led to a greater abundance of hosts with increased susceptibility which, combined with pathogen co-evolution and changing climate conditions, has resulted in the emergence of new pathogens that exhibit altered pathogenic behaviour (Misra and Chaturvedi, 2015).

Cross-kingdom pathogens, typically soil saprophytes, can evolve strategies that enable them to become plant pathogens and cause opportunistic infections in humans. A large part of the literature investigating these virulence determinants focused on bacterial pathogens while few studies have analysed in detail fungal pathogens able to infect distant hosts.

1.2.3 The rise of fungal transkingdom pathogens

Fungal plant pathogens exhibit a remarkable adaptability to thrive in novel environments and hosts. Thereby, climate change may play an important role in increasing the geographic distribution of pathogenic fungi (Nnadi and Carter, 2021) accompanied by the adaptation to the body temperature of the human hosts due to an increased heat tolerance (Casadevall, 2023). Consequently, the increase of clinical

diseases of fungal pathogens and associated infections establishes a growing global public health concern (Fisher and Denning, 2023). Invasive fungal diseases are on the rise, particularly as the at-risk population continues to expand ("One Health - WHO," 2024), it is predictable that fungal cross-kingdom pathogens can become a novel important threat to human and animal health. This urges us to undertake immediate action and no longer overlook the threat pose by this emerging category of pathogens. Generally, cross-kingdom fungal pathogens are considered weak pathogens for both plants and humans. In plants, they often remain asymptomatic but can have clinical significance especially in individuals with compromised immunity or those who have experienced penetrating trauma (Gauthier and Keller, 2013; Van Baarlen et al., 2007). In this context, fungal pathogens capable of crossing kingdom borders and causing diseases in plants, humans, and animals have become a subject of significant interest among researchers. Of special interest are species that have demonstrated the capacity to cycle through ecosystems, infecting animal hosts, transferring back to plants, and multiplying within them (Sharma et al., 2014). Despite the various defence mechanisms and barriers present in different hosts, cross-kingdom pathogens have shown the ability to overcome host-specific barriers and immune defences, potentially due to homologies between target receptors in animals and plants (Gauthier and Keller, 2013; Yasir Rehman, 2015).

It is plausible that fungi associated with plant infections might occasionally develop the ability to jump from one host to another, even if the new host belong to a different kingdom. In doing so, they can become a direct threat to human health.

Both Ascomycota and Mucoromycota fungal species have been reported to cause diseases in humans and plants, and various species have been associated with the ability to infect distant taxonomic groups (Kim et al., 2020; Van Baarlen et al., 2007).

The increase in the use of antifungal treatment of plants as well as the use of similar compounds in treatment of human patients plays a role in prompting alterations in fungi, causing a build-up of drug resistance and the evolution of new survival strategies (Resendiz Sharpe et al., 2018). Consequently, cross-kingdom pathogens can more easily jump on humans and develop resistance that limits therapeutic options for treating new diseases (Gauthier and Keller, 2013). In this scenario, opportunistic fungi have emerged first as an important cause of disease in immunocompromised patients

and, consequently, as an important more general threat to public health (Zhai et al., 2020).

1.2.4 What is known so far

We collected the current knowledge on fungal cross-kingdom pathogens that are able to cause diseases in both, humans and the agricultural/plant sector, and aimed to understand the strategies used by researchers to identify the pathogens as cross-kingdom pathogens. From there, we focussed on the important aspects that scientists should follow to study this complex and newly defined group of pathogens.

An extensive systematic investigation was conducted using the Scopus and PubMed databases with specific keywords: “cross-kingdom virulence”, “trans-kingdom virulence”, “cross-kingdom pathogenicity”, “transkingdom pathogenicity”, “cross-kingdom fungi”, “transkingdom fungi”, “cross-kingdom approach”, “cross-kingdom pathogens”, “transkingdom pathogens”, “cross-species transmission”, “crossover pathogens”, “global analysis trans-kingdom”, “plant human pathogens”, “plant human fungi”, “cross-kingdom plant human”. “Reference” and “cited by” sections were also analysed for all the articles. More than 3000 articles were obtained through this approach. The concept of species capable of infecting both plants and humans had been known for a long time. However, it was first addressed in a scientific publication in 2007 by Van Baarlen *et al.*, who introduced the term 'cross-kingdom pathogen' (Van Baarlen et al., 2007). Later this concept was formally emphasized by Sharma *et al.* and by Gauthier and Keller who introduced another term for this category of fungi, coining the ‘trans-kingdom pathogen’ (Gauthier and Keller, 2013; Sharma et al., 2014).

Results indicated that the field of cross-kingdom pathogenic fungi is still in its infancy. A major challenge is the lack of a universally applicable model to verify the ability of pathogens to jump from one host to another. There is no commonly shared strategy used to investigate species that might be considered as cross-kingdom pathogens. Usually, pathogen identification is based only on morphological characteristics, without necessarily incorporating molecular analysis. In addition, infection is rarely experimentally confirmed, classification as cross-kingdom pathogen is based only on identification of the causal agent isolated from different hosts, rather than on the ability of the microorganisms to actually invade the hosts. Consequently, there is a clear need

for harmonization of experimental work addressing the complex matter of fungal cross-kingdom pathogens.

1.2.5 Which methods are used

Investigation of a pathogen and its virulence potential involves fundamental steps, including accurate identification at the species level and experimental proof of infection. As described in Koch's postulates, to be considered pathogenic to a specific host, a microorganism must be isolated from a diseased host, cultured and reinoculated in a healthy individual where the disease shows the original symptoms as visualised by an approach studying the infection of loggerhead sea turtles by *Fusarium* species from the *F. solani* species complex (Sarmiento-Ramírez et al., 2010). When reisolated, the microorganism must match the original infectious agent and the disease symptoms need to match those observed in the wild. If the pathogen is considered cross-kingdom the postulates must be verified for all hosts.

For a long time, the identification of microorganisms was made only on the morphological characteristics of the isolates. In recent years newer strategies such as molecular methods using the sequencing of informative genes have been introduced for a more accurate identification (Lücking et al., 2021), but they are still not always used.

A considerable number of species has already been classified as cross-kingdom pathogens, as reported by Van Baarlen *et al.* and subsequently by Kim *et al.* (Kim et al., 2020; Van Baarlen et al., 2007). In these articles, authors provided an overview of the species that are currently known to cross the kingdom borders of host infection and describe the mechanisms involved during the invasion of animal and plant hosts. The number of the species presented as cross-kingdom pathogens is high, but most of the studies included do not fully accomplish the above-cited criteria of confirmation of multi-host infection and of the taxonomic accuracy according to the accepted method for species definition. For instance, in studies conducted on *Fusarium* and *Trichoderma* as emerging human pathogens (Ghosh, 2022; Meza-Menchaca et al., 2020), the hypothesis of cross-kingdom pathogenicity was supported by analysing large populations of strains isolated from different hosts through appropriate molecular identification. Many other examples in the literature still lack

experimental confirmation of transmission. Most manuscripts claim that attribution as a cross-kingdom pathogen is based only on the taxonomic identification of the strains isolated from a certain host. A complete verification of the shift of pathogens from one host to the other is frequently lacking and the taxonomic identification of the potential pathogen has been carried out in a different context without the use of transmission proof and without the verification of the symptoms.

Of all the research analysed, we collected a total of 17 papers, summarized in Table 1, that included cross-kingdom transmission tests. In seven papers, transmission from human to plant was analysed and confirmed. Thereby, suitable host plant were infected with strains of human origin and the appearance of disease symptoms was monitored. In another six manuscripts the transmission from plants to animal hosts were analysed whereby *G. mellonella* larvae and mice were used as human proxies to test the ability of strains of plant origin to cause disease. Only in 3 cases, the infection was confirmed in both pathosystems.

This lack of completeness of data is likely due to the complexity of carrying out appropriate investigation in multiple hosts as the experimental approach requires a specialized laboratory with tools and skills to study the interaction of host-pathogens in different settings. In addition, when using animal models to confirm human infections might require a detailed analysis of underlying conditions that allowed infection which need to get replicated in the infection trial.

However, overall the collected research papers revealed numerous species already identified as cross-kingdom pathogens. Looking at the table, we noticed that most of the papers investigated *Cryptococcus* and *Fusarium* genera, both considered critical species by (Fisher and Denning, 2023): *Cryptococcus neoformans* is considered one of the critical species that need urgent attention; *Fusarium spp.* are belonging to the high priority group and *Cryptococcus gattii* is medium priority group. However, compared to the extensive list of possible fungal cross-kingdom pathogens, only a few have yet been appropriately studied.

Table 1. Collection of works dealing with experimental infection proof of infection in animal and plant systems.

Fungal species	***Fungus isolated from***	***Identification method(s) used***	***Transmission from human to plant***	***Transmission from plant to human***
Fusarium oxysporum	plant	phylogenetic	no	yes, mice
	plant	phylogenetic	no	Yes, mice
	plant	phylogenetic	no	yes, mice
	plant	phylogenetic	no	yes, larvae
Fusarium guttiforme	plant and human	designed primers	yes	no
	human	genotipic and phenotipic	yes	no
Fusarium solani	human, plant and environment	phylogenetic	yes	no
Fusarium spp.	human	morphological	yes	yes, *ex vivo* nails
	human and plant	morphological and MLS	no	yes, *G. mellonella* and mice
Exserohilum rostratum	plant and human	morphological and MLS	yes	no
Cladophialophora carrionii	human, plant and environment	morphologicla and phylogenetical	yes	no
Cryptococcus sp.	human	phylogenetic	yes	no
Cryptococcus neformans	human		yes	no
Cryptococcus neoformans	plant	morphological and histological	no	yes, mice
C. gatti	human	morphological and phylogenetical	yes	no
Aspergillus flavus	plant and human	morphological and phylogenetical	yes	yes, larvae
Fonsecaea sp.	plant and human	morphological and phylogenetical	yes	yes, mice

Reference
(Ortoneda et al., 2004)
(Schäfer et al., 2014)
(López-Berges et al., 2013)
(Navarro Velasco et al., 2011)
(Wang et al., 2020)
(Migheli et al., 2010)
(Mehl and Epstein, 2007)
(Meza-Menchaca et al., 2020)
(Coleman et al., 2011)
(Sharma et al., 2014)
(de Hoog et al., 2007)
(Springer et al., 2017)
(Xue et al., 2007)
(Ra et al., 1998)
(Warpeha et al., 2013)
(St. Leger et al., 2000)
(Fornari et al., 2018)

1.2.6 A proposal for standardizing approaches

We, therefore, suggest that two critical aspects must be strongly taken into consideration for an appropriate definition of transkingdom fungal pathogens in order to effectively address the risks of emerging diseases. Firstly, taxonomic approaches must be formalized and uniformly applied to agricultural and medical settings to correctly identify the pathogens and define the best treatment to control the disease. For example, *F. musae*, a recently described species often confused with *F. verticillioides* (Van Hove et al., 2011) when taxonomical identification is not carried out with appropriate molecular markers, shows a lower sensitivity to azoles compared to *F. verticillioides* (Tava et al., 2021), highlighting the importance of taxonomy for appropriate clinical treatment selection.

Secondly, novel appropriate methods for establishing the likelihood of human infection must be developed and used to allow for Koch‘s postulate verification of the disease in human host proxies models. Collaborations and expertise in different fields should be combined and associated with the investigation of fungal shared determinants of adaptation to different hosts to be able to anticipate novel threat to human and animal health as well as select appropriate novel markers for adaptation to different host models.

To summarize, fungal transkingdom pathogens represent a dynamic and evolving field of study, intertwining aspects of microbiology, immunology, plant pathology, and clinical research under the one health paradigm. Here, we highlighted the importance of interdisciplinary research to fight these emerging threats. The ability of transkingdom fungal pathogens to cause diseases in both animals and plants adds complexity to our understanding of host-pathogen interactions. Continued interdisciplinary collaboration

and innovation are essential to effectively mitigate the impact of fungal transkingdom infections on human and plant health, implementing systemic and integrated approaches.

1.2 Fusarium genus

Fusarium spp. are among the fungal species included in the “high priority group” named by the World Health Organization (WHO) in its fungal priority list (Fisher and Denning, 2023; World Health Organization, 2022). This list was formulated to address the emerging challenges of fungal infection, including the rising of antifungal resistances and the need for improved diagnostics and treatments. The list aligns with the One Health approach by recognizing the interconnected nature of human, animal, and environmental health in addressing these fungal threats.

The genus *Fusarium* is a wide and diverse group of fungi known as the primary genera responsible for plant diseases, but also recognized for their ability to infect humans and animals. Thanks to its high variability of species, *Fusarium* represents an interesting example of biodiversity.

Fusarium spp. can infect up to 80% of economically important plants, posing a significant threat to food production by reducing yields and causing major food losses, attracting considerable attention from pathologists (Leslie and Summerell, 2006; Summerell, 2019; Van Diepeningen and De Hoog, 2016). *Fusarium* infections can occur at any stage of a plant's development, from germinating seeds to mature vegetative tissues, depending on the host plant and *Fusarium* species involved. The range of plants known to have at least one *Fusarium*-related infection is so vast that it is frequently said that nearly every plant has at least one *Fusarium*-associated disease (Moretti, 2009).

Fusarium spp. are also known to be great productors of biologically active secondary metabolites (mycotoxins). These compounds can have a big variety of chemical properties and can be harmful not only to plants but are also associated with cancer and other diseases in humans and domesticated animals (Moretti, 2009; Munkvold, 2017; Summerell, 2019).

In addition, the number of human infections attributable to *Fusarium* spp. has increased over the past decades, raising attention also in the medical community. *Fusarium* spp. are now recognized not only as indirect threat to humans correlated to assimilation of mycotoxins, but also as a direct threat to human health as opportunistic human pathogens. The range of diseases caused by *Fusarium* spp. goes from superficial infection, such as skin and nail infection, to more invasive conditions like keratitis and, in rare cases, systemic infection. Immunocompromised individuals are particularly at risk within the affected population (Moretti, 2009; Summerell, 2019; Van Diepeningen and De Hoog, 2016).

Currently, *Fusarium* genus is believed to consist of more than 300 genetically distinct phylogenetic species, though fewer than half have been formally identified and described. Taxonomical studies of *Fusarium* spp. are constantly evolving, with different schools of thought on how to distinguish phylogenetic groups. In plant pathology, the most recognized groups include *F. graminearum* species complex, well-known for causing *Fusarium* head blight in cereals, and *F. oxysporum* species complex, responsible for vascular wilt agents of over 100 agronomically important crops. The *F. solani* species complex is highly diverse, causing various plant diseases, and includes the most aggressive human pathogens. Finally, *F. fujikuroi* species complex is the largest and best studied, containing the highest number of opportunistic human pathogens (Aoki et al., 2014; Dean et al., 2012; Moretti, 2009; O'Donnell et al., 1998; O'Donnell and Cigelnik, 1997; Yilmaz et al., 2021).

Indeed, a significant number of *Fusarium* spp. are already known for their ability to cause infection in multiple hosts belonging to both plant and animal kingdoms. In addition, continuous updates in their phylogeny and characterization reveal new species (Moretti, 2009; Summerell, 2019; Van Diepeningen and De Hoog, 2016).

1.3 Fusarium musae

The number of *Fusarium* species considered capable of transkingdom infection is notable, with one of the most recently identified being *F. musae*.

Described for the first time in 2011 by Van Hove *et al.*, *F. musae* is considered a "sister species" to *F. verticillioides* due to their morphological similarity, which initially lead to

their classification under the same species (Van Hove et al., 2011). However, multilocus phylogeny and mating experiments allowed *F. musae* to be classified as a distinct species within the *F. fujikuroi* species complex.

F. musae was first isolated from banana fruits and identified as one of the causative agents of the crown rot disease, one of the most serious and important diseases of bananas worldwide at postharvest level (Kamel et al., 2016). When harvested from the plant, crowns of fruits appear to be healthy and safe with no notice signs of disease, however within 7 days a greyish white, pink or white mold, commonly referred to as "crown mold", may appear on the cut crown surface. Rot can then spread into the pedicel and eventually into the pulp of the fruit reaching the most pronounced signs around 14 days post-harvest (Demerutis et al., 2008).

Kamel *et al.* demonstrated that fungi are the causal agents of crown rot disease and *Colletotrichum musae* and *Fusarium* spp. seem to be the main species involved in the infection (Kamel et al., 2016). Infection begins at harvesting and continues during packaging processes, with rot developing and spreading very rapidly during the banana ripening process. The aggressivity and late appearance of the disease are the main reasons for more cases of crown rot have been collected and studied in Europe, rather than America, where the number of bananas consumed is higher. Longer shipments transit times contribute to significant yearly losses in banana fruits and economic damage.

Geographical and seasonal variations (temperature and rainfall) have been shown to play a role in the incidence of post-harvest diseases in bananas. It has been suggested that these spatiotemporal fluctuations could reflect the variations in the quality potential of the fruit, acquired in the field. This quality potential would include two components: the fruit's susceptibility to the post-harvest diseases (physiological component) and the level of fruit contamination by fungal pathogens (pathological component). Both components depend on pre-harvest factors including agronomic practices and soil–climate factors (Ewané et al., 2012).

In 2016 multilocus sequence analysis revealed that few *Fusarium* isolates collected from human patients and previously identified as *F. verticillioides* actually belonged to *F. musae* species, making *F. musae* an opportunistic human pathogen and a potential transkingdom pathogen (Esposto et al., 2016). Reported cases of human infection by

F. musae involve patients with typical Fusariosis symptoms such as nail and skin lesions as well as systemic infections in immunocompromised patients mostly hospitalized in Belgium, France or the United States of America refs here. Overall, it is estimated that approximately 20% of human pathogenic *F. verticillioides* infections are in fact infections caused by *F. musae*. Since infections associated with *F. verticillioides* account for approximately 10% of the total amount of *Fusarium* infections, *F. musae* human infections could be more common than we assume (Triest and Hendrickx, 2016).

It's not clear yet how human patients acquire the infection with *F. musae*, the main hypothesis is the one stated by (Triest et al., 2015) where banana fruits acquire the infection when harvested, fruits act as carriers of spores when imported and in this way, they reach the consumers. But transmission from one host to the other has not been proved yet, and other hypotheses cannot be excluded. Patients could have acquired their infection after travelling to a banana-producing country, where they came into contact with *F. musae* contaminated banana material or cleaning water; or the habitat and distribution of *F. musae* could have a broader range of plant or environmental substrates beyond bananas, which remains undiscovered.

Chapter 2

Research objectives

Chapter 2

Research objectives

F. musae has been identifies as a potential transkingdom pathogen due to its isolation from banana fruits as one of causative agent of crown rot disease. A few years later, it was isolated from human immunocompromised patients as an opportunistic pathogen causing typical fusariosis symptoms.

Reports of *F. musae* infections are scarce in both agricultural and medical contexts, with only a few publications available at the start of our investigation in 2020. Our interest in this novel potential transkingdom pathogen, alongside growing public concern over fungal infections, motivated us to explore *F. musae* as a model species for studying transkingdom pathogens.

The primary aim of this thesis was to characterize *Fusarium musae* as a model organism for studying transkingdom pathogens, utilizing an interdisciplinary approach to deepen our understanding of its interactions with various hosts.

To achieve this ambitious goal, we began by budling a worldwide collection of *F. musae* strains from both banana fruits and human patients across different time periods and geographical locations. Our aim was to observe the incidence of *F. musae* infection cases and represent distribution.

The entire collection was genomically characterized. Through multilocus phylogenetic analyses, we sought to uncover the genetic diversity within *F. musae* and elucidate its phylogenetic relationship to *F. verticillioides*, shedding light on the evolutionary dynamics of these closely related species.

Understanding the population homogeneity infecting both human and plant hosts emerged as another critical objective. We investigated mitochondrial genome diversity among our *F. musae* strains to assess the taxonomic identity of this species and explore its potential transmissibility across different hosts, which is crucial for understanding its epidemiology.

Given the inherent resistance to most antifungal agents of *Fusarium* spp., we then tested the sensitivity *in vitro* of our *F. musae* collection to different azole treatments used in both agricultural and clinical settings. This investigation aimed to observe the

fitness of *F. musae* and its potential adaptive advantages compared to its sister species, *F. verticillioides.*

A key aspect of this research is to validate the transkingdom pathogenicity of *F. musae*. We accomplished this by fulfilling Koch's postulates through established infection models in both the plant and human kingdoms, providing experimental evidence of its pathogenic capacity across species. Finally, we aimed to develop innovative quantitative methodologies that allow for non-invasive, real-time observation of host-pathogen interactions over time. These methodologies will be adaptable for use in different host systems, paving the way for future investigations into transkingdom pathogenicity.

In conclusion, through these objectives, this thesis aims to contribute significantly to our understanding of *F. musae* and its role as an emerging transkingdom pathogen. In addition, this research aimed contribute to establish novel standards of food safety and awareness in medical and agricultural field about the importance of fungal infection within the One Health concept and the risk posed by fungal transkingdom pathogens.

Chapter 3

F. musae distribution worldwide

Chapter 3

F. musae distribution worldwide

3.1 Building a collection of F. musae strains

To start our investigation of *F. musae*, we built a collection of 19 strains isolated from different hosts, countries and timeframes in order to represent the global diversity of this species (Table 2).

Table 2 Complete working collection of F. musae strains used in my PhD. The table provides information on the geographical origin, the host and the year of isolation of each strain.

STRAIN	COUNTRY	HOST (TISSUE)	YEAR	REFERENCE
F31	Dominican Republic	Banana (fruit)	2013	(Kamel et al. 2016)
IUM 11-0507	Greece	Human (blood)	2011	(Esposto *et al.* 2016)
IUM 11-0508	Greece	Human (cornea)	2011	(Esposto *et al.* 2016)
NRRL 28893	Mexico	Banana (fruit)	1996	(Van Hove *et al.* 2011)
NRRL 28895	Mexico	Banana (fruit)	1996	(Hirata et al. 2001)
NRRL 28897	Mexico	Banana (fruit)	1996	(Hirata et al. 2001)
NRRL 43601	Maryland, USA	Human (skin)	2005	(O'Donnell *et al.* 2007)
NRRL 43604	Ohio, USA	Human (nasal sinus)	2005	(O'Donnell *et al.* 2007)
NRRL 43658	Minnesota, USA	Human (contact lens)	NO DATA	(O'Donnell *et al.* 2007)
NRRL 43682	Minnesota, USA	Human (cornea)	2006	(O'Donnell *et al.* 2007)
NRRL 25673 (MUCL 53204)	Guatemala	Banana (fruit)	NO DATA	(Van Hove *et al.* 2011)
NRRL 25059 (CBS 624.87, MUCL 52574)	Honduras	Banana (fruit)	NO DATA	(Van Hove *et al.* 2011)
IHEM 20180	Brussels, Belgium	Human (sinus biopsy)	2003	(Shi *et al.* 2016)
IHEM 19881	Brest, France	Human (shoulder biopsy)	2003	(Triest *et al.* 2015)
ITEM 1121 (MUCL 52573)	Panama	Banana (fruit)	1991	(Triest *et al.* 2015)
ITEM 1142 (MUCL 53196)	Equador	Banana (fruit)	1991	(Van Hove *et al.* 2011)
ITEM 1149 (MUCL 52201)	Panama	Banana (fruit)	1991	(Van Hove *et al.* 2011)
ITEM 1250 (MUCL 53203)	Canary Islands	Banana (fruit)	1991	(Van Hove *et al.* 2011)
MUCL 51371	Philippines	Banana (fruit)	2007	(Van Hove *et al.* 2011)

A set of three strains was obtained at the University of Milan, other 16 strains were obtained from public databases named ARS Culture Collection Database (USA), Belgian coordinated collections of Microorganisms, Institute of Science of Food Production, Bari, Italy. Infection with *F. musae* has a low incidence, as made clear by our database research, which revealed a limited number of deposited strains. Plant strains were exclusively isolated from banana fruits, the only known host of *F. musae* in the plant kingdom, and in big banana-producing countries as Ecuador, Panama and Canary Islands. On the other hand, clinical strains were isolated from patients hospitalized in countries known as big banana-importers as USA and Europe. There are no documented cases of infection with *F. musae* in hospitalized patients in banana-producing countries, probably due to a lack of investigation. Therefore, our working collection of strains reflects this distribution highlighting the geographical distance between reported *F. musae* infection human and plant.

In addition, the isolation timeline revealed that most strains were collected between the 1990s and early 2010s. With no further reports of this pathogen publicly deposited outside this period, this made us wonder whether infection with *F. musae* is an historical concern or it is still a relevant threat.

In literature, the number of papers addressing *F. muse* and its infection cases is very limited. Moretti and Van Hove *et al*. were the first to explore the appearance of infection with *F. musae*, establishing a molecular approach to identify this novel pathogen (Moretti, 2009; Van Hove et al., 2011). Later, Molnàr *et al.* investigated the presence of *F. musae* where *F. verticillioides* like isolates obtained from banana fruits marketed in Hungary and characterized (Molnár et al., 2015). Esposto *et al*. were the first to confront the appearance of *F. musae* in clinical cases, detecting it among *F. verticillioides* clinical strains in the collection of the Laboratory of Medical Mycology of University of Milan (Esposto et al., 2016). Since these publications, no further studies have investigated the presence and rise of *F. musae* infection and research on this pathogen still remains a niche for only few groups of experts.

3.2 Survey in market surrounding Milan area to detect presence of F. musae

3.2.1 Introduction

Bananas are the fourth most important food crop after rice, wheat and corn, accounting for 16% of world fruit production. Their high calories, vitamins and fiber content together with appealing sensory characteristics, make them one of the most important staple foods worldwide. It is estimated that bananas contribute up to 25% of carbohydrate intake of about 60 million people (Alzate Acevedo et al., 2021; Heslop-Harrison and Schwarzacher, 2007; Lamessa, 2021).

Although bananas are commercially grown in more than 130 countries, the largest exporters are Latin America and the Caribbean, with Ecuador leading with approximately 6.2 million tons bananas grown in 2023. Europe and USA are the major importers, each reaching up to 5 million tons for the full year of 2023 (Bonavita, 2024; Evans et al., 2020).

Bananas are produced and transported year-round, however irregular weather patterns and inappropriate transport conditions are the main cause of important fruit losses. Banana fruits are harvested from the tree at full-mature (green) stage and hung in cool places, where they go under ripening phases. Once they reach full natural ripening stage, they can be shipped and distributed. Storage and transport are critical steps, as most of the postharvest losses appear at these stages. The storage conditions are not often optimal and too small, or damaged fruits are transported, increasing the chances of fungal contamination with the bunch (Evans et al., 2020).

Among the postharvest losses caused by fungi, crown rot disease is the most significant and devastating in bananas, having a major negative impact on fruit quality and causing important losses. Crown rot is caused exclusively by fungal species, with *Fusarium* being the most frequent genus, and *F. musae* as a new emerging threatening for food safety (Kamel et al., 2016).

Cases of infection with *F. musae* have been found in banana primarily from banana-producing countries as Ecuador and Panama. In bananas, the hypothetical entry route of *F. musae* is through the crown when fruits are harvested from the plant. In this way, bananas acquire infection with *F. musae* and the shipping period, from the producing

country to the consuming country, provides an ideal incubation period for the pathogen to grow, allowing it to reach the consumer when bananas are distributed (Hirata et al., 2001; Kamel et al., 2016; Molnár et al., 2015; Shi et al., 2017; Triest et al., 2015; Van Hove et al., 2008). *F. musae* has been described not only as a plant pathogen, involved in crow rot disease, but also as human pathogens. It has been isolated from hospitalized patients who showed typical symptoms of fusariosis such as keratitis and skin infections as well as systemic infections in immunocompromised patients. Cases have been reported mainly in major importing countries as USA and Europe (Esposto et al., 2016; O'Donnell and Cigelnik, 1997; Triest, 2016; Triest et al., 2016; Triest and Hendrickx, 2016).

Given the distribution of the cases of *F. musae* infection, the limited literature available and the potential threat that this pathogen poses, this survey aimed to sample symptomatic bananas from markets in the areas surrounding Milan (Italy) to look for *F. musae*. We specifically targeted bananas with visible disease symptoms or at advanced stages of ripeness, often discarded by wholesale markets and supermarkets for not meeting market standards. Our goal was to isolate potential pathogens in the collected bananas and verify the presence of *F. musae*. And in this way demonstrates that even though infection with *F. musae* has a low incidence, the pathogen remains a real threat present in the markets.

3.2.2 Material and methods

3.2.2.1 Sampling and isolation

Surveys in markets in the Milan (Italy) area were conducted in two different moments of the year: once in spring 2022 and again in winter 2023. We collected a total of 11 Cavendish bananas, 3 imported from Colombia, 6 imported from Ecuador, 2 imported from Costa Rica and 1 imported from Panama. Selected fruits presented visible diseases symptoms due to possible fungal infection. Samples were isolated from the fruits and incubated at 25°C in Petri dished containing Komada *Fusarium*-selective medium (Na2B4O7 10 H20 1g/L, K2HPO4 1g/L, KC1 0.5g/L, MgSO4 7H2O 0.5g/L, Fe-Na-EDTA 0.01g/L, D-Galactose 20g/L, agar 15g/L, pentachloronitrobenzene 1g/L, streptomycin sulfate 0.3g/L). Fungi successfully isolated were then transferred on petri

dishes containing PDA medium (Potato Dextrose Agar: Difco Potato Dextrose Agar 38g/L) and incubated at 25°C to favorite fungal growth.
Isolates were at first morphologically characterized with an electronic microscope (Olimpus BX51, 40X magnification) and selected for molecular characterization.

3.2.2.2 DNA extraction

DNA was extracted using DNeasy PowerSoil Pro Kit (Qiagen, Germantown, MD, USA following the protocol) following manufacture's protocol. Mycelia (250 mg) were placed in PowerBead Pro Tube with addition of 800 µl of Solution CD1 and vortexed for 10 min at maximum speed for mechanical homogenization. Tubes were then centrifuged at 15,000 x g for 1 minute and the maximum volume of the obtained supernatants were transferred to a clean 2 ml microcentrifuge tube without disturbing the precipitate at the bottom of the tube. A volume of 200µL of solution CD2 was added and the tubes were briefly vortexed and centrifugated at 15,000 x g for 1 minute at room temperature to precipitate non-DNA organic and inorganic material. A volume up to 700 µl of supernatant was transferred to a clean 2 ml microcentrifuge tube (provided by the kit), with addition of 600 µl of Solution CD3 to promote binding of DNA to MB Spin Column. Samples were vortexed for 5 seconds and a volume of 650 µl was placed onto an MB Spin Column and centrifuging at 15,000 x g for 1 minute. Flow-through was discarded and a second round of centrifugation was performed. The MB Spin Column was then carefully placed into a clean 1 ml Collection Tubes (provided) avoiding splashing any flow-through, 500 µl of Solution EA were added to wash the sample, and tubes were centrifugated two times at 15,000 g for 1 minute f. Contaminants were then washed by addition of dd 500 µl of Solution C5 to the MB Spin Column, followed by centrifugation step at 15,000 g for 1 min. Flow-through was discarded again and the columns were then transferred to a new microcentrifuge tube and 200 µl of Solution C6 was pipetted directly to the center of the white filter membrane and centrifugated to allow DNA elution. DNA was then quantified by Qbit and checked with electrophoresis onto a 1% (w/v) agarose gel, stained with ethidium bromide and photographed under UV light to verify the success of the extraction.

3.2.2.3 Molecular identification

Amplification of Internal Transcribed Spacer (ITS), Elongation Factor 1α (EF) and RNA polymerase second largest subunit (RPB2) was performed directly from genomic DNA. For ITS we used primers ITS1 (5'-TCCGTAGGTGAACCTGCGG-3') and ITS4 (5'-TCCTCCGCTTATTGAT ATGC-3') (Peeran et al., 2019) with the following program: 94°C for 2 min, followed by 35 cycles of denaturation at 94°C for 20 sec, annealing at 57°C for 30 sec, elongation at 72°C for 1 min and 72°C for 7 min for final extension followed by 4°C until gel loading. For EF we used primers EF1 (5'-ATGGGTAAGGAG GACAAGAC-3') and EF2 (5'-GGAAGTACCAGTGATCATGTT-3') and for RPB2 primers was 5F2 (5'- GGGGWGAYCAGAA GAAGGC-3') and 7CR (5'-CCCATRGCTTGYTTRC CCAT-3') (Reeb et al., 2004) following the program: 94°C for 2 minutes for DNA strand separation, then 35 cycles of denaturation at 94°C for 20 sec, annealing at 61°C for 30 sec, elongation at 72°C for 2 min and 72°C f or 7 minutes final extension, finishing at 4°C until gel loading. Every time was prepared a PCR reaction mixtures (total volume 25 µL) containing 2 µL of fungal genomic DNA template, 5 µL PCR buffer (5x green GoTaq reaction buffer), 0.5 µL deoxynucleoside triphosphate (dNTPs), 0.2 µL of GoTaq G2 DNA polymerase and 0.25 µL of each primer. An aliquot of 5 µl of amplified products was separated by electrophoresis onto 1% (w/v) agarose gel, stained with ethidium bromide and photographed under UV light to observe the result of the amplification. DNA was quantified using 1 kb plus NEB ladder by comparing fluorescence intensity of a known amount of ladder as specified by NEB guidelines. The appropriate amount of PCR product was sent to Eurofins Genomics (Vimodrone, Italy) for Sanger sequencing.

A consensus sequence was computed from the forward and reverse sequences using Geneious software (Version: 2020.2). Identification of the species was carried out using the Fusarium MycoBank database and NCBI nucleotide BLAST (nBLAST) (Bonavita, 2024).

3.2.3 Results

3.2.3.1 Morphological characterization

We collected 11 symptomatic bananas from markets surrounding the Milan area, from which we sampled potential fungal isolates. These fungal isolates were firstly grown

on Komada *Fusarium*-selective medium and then on PDA medium, the standard media for the identification of *Fusarium* species. As a result, we obtained more than 50 potential fungal isolates.

Morphological characterization of the colonies grown in PDA media, followed by examination with an optical microscope led to the selection of 18 isolates that could be reconducted to *Fusarium* species. Typical morphological traits, such as the production of numerous canoe- or banana-shaped conidia, the appearance of white, pink, or purple colonies and the presence of fluffy aerial mycelium were observed in all the samples

3.2.3.2 Molecular characterization

DNA extracted from the 18 isolates selected as potential *Fusarium* species was used for PCR amplification and DNA sequencing to confirm their identification with the MLS approach.

PCR amplification resulted in successful amplification of ITS gene of all the isolates, amplification of EF was obtained from 9 out of 17 isolates, while RPB2 resulted in the amplification of 13 samples. Sequences obtain were then inserted in Fusarium MycoBank database (https://fusarium.mycobank.org/) and NCBI nucleotide BLAST (nBLAST) for identification of the species.

Molecular identification confirmed 15 of the isolates as *Fusarium* species, one *Sarocladium strictum* commonly found in soil and decaying plant matter but also as opportunistic human pathogen, one *Aspergillus neoniger* an ecologically versatile fungus and one *Pestalotiopsis microspore* a significant plant fungal species (Table 3).

Table 3 Identification of strains isolated from bananas collected in markets surrounding Milan (Italy) area. The table describe name of the isolate, species identification, geographical provenience of the banana sampled, year and location of sampling.

ISOLATE	SPECIES	SAMPLING	COUNTRY	YEAR	MARKET
2022_A	*Fusarium spp.*	banana 1 (bio)	Ecuador	2022	Milan (Italy)
2022_L	*Fusarium spp*	banana 1 (bio)	Ecuador	2022	Milan (Italy)
2022_E	*Fusarium sacchari*	banana 10	Colombia	2023	Milan (Italy)
2022_B	*Fusarium sacchari*	banana 2	Costa Rica	2022	Milan (Italy)
2022_K	*Fusarium musae*	banana 2	Costa Rica	2022	Milan (Italy)
2022_M	*Fusarium oxysporum*	banana 2	Costa Rica	2022	Milan (Italy)

2022_G	*Pestalotiopsis microspora*	banana 3	Ecuador	2022	Milan (Italy)
2022_D	*Fusarium sacchari*	banana 4	Panama	2022	Milan (Italy)
2022_N	*Fusarium musae*	banana 5 (bio)	Ecuador	2022	Milan (Italy)
2022_I	*Fusarium spp.*	banana 6	Colombia	2022	Milan (Italy)
2022_II	*Fusarium spp.*	banana 6	Colombia	2022	Milan (Italy)
2022_IV	*Sarocladium strictum*	banana 6	Colombia	2022	Milan (Italy)
2022_V	*Fusarium spp.*	banana 6	Colombia	2022	Milan (Italy)
2022_VI	*Fusarium spp.*	banana 6	Colombia	2022	Milan (Italy)
2022_III	*Fusarium musae*	banana 7	Ecuador	2022	Milan (Italy)
2022_VII	*Fusarium musae*	banana 8	Colombia	2022	Milan (Italy)
2022_VIII	*Aspergillus neoniger*	banana 8	Colombia	2022	Milan (Italy)
2022_C	*Fusarium musae*	banana 9	Ecuador	2022	Milan (Italy)

3.2.4 Discussion

F. musae is the most recently identified causal agent of the devasting postharvest disease known as crown rot in banana fruits (Kamel et al., 2016). In addition, it has been isolated from hospitalized patients exhibiting fusariosis symptoms (Esposto et al., 2016; Triest and Hendrickx, 2016). Literature addressing the investigation of *F. musae* is quite limited and since 2016 very few studies have been published on this topic, moreover no additional cases have been reported.

With this survey we aimed at looking for *F. musae* by sampling symptomatic bananas found in the markets surrounding the area of Milan. Our goal was to assess whether *F. musae* is still present and can still be considered as a threat.

We visited various markets and collected symptomatic bananas presenting damages, both mechanical and indicative of fungal infection. It became immediately clear that this type of fruit is excluded from distribution and often discarded, making it challenging to collect symptomatic bananas. However, we menage to obtain 10 fruits with the desired characteristics. We sampled the fruits isolating potential fungi involved in their damage. By cultivating the isolates on Komada *Fusarium*-selective medium media, we aimed to promote the growth of only *Fusarium* species, specifically targeting *F. musae*, while excluding other microbial species that might be present on the fruit peel. Subsequent cultivation on PDA was used to facilitate fungal growth and the development of reproductive or peculiar structures, which helped us to initially identify isolates that match *Fusarium* spp. description.

Sampling of bananas resulted in obtaining more than 50 possible isolates, of which we made a selection to ensure that the same isolate was not counted multiple times from the same banana. A total of 18 isolates were picked as possible *Fusarium* species through morphological characterization with an electronic microscope and included for molecular characterization. MLS approach with informative genes, then, confirmed us the identification of our isolates at species level. As informative genes we selected ITS, commonly used to identify eukaryotes, EF and RPB2 for the identification at species level. Since we focused on identifying *F. musae*, we used EF and RPB2 primers already tested and constructed specifically to tailor for this species. Due to their high specificity, amplification was not successful for all the isolates. Amplification with ITS was successful for all the isolates, confirming them as fungi and allowing us to identify them at genus level. RPB2 amplified for 12 strains out of 18 and EF for 9 strains out of 18 enabling us to identify these isolates as species level.

Consensus sequences obtained from sequencing of informative genes were then uploaded in databased for the identification. NCBI nucleotide BLAST (nBLAST) is a database for general nucleotide sequence comparisons, while when using MycoBank database a filter for identification of mainly *Fusarium* species was applied. For this reason, some isolates presented a very low identification percentage and at these times they were identified as *Fusarium* even if the identity percentage or coverage was minimal. This indirectly suggested that they are non-*Fusarium* species, which was subsequently confirmed by results from NCBI.

With genomic characterization we were able to assign an identity to all isolates obtained. Out of the 18 isolates, we labeled 15 as *Fusarium* species, overall validating our procedure to isolate *Fusarium* from bananas. The use of Komada *Fusarium*-selective medium media reduced non-*Fusarium* isolates, though it was not fully selective, as some non-*Fusarium* fungi were recovered. It nonetheless favored the isolation of *Fusarium* species. Identification at species level was not possible for 6 of the *Fusarium* isolates. However, we demonstrate the presence of *F. sacchari* (3 isolates), *F. oxysporum* (1 isolate) and, most importantly, *F. musae* (5 isolates) on banana fruits sourced from different markets and imported from multiple countries.

Overall, with our survey we demonstrated that *Fusarium* species are commonly found on banana fruits. In particular, we assess the presence of *F. musae* emphasizing the current presence of this pathogen and the relevance of investigating it.

Isolates identified as *F. musae* were multiple and all of them were obtained from different fruits, highlighting once more its presence. However, deeper characterization of these isolates is required to prove them as different strains. This has to be done to exclude the possibility that the same strain was transferred from one fruit to another during transport to our facility or while handling the fruits during sampling.

In addition, provenance of banana from major banana-producing countries as Ecuador and Costa Rica combined with the isolation of the fungus in a banana-consuming country as Italy, support the hypothetical transmission route of *F. musae (Triest and Hendrickx, 2016)*. In this scenario, fruits may acquire the infection when harvested and, after incubation during transport, the infection reaches people at risk. However, further sampling is needed in banana-producing countries to detect the fungus in both bananas and the surrounding environment, including soil and plantations to confirm bananas as the primary host of *F. musae*. As well, it would be valuable to research for *F. musae* in hospitals within these regions by monitoring patients with fusariosis symptoms to assess potential links between human infections and contact with infected bananas.

To conclude, with our survey we confirm the presence of *F. musae* in the markets surrounding the area of Milan. Despite the low incidence of reported cases of infection with *F. musae*, our results underline once more the importance of study *F. musae*. This species remains a real threat present in the markets and an emerging concern for food security and human health, crossing the full spectrum of One Heath.

Chapter 4

Telomere to telomere genome assembly of *Fusarium musae* F31, causal agent of crown rot disease of banana

The chapter was adapted from:

Degradi, L.; Tava, V.; Kunova, A.; Cortesi, P.; Saracchi, M.; Pasquali, M. Telomere to Telomere Genome Assembly of Fusarium musae F31, Causal Agent of Crown Rot Disease of Banana. Mol. Plant Microbe Interact. 2021, 34, 1455–1457

DOI: 10.1094/MPMI-05-21-0127-A

Chapter 4:

Telomere to telomere genome assembly of *Fusarium musae* F31, causal agent of crown rot disease of banana

4.1 Abstract

Fusarium musae causes crown rot of banana and it is also associated to clinical fusariosis. A chromosome-level genome assembly of *Fusarium musae* F31 obtained combining Nanopore long reads, and Illumina paired end reads resulted in 12 chromosomes plus one contig with overall N_{50} of 4.36 Mb, and is presented together with its mitochondrial genome (58072 bp). F31 genome includes telomeric regions for 11 of the 12 chromosomes representing one of the most complete genome available in the *Fusarium fujikuroi* species complex. The high-quality assembly of the F31 genome will be a valuable resource for studying the pathogenic interactions occurring between *F. musae* and banana. Moreover, it represents an important esource for understanding the genome evolution in the *Fusarium fujikuroi* species complex.

4.2 Assay

Fusarium musae Van Hove is a filamentous fungus (Class Sordariomycetes, phylum Ascomycota) able to infect banana, but it is also found in clinical settings (Kamel et al., 2016; Triest et al., 2016; Van Hove et al., 2011). This fungus is one of the causal agents of crown rot of banana, a major cause of postharvest losses in banana (Van Hove et al., 2011). It belongs to the *Fusarium fujikuroi* species complex (FFSC), which includes at least 50 (O'Donnell et al., 1998; Yilmaz et al., 2021). Improving the quality of the available assembly in the FFSC will provide a valuable resource for the identification of pathogenic genes and for comparative genomic studies. The complete genome of *F. musae* will contribute to study genomes evolution within the FFSC. Actual reference for the FFSC is *F. verticillioides* 7600 (AN: GCA_000149555.1). Only one assembly of *F. musae* species is available up to date (AN: GCA_013623345.1).

To obtain a complete genome, a hybrid sequencing approach was used. The F31 strain was originally isolated from infected banana from the Dominican Republic and proved to be pathogenic on banana and deposited in the German Collection of Microorganisms and Cell Cultures GmbH (Leibniz, GER) under the accession number DSM 112727 (Kamel et al., 2016).

In our work, high-molecular weight DNA was extracted from F31 strain lyophilized tissue using the CTAB extraction method (Breakspear *et al.,* 2011) followed by Qiagen genomic tip (Qiagen, USA) cleaning procedure according to manufacturer's instructions. MiSeq Reagent Kit v2 (Illumina, USA) led to a total of 11.812.123 paired-end short reads (2 x 151) and SQK- LSK109 sequencing kit (Nanopore, UK) led to 2.221.411 reads of single molecule long read sequencing using MinION MIN101B platform, R9.4.1 flow cell (Nanopore, UK). Obtained coverage was 60X by Illumina and 250X by Nanopore reads.

Assembly was performed on NanoLyse processed sequences (to remove lambda reads) using Canu v.2.1.1+galaxy0 (Koren *et al.*, 2017) with default settings. Autopolishing was performed using Medaka v.1.0.3+galaxy2. Minimap2 v.2.17+galaxy4 (Li and Durbin, 2010) was used to align short reads on the obtained assembly and Pilon v.1.20.1 (Walker et al., 2014) was used to extract the consensus sequence giving 0.48% of corrected erroneous positions (n=214.296).

Manual correction was done using Geneious Prime software v11 (Biomatters, NZ). Minimap2 plugin (default settings) tool aligning long reads on the obtained assembly validated 7 contiguous contigs. Others had errors corrected using short reads assembly obtained with Shovill v1.1.0+galaxy0 with default settings. Manual correction allowed to connect different contigs. Telomeric regions, based on Telomerase DB, were annotated to validate chromosomes.

Final assembly statistics were evaluated using Quast tool v.5.0.2+galaxy1 (Mikheenko et al., 2018). The ultimate genome size of *F. musae* F31 was 44.07 Mb (1.5 Mb more than the reference), divided into 12 chromosomes, the circular mtDNA and 1 unplaced contig. N50 of the final assembly was 4.36 Mb confirming high contiguity of the obtained assembly. Of the 12 chromosomes, 11 had both telomeres (TTAGGG) included, while one had only one telomeric region. Compared with previous assembly of *F. musae* (*GCA_013623345.1*) and *F. verticilloides* (*GCA_000149555.1*) present on

NCBI, this genome improves substantially completeness within the *F. fujikuroi* species complex. Completeness measured using BUSCO v.5.0.0+galaxy0 tool (Simao *et al.*, 2015) on *hypocreales*_odb10 database was higher for F31 compared to NRRL25059 strain of *F. musae*. Moreover, contig number and N50 results were significantly improved for F31 genome assembly (Table 4).

Table 4 Summary of the genome assembly and annotation statistics of F. musae F31 strain, compared with a previous assembly of F. musae NRRL 25059 strain and with the best reference available in the FFSC, F. verticillioides 7600.

Strains	F31 (this study)	NRRL 25059 (GCA_013623345.1)	*F. verticillioides* 7600[a] (GCA_000149555.1)
Number of contigs	14	1149	37 (scaffold)
Number of chromosomes	12	N.A.[b]	11
MtDNA (size)	Yes (58072 bp)	Yes (57891 bp)	Yes (53743 bp)
Genome size (Mb)	44.07	42.5	41.8
GC content (%)	47.22	48.70	48.68
Contig N50 (Mb)	4.36	0.09	1.96 (scaffold)
Number of protein coding genes	13963	13931	13699
BUSCO completeness[c]	4485/4494	4463/4494	4372/4494

[a]nearest species belonging to FFSC with chromosome level assembly.
[b]Not Available
[c]Completed BUSCO (single and multiple copy)/Total *hypocreales_odb10* BUSCO

Annotation was performed using Funannotate software v. 1.8.7. After first step of repeat

sequences masking done with repeat mask v. 4.0.7, Augustus tool v.3.3.3, (Keller *et al.*, 2011) trained with *Fusarium graminearum* protein database, was used for nuclear “ab initio” annotation. Functional annotation of the predicted coding region was performed using Antismash v. 5.0, Interproscan v. 5.51-85.0, EggNOG mapper v. 5.0.0, database. For mtDNA annotation, Mfannot and RNAWeasel were used with NOVOplasty v.4.2+galaxy0 (Dierckxsens *et al.*, 2019) assembly using the *F. verticillioides* 7600 (AN: GCA_000149555.1) strain mtDNA as a reference and a sequence of 1700 bp length as a seed sequence.

After masking sequences process, which masked 4.32% of sequences, ab initio gene prediction generates the prediction position of coding region. Final functional annotation finalized to assign function to predicted sequences lead to a total of 13963 annotated genes, 13661 of which are proteins and 302 are tRNA for nuclear DNA. For

mtDNA 15 proteins, the small subunit ribosomial RNA (rns) and 27 tRNA were annotated.

The genome assembly of F31 will be a useful resource for comparative analysis of *Fusarium musae* species and represents a reference for completeness in the *Fusarium fujikuroi* species complex.

The F31 genome project can be found at GenBank under BioProject accession number PRJNA718489. The chromosomal sequence and genes annotation of F31 can be found at GenBank with the accession number JAHBCI000000000. Nanopore reads and Illumina paired end reads are available in the NCBI Sequenced Read Archive under the accession numbers SRR14117444 and SRR14117445 respectively.

Chapter 5

Exploring Mitogenomes Diversity of *Fusarium musae* from Banana Fruits and Human Patients

The chapter was adapted from:
Degradi, L.; Tava, V.; Prigitano, A.; Esposto, M.C.; Tortorano, A.M.; Saracchi, M.; Kunova, A.; Cortesi, P.; Pasquali, M. Exploring Mitogenomes Diversity of Fusarium musae from Banana Fruits and Human Patients. Microorganisms 2022, 10, 1115.
DOI: 10.3390/microorganisms10061115

Chapter 5

Exploring Mitogenomes Diversity of *Fusarium musae* from Banana Fruits and Human Patients

5.1 Abstract

Fusarium musae has recently been described as a cross-kingdom pathogen causing post-harvest disease in bananas and systemic and superficial infection in humans. The taxonomic identity of fungal cross-kingdom pathogens is essential for confirming the identification of the species on distant infected hosts. Understanding the level of variability within the species is essential to decipher the population homogeneity infecting human and plant hosts. In order to verify that *F. musae* strains isolated from fruits and patients are part of a common population and to estimate their overall diversity, we assembled, annotated and explored the diversity of the mitogenomes of 18 *F. musae* strains obtained from banana fruits and human patients. The mitogenomes showed a high level of similarity among strains with different hosts' origins, with sizes ranging from 56,493 to 59,256 bp. All contained 27 tRNA genes and 14 protein-coding genes, rps3 protein, and small and large ribosomal subunits (rns and rnl). Variations in the number of endonucleases were detected. A comparison of mitochondrial endonucleases distribution with a diverse set of *Fusarium* mitogenomes allowed us to specifically discriminate *F. musae* from its sister species *F. verticillioides* and the other *Fusarium* species. Despite the diversity in *F. musae* mitochondria, strains from bananas and strains from human patients group together, indirectly confirming *F. musae* as a cross-kingdom pathogen.

5.2 Introduction

Different fungal species are able to cross hosts, causing diseases not only in plants but also in humans and animals. In general, cross-kingdom fungi are weak pathogens for both plants and humans; they can also be asymptomatic in plants but can have clinical significance, especially in people with impaired immunity or those who have sustained penetrating trauma (Gauthier and Keller, 2013). The

role of food and agriculture in the transmissibility of cross-kingdom pathogens deserves to be studied accurately.

Fusarium musae VanHove is a pathogenic species belonging to the *F. fujikuroi* species Complex (Van Hove et al., 2011). It causes crown rot in bananas, a post-harvest disease (Kamel et al., 2016; Molnár et al., 2015), and it also causes keratitis and skin infections as well as systemic infections in immunocompromised patients (Triest et al., 2015; Verbeke et al., 2020).

Based on multilocus sequence typing, *F. musae* can be distinguished from its sister species *F. verticillioides (Van Hove et al., 2011)*. The two species show a diverse susceptibility to azoles, with *F. musae* having a higher tolerance to some fungicides compared to *F. verticillioides* (Tava et al., 2021).

F. musae has been identified on banana fruits in Central American regions, in the Philippines and Canary Islands and in European and Japanese markets of banana fruits. In patients, it has been identified in the US and Europe (Esposto et al., 2016; Triest et al., 2015). Understanding the level of diversity of strains infecting humans and banana fruits may help address the question about the transmissibility of *F. musae* in different hosts (Triest and Hendrickx, 2016).

Mitochondrial genomes evolve independently of and faster than the nuclear genome (Almeida et al., 2021). Mitogenomes have also been proposed as a useful tool for diagnostic purposes in *Fusarium* species (Wyrębek et al., 2021). The concept of using mitogenome diversity for the identification of species mainly derives from their higher DNA copy number compared with nuclear DNA, and hence the high recovery and amplification success in eukaryotes where insufficient phylogenetic signals have accumulated in nuclear genes (Kulik et al., 2020).

Fungal mitochondrial genomes are typically small, circular and double-stranded DNA molecules, with a typical set of mitochondrial genes with identical gene order. Extensive mitochondrial genome comparisons within the fungal kingdom have shown that any gene has a mitochondrial localization in all fungal species (Fonseca et al., 2021), suggesting that the use of mitochondrial gene diversity cannot be applied as a universal marker for fungi. Nonetheless, the analysis of mitochondrial diversity can be successfully applied to differentiate species within orders (Valenti et al., 2022) or species (Ma et al., 2021; Theelen et al., 2021). For example, a unique feature

apparently common in all *Fusarium* species is the presence of a large open reading frame with an unknown function (LV-uORF) firstly described in mitogenomes of *F. graminearum*, *F. verticillioides* and *F. solani* (Al-Reedy et al., 2012) and probably acquired prior to the divergence of *Fusarium* species.

In addition, fungal mitogenomes harbour a variable number of mobile genetic elements (MGEs) such as intron-associated homing endonucleases (HEGs), which have invaded mitogenomes throughout their evolution. Most of the MGEs insertion sites are highly conserved (Hamari et al., 2005) and occur in mitochondrial protein-coding genes but can display remarkably different MGE densities. The same MGEs can be irregularly distributed in evolutionarily distant species and mosaicism in MGE patterns can be found between different populations or even strains of the same species, driving large genome size differences among them. Exploring MGE distribution can help discriminate species and subgroups, tracking the spread of fungal populations (Yang et al., 2020). We, therefore, explored the mitogenomes of a collection of 18 *F. musae* strains in order to describe their mitochondrial diversity. The other objective of this study was to discover whether the pattern of MGE diversity might facilitate the identification of *F. musae* species within the *Fusarium* genus. Moreover, we explored whether *F. musae* from bananas and human patients shared the same mitochondrial sequence in order to see if genetic subgroups associated with the host origin could be identified.

5.3 Material and Methods

5.3.1 DNA Extraction and Sequencing

DNA used for sequencing was obtained from fresh mycelia of 16 strains according to a modified CTAB method, followed by Genomic tips column purification (Qiagen, Germantown, MD, USA) (Pasquali et al., 2004). Sequencing was carried out using Illumina Hiseq 2000 (151 bp x2) by Novogene (Cambridge, UK). Mitogenomes of NRRL25059 (Brankovics et al., 2020) and F31 (Degradi et al., 2021) strains were obtained from the NCBI database.

5.3.2 Other Fungal Mitochondrial Genomes

Mitogenomes from fungal strains belonging to different *Fusarium* species were retrieved from NCBI and partially annotated if the annotation was missing (protein genes) using MFannot online software (University of Montreal, Montreal, QC, Canada), (https://megasun.bch.umontreal.ca/cgi-bin/mfannot/mfannotInterface.pl (accessed on 4 March 2022)).

5.3.3 Assembly and Annotation of Mitogenome

Assembly for all *F. musae* mitochondrial DNAs was carried out de novo with NOVO-plasty 4.2 (Dierckxsens et al., 2020) using *F. musae* F31 strain as a reference and the first 715 bp from *cox1* gene as seed sequence. The obtained mitogenomes were then annotated by integrating MFannot and RNAWeasel (Lowe and Chan, 2016). In order to improve the final annotation, the BlastX tool was used to define the nature of the different annotated ORFs and endonucleases.

5.3.4 Alignment of Protein Genes

Mitogenomes comparison included a total of 14 concatenated sequences, which rep-resent the 14 coding protein nucleotide sequences corresponding to the set of conserved mitochondrial genes, using the “concatenated sequences” tool on Geneious Prime Software (Biomatters Ltd., Auckland, Australia). Sequences were then aligned using the MAFFT alignment tool with default parameters and visually checked.

5.3.5 MGE Analysis (Minimap2)

Mobile genetic element analysis was performed using the distribution pattern of *F. musae* IUM_11-0508 as a reference. The goal was to identify the distribution of the same MGEs across *Fusarium* genus diversity. After MGE sequences collection, the Minimap2 tool on Geneoius Prime Software (setting a threshold of identity at 90% and minimum coverage of 75%) against all other *Fusarium* mtDNA and BlastX (coverage and identity threshold: 75 and 90% respectively) analyses were used to identify the presence of those sequences in other *Fusarium* species and other fungal species.

5.3.6 Analysis of Nad1 Intron

To confirm the sequence of the intron in nad1 in order to describe the possible path of inactivation of the nad1 endonuclease present in *F. verticillioides*, primers musaeendoF1- (5′-TGGAAAATCAGCAGGTTGACC-3′) and musaeendoR1- (5′-ACTGCTGCGTGTTCTGTCAT-3′) were designed on the coding region of the nad1 gene using primer 3 software online (https://primer3.ut.ee/, accessed on 4 November 2021). PCR amplification was carried out using Q5 master mix (NEB, Ipswich, MA, UK) in a total of 25 microliters of reaction using a PCR program that included 3 min at 95 °C, 35 cycles including 20 s at 95 °C, 20 s at 60 °C and 1 min at 72 °C, followed by a last step at 72 °C for 5 min, which was carried out in a VeritiPRO Thermal Cycler (Applied Byosystem, Waltham, MA, USA). Sequences were obtained by PCR purification and Sanger sequencing (Eurofins genomics, GER, Ebersberg, Germany). The obtained sequences were then manually checked and assembled and then aligned using the MAFFT tool in Geneious Prime Software to verify the correctness of the assembly. Moreover, BlastN, BlastX and BlastP were used to characterize the mutations occurring in the region and to identify the inactivation of endonuclease functional domains.

5.3.7 Haplotype Analysis of Mitogenomes

Whole MAFFT aligned mitogenomes using Geneious prime software were manually checked and analysed using Median Joining Network in Popart (Bandelt et al., 1999).

5.4 Results

5.4.1 F. musae Mitogenomes

Mitogenomes of *F. musae* strains ranges from 56,439 to 59,256 bp (Table 5).

All mitogenomes had identical gene and tRNA distribution. Analysis carried out on the nine annotated ORFs, using the BlastP tool, showed that six of these ORFs represent mobile genetic elements (MGEs) of LAGLIDADG and GIY-YIG family, one represents a hypothetical protein, while two have to be considered ORFs with unassigned functions.

Further investigation of *nad1*_intron revealed the presence of an inactivated endonuclease with very high similarity to the *F. verticillioides* GIY-YIG endonuclease positioned within the *nad1* gene.

*Table 5 List of F. musae strains used in this study with GeneBank accession numbers and mitogenome size and composition. *Protein list: atp6, atp8, atp9, cob, cox1, cox2, cox3, nad1, nad2, nad3, nad4, nad4L, nad5, nad6, rps3; ** +1 represent the inactivated endonuclease; *** identity not calculated due to differences in number of endonucleases.*

Strain/Feature	110508		43682								
mtDNA	MW 307784	MW 296866	ON 240679	ON 240982	ON 240983	ON 240980	ON 240981	ON 240987	ON 240984	ON 240985	ON 240992
Length (bp)	58,111	58,072	58,076	58,078	58,089	58,063	59,252	59,252	58,080	59,256	58,105
Identity (%)	REF	99.8	99.9	99.9	99.9	99.9	99.5	99.5	99.9	99.9	99.97
Protein genes *											
Number	15	15	15	15	15	15	15	15	15	15	15
Length (bp)	14,148	14,148	14,148	14,148	14,148	14,148	14,148	14,148	14,148	14,148	14,148
Identity (%)	REF	99.96	100	100	100	100	99.99	99.99	100	100	100
Differences	REF	2	0	0	0	0	1	1	0	0	0
Transversion	REF	1	0	0	0	0	0	0	0	0	0
MGEs											
Number **	6 + 1	6 + 1	6 + 1	6 + 1	6 + 1	6 + 1	7 + 1	7 + 1	6 + 1	7 + 1	6 + 1
Length (bp)	7009	7010	7009	7009	7009	7009	7464	7464	7009	7448	7009
Identity (%)	REF	100%	100%	100%	100%	100%	– ***	– ***	100%	– ***	100%
ORF											
Number	3	3	3	3	3	3	3	3	3	3	3
Length (bp)	8952	8952	8952	8952	8952	8952	8949	8949	8952	8952	8952
Identitcal sites	REF	8948	8945	8945	8945	8944	8931	8931	8946	8943	8944
rns + tRNA											
Length (bp)	1668 + 2005	1668 + 2005	1668 + 2005	1668 + 2005	1668 + 2005	1668 + 2005	1668 + 2005	1668 + 2005	1668 + 2005	1668 + 2005	1668 + 2005
Identity (%)	REF	100	100	100	100	100	100	100	100	100	100

The final annotation of the mitogenomes of *F. musae* strains includes all the 14 protein-coding genes (atp6, atp8, atp9, cob, cox1, cox2, cox3, nad1, nad2, nad3, nad4, nad4 L, nad5, nad6); the ribosomal protein rps3 and two ribosomal rRNA (rns and rnl); 27 tRNA genes and 2 ORFs; 6 MGEs (3 LAGLIDADG and 3 GIY-YIG positioned in nad2 intron (n = 1), in cob introns (n = 2) and in cox1 introns (n = 3)); 1 hypothetical protein; and 1 inactivated GIY-YIG endonuclease present in nad1 intron (not annotated). Figure 1 shows the example of the IUM_11-0508 strain mitogenome.

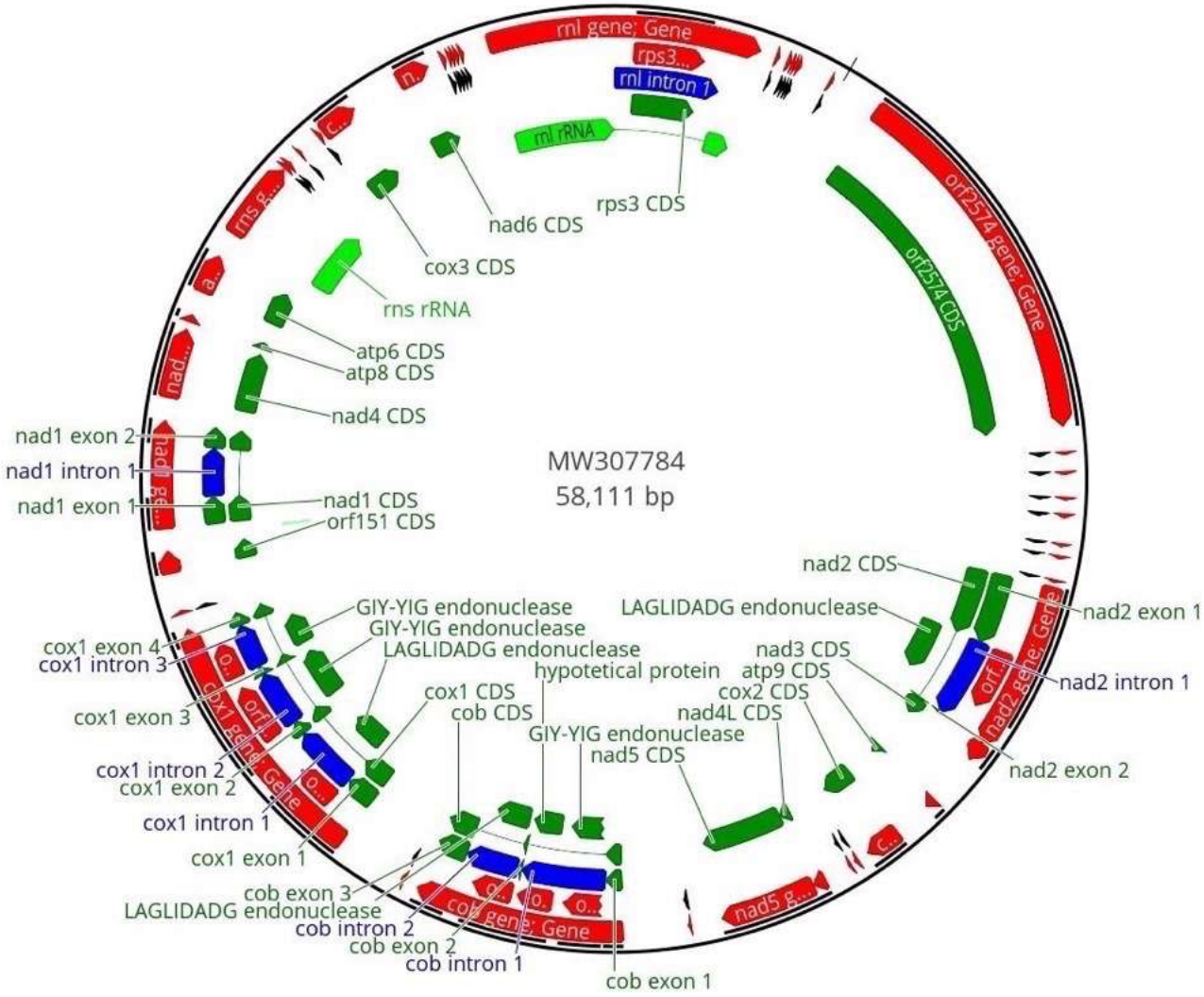

Figure 1. Graphical representation of circular mtDNA of Fusarium musae IUM_11-0508. The red colour indicates genes, the green colour refers to the coding sequences, light green refers to ribosomal subunits and the blue colour represents the introns. tRNA are represented in black.The analysis of codon usage in coding sequences did not reveal any significant difference among the whole set of analysed strains (not shown). Indeed, all the F. musae strains showed a high similarity for protein-coding regions. Two differences were present in strain F31: a triplet change for coding the same amino acid (Leu) and a single SNP, which causes a transversion. Strains FM_IHEM20180, FM_NRRL28993 and NRRL28997 showed one SNP with no effect on the amino acid sequence. All changes were localized in the nad5 gene

Size difference among mitogenomes was mostly due to variations in two regions: for strain ITEM_1149, a deletion in the ORF located between rps3 and nad2 reduces the mitogenome to 56,493, while for strains IHEM_20180, MUCL_51371, NRRL_28893 and NRRL_28897, the increased size above 59 kb is due to changes in the cob region. The *cob*gene in *F. musae* includes three exons and two introns (Figure 2). The first intron is composed of an endonuclease with GIY-YIG domain and a hypothetical protein, common in all the *F. musae* strains. The second intron shows differences within the species: in four strains (IHEM_20180, NRRL_28893,

NRRL_28897, MUCL_51371), it shows a duplication of a 247 AA LAGLIDADG endonuclease, while in all the other strains, a single LAGLIDAGD of 296 AA is present (Figure 2).

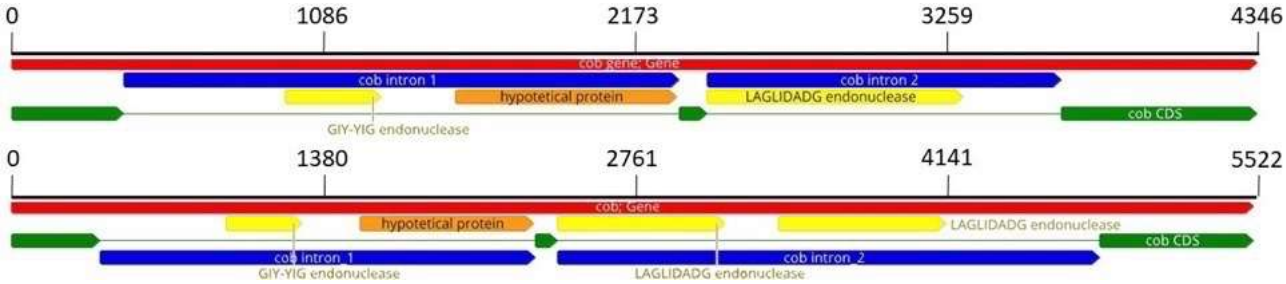

Figure 2. The two different patterns of the cob gene. On the top, the most common configuration with only one endonuclease inside the intron_2; on the bottom, the other configuration of the 4 F. musae strains with 2 endonucleases in intron_2. Red colour represents the gene, yellow and orange are respectively endonucleases and hypothetical protein while introns are in blue.

BlastX analysis on these two endonucleases showed different LAGLIDADG domains for the two endonucleases (LAGLIDADG_1 and LAGLIDADG_2). Investigation for a similar pattern in other species showed that a similar duplication could be observed in *F. bactridioides*, *F. begoniae* and *F. pseudograminearum* as well as in *Cladobotryum mycophilum*.

F. verticillioides has an endonuclease within the nad1 gene. Interestingly, *F. musae* strains also have an intron in nad1. Intron annotation using alignment and BlastX tool showed that *F. musae* introns have highly similar sequences to the endonuclease of *F. verticillioides*, but the presence of different mutations leading to stop codons and frame shifts suggest the inactivation of the endonuclease and the loss of functional domains. Analyzing endonad1 (the most variable endonuclease within *F. musae* species) using *F. verticillioides* as a reference, we could identify three different ways of silencing the endonuclease in our *F. musae* population that are caused by insertion and nonsynonymous substitution to add stop codons in the sequence of the endonuclease (Figure 3).

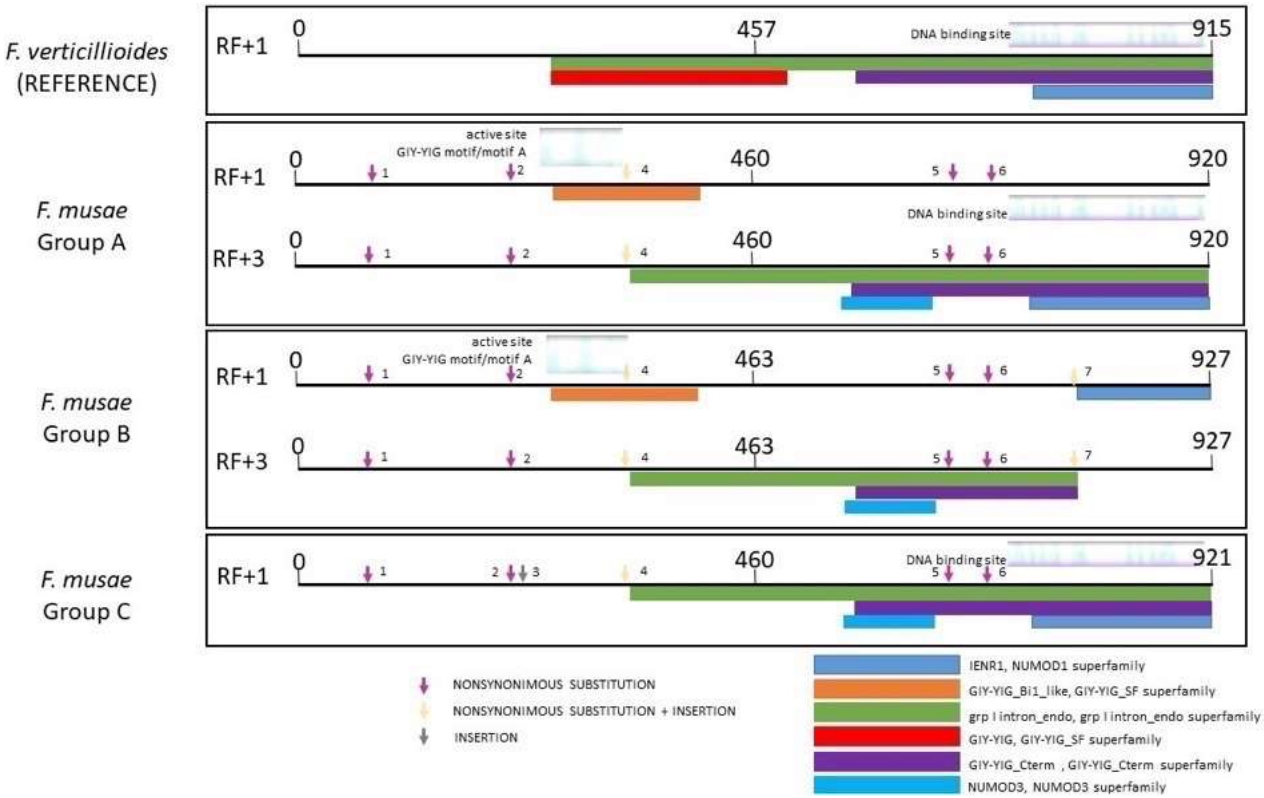

Figure 3. BlastX results of the intron of nad1 gene in F. verticillioides and in F. musae strains. Types of endonuclease functional domains are visible. Numbers near arrows indicate different types of variations of the intron gene in F. musae strains compared to functional endonuclease in F. verticillioides. Group A includes: IHEM19981, ITEM1121, ITEM1142, ITEM1149, ITEM1250, IUM_11-0508, IUM_11-0507, MUCL51371, NRRL25673, NRRL43601, NRRL43604, NRRL43658, NRRL43682; group B: IHEM20180, NRRL25059, NRRL28893, NRRL28897; group C: F31.

5.4.2 Diversity within F. musae

Given the limited exploitation of mitogenomes for population studies, the other goal of our work was to assess whether mitochondrial diversity observed within the species could be explored to differentiate species subgroups.

Triest and Hendrickx hypothesized that *F. musae* may have been transmitted from bananas to patients (Triest and Hendrickx, 2016). To confute this hypothesis, we would expect that the hosts' origin can be associated with different subgroups within the species, suggesting a host specialization driven by evolutionary constraints (Hartmann et al., 2020). We therefore tested whether *F. musae* mitochondria diversity could be used to clearly separate strains obtained from humans and bananas. The overall diversity of mitogenome haplotypes (Figure 4) suggests that different subgroups of *F. musae* strains exist within the analyzed population.

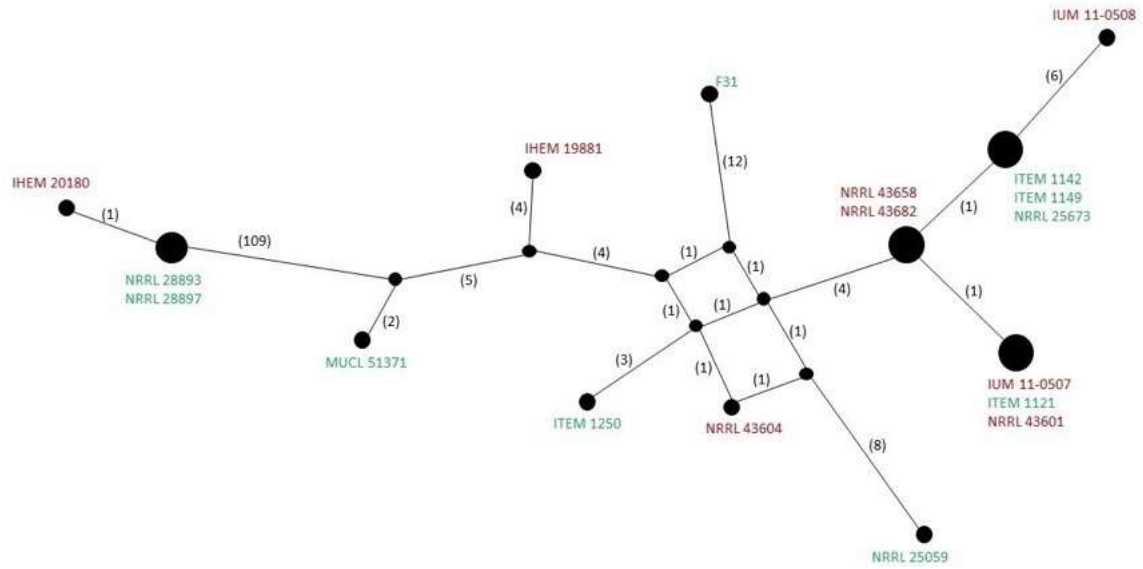

Figure 4 . Representation of mitogenomes network haplotypes using Popart software. The red colour indicates strains isolated from human patients; the green colour indicates strains isolated from banana fruits.

This is consistent with the existence of different nuclear gene haplotypes (Van Hove et al., 2011). Interestingly, at least one set of strains belonging to the same mitochondrial haplotype includes both human and banana derived strains from different geographic regions (ITEM_1121 from a banana fruit from Panama, IUM_11-0507 from a patient in Greece and NRRL_43601 from a patient in Maryland, USA), supporting the hypothesis that the infection of banana fruits and human patients occurs from strains with similar genetic profile.

5.4.3 The Diagnostic Power of Mitochondrial Genomes

Another objective of the paper was to explore the use of mitochondrial diversity as a tool for the detection of species. The distribution of MEGs in a mitogenome may differentiate species. The hypothesis has been validated for other *Fusarium* species (Kulik et al., 2020). One of the major diagnostic challenges in *F. musae* is to discriminate it from *F. verticillioides*, as morphologically, the species are often misclassified (Esposto et al., 2016; Triest et al., 2015).

We therefore compared the *F. musae* pattern of MGE with all the other available Fusarium mtDNAs. The 6 + 1 MGEs were extracted and searched in all other mtDNAs. MGE distribution within the *Fusarium* genus showed discontinuity. In particular, *F.*

musae species showed a specific pattern of MGE distribution that is unique within the *Fusarium* genus. It is possible to identify
F. musae species based on the unique presence of two MGEs (nad1 intron that is showing polymorphic inactivation and endo1cox), offering potentially a very powerful methodology to identify *F. musae*.

5.5 Discussion

This study, analyzing the mitochondrial genomes of 18 *F. musae* strains, confirms previous observations based on nuclear genes (*TEF* and *RPB2*) (Tava et al., 2021; Triest, 2016), which showed that *F. musae* strains from banana and human patients are interspersed in the species tree. This indirectly confirms the ability of *F. musae* to cross-infect distant hosts. One strain, F31, showed a non-synonymous substitution that may indicate some divergence within the species. Further analyses to appropriately characterize the strain are warranted. Within *F. musae* species, *nad5* proved to be the gene with higher recombination, as observed previously in other species within the *F. fujikuroi* species complex (Fourie et al., 2018). Our mitogenome study of the *F. musae* population confirms that intergenic regions and endonucleases may be exploited to identify subgroups within a species (Theelen et al., 2021). As observed in other fungal species (Li et al., 2023; Sommerhalder et al., 2007), we also observed that major contributors to mitogenome size diversity within a species are intron rearrangements. In our population, two regions showed variability in size: the ORF located between *rps3* and *nad2* and the intron between exon2_*cob* and exon3_*cob*. Future studies may focus on the diversity of these regions in a larger *F. musae* population.
We observed different haplotype groups comparing whole mitochondrial diversity in *F. musae*. Previous analysis of nuclear gene haplotype diversity carried out on *F. musae* strains (Van Hove et al., 2011) showed the existence of nine haplotypes based on *RPB2*, *B-tub* and *TEF* diversity. Our panel of strains included representatives of six haplotypes. We could verify that nuclear gene haplotypes were all distinguished in different mitogenome groups. A larger dataset of mitogenomes needs to be analyzed to verify the correspondence of nuclear gene haplotypes and mitochondrial whole diversity haplotypes. This preliminary observation seems to confirm that in *F. musae*,

mitochondrial diversity is concordant with nuclear gene variations, as observed for other fungal pathogens (Sommerhalder et al., 2007), and it is therefore a valuable tool for strain typing.

The use of mitochondrial genomes for diagnostic purposes has been often proposed and explored (Jelen et al., 2016; Misas et al., 2020; Santamaria et al., 2009; Yang et al., 2020). We could verify that all *F. musae* strains with different geographic origins (Europe, Asia, America) and different years of isolation (from 1991 to 2013) share the same specific co-occurrence of two endonucleases that allow us to differentiate them from all other *Fusarium* species whose mitogenome is available. With the increased number of available genomes within single species, the possibility to test the hypothesis of using MGE distribution for species discrimination will be tested thoroughly.

Chapter 6

Fusarium musae from diseased bananas and human patients: susceptibility to fungicides used in clinical and agricultural settings

The chapter was adapted from:

Tava, V.; Prigitano, A.; Cortesi, P.; Esposto, M.C.; Pasquali, M. Fusarium musae from Diseased Bananas and Human Patients: Susceptibility to Fungicides Used in Clinical and Agricultural Settings. J. Fungi 2021, 7, 784. [CrossRef] 8. Esposto, M.C.; Prigitano, A.; Tortorano, A.M. Fusarium musae as Cause of Superficial and Deep-Seated Human Infections. J. Mycol. Med. 2016, 26, 403–405.

DOI: 10.1016/j.mycmed.2016.02.021

Chapter 6

Fusarium musae from diseased bananas and human patients: susceptibility to fungicides used in clinical and agricultural settings

6.1 Abstract

Fusarium musae belongs to the *Fusarium fujikuroi* species complex. It causes crown rot disease in banana but also keratitis and skin infections as well as systemic infections in immunocompromised patients. Antifungal treatments in clinical and agricultural settings rely mostly on molecules belonging to the azole class. Given the potential risk of pathogen spread from food to clinical settings, the goal of the work was to define the level of susceptibility to different azoles of a worldwide population of *F. musae*. Eight fungicides used in agriculture and five antifungals used in clinical settings (4 azoles and amphotericin B) were tested using the CLSI (Clinical and Laboratory Standards Institute) protocol methodology on 19 *F. musae* strains collected from both infected patients and bananas. The level of susceptibility to the different active molecules was not dependent on the source of isolation with the exception of fenbuconazole and difenoconazole which had a higher efficiency on banana-isolated strains. Minimal inhibitory concentrations (MICs) of the different molecules ranged from 0.12–0.25 mg/L for prochloraz to more than 16 mg/L for tetraconazole and fenbuconazole. Compared to the *F. verticillioides*, *F. musae* MICs were higher suggesting the importance of monitoring the potential future spread of this species also in clinical settings.

6.2 Introduction

Fusariosis is one of the most common mold infections in humans ranging from superficial diseases, such as onychomycosis and keratitis, to disseminated infections, particularly in hematological cancer and neutropenic patients (Guarro, 2013). The genus *Fusarium* comprises at least 200 species that are not only human pathogens, but they have been isolated also from animals, plants and in specific cases also from the surrounding environment (Guarro, 2013; Sáenz et al., 2020). Numerous *Fusarium*

species have been classified as cross-kingdom pathogens given their ability to jump from one host to a taxonomically distant one. Among those, *Fusarium musae*, sister species of *Fusarium verticillioides* in the *Fusarium fujikuroi* species complex, is one of the causative agents of crown rot of banana, a devastating postharvest disease (Kamel et al., 2016; O'Donnell et al., 1998; Triest, 2016; Triest and Hendrickx, 2016; Van Hove et al., 2011). The late appearance after distribution in consuming countries make signs of disease impossible to notice during harvest and determine significant losses in banana fruits. Recent studies showed that *F. musae* has also been isolated from human patients where it causes nail and eyes lesions as well as systemic infection in immunocompromised patients (Esposto et al., 2016; Triest et al., 2016). It is not clear yet how human beings are infected by *F. musae*. Banana fruits probably act as carriers of *F. musae* spores that reach the consumers after shipping in banana-consuming countries where humans acquire the infection (Triest and Hendrickx, 2016). However, it cannot be excluded that humans acquire the infection after traveling to a banana producing country or through unknown plants or other environmental substrates (Triest et al., 2016). It is estimated that 10–30% of the total amount of human Fusariosis are caused by *F. verticillioides* of which 7–20% are actually *F. musae* (Tortorano et al., 2014; Triest et al., 2016).

F. musae has been reported so far as a cause of banana disease in Dominican Republic (Kamel et al., 2016), Hungary (Molnár et al., 2015), "Neotropical" countries (Hirata et al., 2001; Shi et al., 2017) and Philippines (Van Hove et al., 2011), and cause of infections in humans in Italy, Greece (Esposto et al., 2016), France, Belgium (Triest et al., 2015) and the USA (O'Donnell et al., 2007) although it is probable that other *Fusarium* infections have gone undetected due to the difficulty of identifying species. Indeed, species classification relies on multigene sequencing. Differences between *F. verticillioides* and *F. musae* include the excision of the fumonisin gene cluster (Van Hove et al., 2011).

The lack of consensus regarding treatment protocols for human fusariosis make the infections difficult to treat (Batista et al., 2020). Reference methods for in vitro antifungal susceptibility testing are those of Clinical and Laboratory Standards Institute (CLSI) and European Committee on Antimicrobial Susceptibility (EUCAST), but breakpoints (BPs) have not yet been established (Al-Hatmi et al., 2016a, 2018).

So far most of the clinical and agricultural treatments of *Fusarium* infections rely on the use of azoles, imidazoles and triazoles, which act as inhibitors of ergosterol biosynthesis by blocking 14a demethylation with a selectivity for fungal CYP51 (Lamb et al., 1999). It has been shown that various azole derivatives can show differences in the spectrum of activity and power of action (Pasquali et al., 2020), therefore it is important to know the antifungal effectiveness of different antifungal drugs (Hof, 2006). In particular knowledge on *F. musae* sensitivity to azoles is limited to few strains from clinical samples (Al-Hatmi et al., 2016a, 2018; Batista et al., 2020; Hirata et al., 2001; Hof, 2006; Lamb et al., 1999; Molnár et al., 2015; O'Donnell et al., 2007; Pasquali et al., 2020; Shi et al., 2017; Tortorano et al., 2014; Triest et al., 2015) and no comparative analysis of strains obtained from agricultural and clinical settings is available. To have a better understanding on the potential treatments useful against *F. musae*, the aim of this work was to assess the level of susceptibility to 13 antifungal drugs (five from clinical settings and 8 from agricultural settings) of 19 *F. musae* strains isolated from patients and infected bananas. Moreover, we aimed to evaluate whether different sources of the strains could determine differences in antifungal susceptibility. Our work identifies the most effective antifungal compounds for *F. musae* population and suggests that *F. musae* has a lower sensitivity to azoles compared to *F. verticillioides*.

6.3 Materials and Methods

6.3.1 Strains Collection

A worldwide collection of *F. musae* strains was analysed together with a set of four strains obtained at the University of Milan. Five strains of *F. musae* (NRRL 25059, NRRL 25673, NRRL 28893, NRRL 28895, NRRL 28897) isolated from banana fruits, and four strains of *F. musae* isolated from human patient (NRRL 43601, NRRL 43604, NRRL 43658, NRRL 43682) were obtained from ARS Culture Collection Database (USA), two strains of *F. musae* isolated from human patient, and one strain isolated from banana fruits (respectively IHEM 19881, IHEM 20180 and MUCL 52574) from the Belgian coordinated collections of Microorganisms, and four strains of *F. musae* (ITEM 1121, ITEM 1142, ITEM 1149, ITEM 1250) isolated from banana fruits obtained from the Institute of Science of Food Production, Bari, Italy (Table 6).

*Table 6. Collection of strains of F. musae and F. verticillioides used in this work. The name of each strain, its species, country of origin, host species and tissue type, [references] and GenBank accession numbers for TEF-1α and RPB2 are reported. * The strain was obtained from two culture collections. [a] Sequenced and deposited as part of this work*

COUNTRY	HOST (TISSUE)	REFERENCE	ACCESSION NUMBER TEF-1α	ACCESSION NUMBER RPB2
Dominican Republic	Banana (fruit)	(Kamel et al. 2016)	MW916961	MW916958
Greece	Human (blood)	(Esposto *et al.* 2016)	MW916959	MW916956
Greece	Human (cornea)	(Esposto *et al.* 2016)	MW916960	MW916957
Mexico	Banana (fruit)	(Van Hove *et al.* 2011)	FN552092	FN552114
Mexico	Banana	(Hirata et al. 2001)	AF273314.1	MZ346032
Mexico	Banana	(Hirata et al. 2001)	AF273316.1	MZ346033
Maryland, USA	Human (skin)	(O'Donnell *et al.* 2007)	MZ346030	EF470191
Ohio, USA	Human (nasal sinus)	(O'Donnell *et al.* 2007)	MZ346031	EF470194
Minnesota, USA	Human (contact lens)	(O'Donnell *et al.* 2007)	EF452989	EF470028
Minnesota, USA	Human (cornea)	(O'Donnell *et al.* 2007)	EF453009	EF470048
Guatemala	Banana (fruit)	(Van Hove *et al.* 2011)	FN552091	FN552113
Honduras	Banana (fruit)	(Van Hove *et al.* 2011)	FN552086	FN552108
Brussels, Belgium	Human (sinus biopsy)	(Triest *et al.* 2015)	KJ865533	KM582792
Brest, France	Human (shoulder biopsy)	(Triest *et al.* 2015)	KJ865532	KM582791
Honduras	Banana (fruit)	(Shi *et al.* 2016)	FN552087	FN552109
Panama	Banana (fruit)	(Van Hove *et al.* 2011)	FN552093	FN552115
Equador	Banana (fruit)	(Van Hove *et al.* 2011)	FN552094	FN552116
Panama	Banana (fruit)	(Van Hove *et al.* 2011)	FN552095	FN552117
Canary Islands	Banana (fruit)	(Van Hove *et al.* 2011)	FN552090	FN552112
Italy	Human (blood)	(Esposto *et al.* 2016)	MW915565	MW915564
Kansas, USA	Corn	(Van Hove *et al.* 2011)	FN552074	FN552096

6.3.2 DNA Isolation, PCR and Sequencing

Fusarium isolates were grown on V8 media (200 mL V8 juice Campbell, Camden, NJ, USA); 2 g/L $CaCO_3$ Carlo Erba Reagents S.r.l, Cornaredo, Milano, Italy; 15 g/L agar NeoFroxx GmbH, Einhausen, Germany) where a cellophane membrane was previously placed. After 5 days plates were gently scraped with an inoculation loop and mycelia were collected in plastic tubes, stored at −80 °C and lyophilised the day after. DNA was extracted from lyophilised mycelia following the protocol (200 microL) of the DNeasy Mericon food Kit (Qiagen, Germantown, MD, USA). Lyophilised mycelia (200 mg) were weighted and placed in a 2 mL microcentrifuge tube in presence of 1 mL food lysis buffer (provided by the kit) and 2.5 µL Proteinase K solution (provided by the kit). Samples were briefly vortexed to ensure complete distribution of the material and incubated in a water bath at 60 °C for 30 min while manually vortex-shaking the samples every two minutes. After incubation, samples were cooled at room temperature on ice to enhance inhibitor precipitation. Centrifugation of microcentrifuge tubes was performed for 5 min at 2500× g. The maximum volume of clear supernatant was drawn from each lysis tube without disturbing the precipitate at the bottom of the tube and the supernatant aliquots were combined in one microcentrifuge tube and

mixed by pipetting up and down several times to ensure a homogenous solution. A volume of 700 µL of the clear supernatant pool was transferred to a new microcentrifuge tube already containing 500 µL of chloroform. Tubes were vortexed and centrifuged again for 15 min at 14,000× g. New microcentrifuge tubes were prepared containing 350 µL of Buffer PB (provided by the kit) and an aliquot of 350 µL of the upper aqueous phase from our samples was added. One QIAquick spin column (provided by the kit) was prepared per each strain by placing them in a 2 mL collection tube. Samples were vortexed for a few seconds and then pipetted into the columns. Tubes and columns were centrifuged at 17,900× g for 1 min and the flow-through was discarded. An aliquot of 500 µL Buffer AW2 (provided by the kit) was added, and the centrifugation step was repeated. A second centrifuge step was performed with an empty QIAquick spin column to dry the membrane. The columns were then transferred to new microcentrifuge tubes and 150 µL of Buffer EB (provided by the kit) was pipetted directly onto the QIAquick membrane, samples were incubated at room temperature for 1 min and centrifuged at 17,900× g for 1 min to elute the final extracted DNA. Samples were separated by electrophoresis onto a 1% (w/v) agarose gel, stained with ethidium bromide and photographed under UV light to verify the success of the extraction.

Two regions were amplified directly from the genomic DNA. Fragments of the Translation Elongation Factor 1α (EF) and RNA polymerase second largest subunit (RPB2) were amplified and sequenced using PCR protocols with the following primers: EF1 (5′-ATGGGTAAGGARGACA-3′) and EF2 (5′-GGARGTACCAGTSATCATG -3′) (Peeran et al., 2019); 5F2 (5′-GGGGWGAYCAGAAGAAGGC-3′), 7cR (5′-CCCATRGCTTGYTTRCCCAT-3′), 7cF (5′-ATGGGYAARCAAGCYATGGG-3′) and 11aR (5′-GCRTGGATCTTRTCRTCSACC-3′) (Reeb et al., 2004). PCR reaction mixtures (total volume 25 µL) contained 2 µL of fungal genomic DNA template, 5 µL PCR buffer (5x green GoTaq reaction buffer), 0.5 µL deoxynucleoside triphosphate (dNTPs), 0.2 µL of GoTaq G2 DNA polymerase and 0.25 µL of each primer. The condition for thermal cycler consists of an initial denaturation step at 94 °C for 2 min, followed by 35 cycles of denaturation at 94 °C for 20 s, annealing at 61 °C for 30 s and extension at 72 °C for 2 min, then a final extension of 72 °C for 7 min.

The fumonisin gene cluster excision site (ΔFGC) was also investigated by PCR as a determinant for the identification of this species. Fvh55 (59-CGCTGCTGTGTGTGGTAACT-39) and Fvh59 (59-AGCTTGTCAACCCAGCAGAT-39) were used as primers (Van Hove et al., 2008) and the PCR reaction mixture was prepared as described before. The condition for thermal cycler consists of an initial denaturation step at 94 °C for 2 min, followed by 35 cycles of denaturation at 94 °C for 20 s, annealing at 60 °C for 30 s and extension at 72 °C for 2 min, then a final extension of 72 °C for 7 min. An aliquot of 5 µL of amplified products was separated by electrophoresis onto a 1.5% (*w*/*v*) agarose gel, stained with ethidium bromide and photographed under UV light to observe the result of the amplification. DNA was quantified using 1 kb plus NEB ladder by comparing fluorescence intensity of a known amount of ladder as specified by NEB guidelines. Appropriate amount of PCR product was obtained for further purification and Sanger sequencing with each primer was used during previous amplification. Sanger sequencing service was performed by Eurofins Genomics, Vimodrone (Italy).

6.3.3 Phylogenetic Analysis

A consensus sequence was computed from the forward and reverse sequences using Geneious software (Version: 2020.2). Phylogenetic analyses of our collection were conducted on the sequences of two protein-encoding nuclear genes: translation elongation factor 1α and RNA polymerase second largest subunit (RPB2). Sequence of genes were obtained from published articles covering *Fusarium fujikuroi* species complex diversity (Al-Hatmi et al., 2019; Laraba et al., 2020; Moussa et al., 2017; Van Hove et al., 2011). Sequences were aligned using Muscle plugin of Geneious and manually checked and concatenated. A consensus phylogenetic tree of major *Fusarium* species including the *F. verticillioides* and *F. musae* diversity on a total of 733.047 bases was built applying a Bayesian inference using the MrBayes plugin (Version: 2.2.4) in Geneious software (Version: 2020.2). GTR model was selected based on AKAIKE test implemented in Modeltest 3.2. The consensus tree was obtained by 110,000 generations sampling every 200 generation and burn in of 100,000 initial generations.

6.3.4 Antifungal Susceptibility

Nineteen *F. musae* and two *F. verticillioides* strains were tested for in vitro susceptibility to five medical antifungals—itraconazole, voriconazole, posaconazole, isavuconazole and amphotericin B (all Sigma-Aldrich, St. Louis, MO, USA)—and to eight DMIs used for crop protection—prochloraz, tebuconazole, epoxiconazole, difenoconazole, propiconazole, tetraconazole, flusilazole and fenbuconazole (all Sigma- Aldrich). Susceptibility was performed with broth microdilution method according to the Clinical and Laboratory Standards Institute (CLSI) guidelines for filamentous fungi (Reference CLSI M38-A2). All molecules were prepared at final concentrations ranging from 0.03 to 16 mg/L. Broth microdilution assay was performed in RPMI-1640 with glutamine, without bicarbonate (Sigma-Aldrich, St. Louis, MO, USA). Inoculum suspensions were prepared from 2–5-day-old cultures. The conidia suspensions were counted in a haemocytometer chamber and diluted to a final working inoculum of $0.5–5\times10^4$ CFU/mL. Plates were incubated at 28 °C for 48 h. The minimum inhibitory concentration (MIC) value was the concentration of drug yielding no fungal growth at visual reading: no mycelium was visible, and the medium appeared crystal clear by looking through naked eye. Tests were performed in duplicate. Reference strains *Candida parapsilosis* ATCC 22019 and *Candida krusei* ATCC 6258 were used as quality controls.

6.3.5 Statistical Analysis

Statistical analysis was performed using JAPS software v0.10.2 considering the confidence interval of 95% as significant. Bayesian Mann-Whitney T-test sample was used to assess the discriminatory effect of each fungicide on the origin of the strain.

6.4 Results

6.4.1 Strain Classification

Four strains isolated in our laboratories from banana fruits and human patients (respectively F31 and IUM 11-0507, IUM 11-0508, IUM 09-1037, Table 6*) identified at first as *Fusarium musae* were further investigated in this work. Their initial identification was verified using an EF-1 and RPB2 sequencing approach. Their phylogenetic

position was observed in relation to other *F. musae* strains and other *Fusarium* species (Figure 5) confirming position of all the *F. musae* strains as a clade close to *F. verticillioides*. The use of fumonisin excision primers confirmed the species attribution of the *F. musae* strains investigated in this work and to confirm reclassification of IUM 09-1037 as *F. verticillioides* that grouped with *F. verticillioides* in the phylogenetic tree.

Figure 5 Phylogenetic tree position F. musae strains on a Fusarium tree based on EF1 and RPB2 sequence diversity. Bayesian posterior probability tree obtained with mr.Bayes plugin in the Geneious software. Branch labels are shown as a measure in support of the nodes

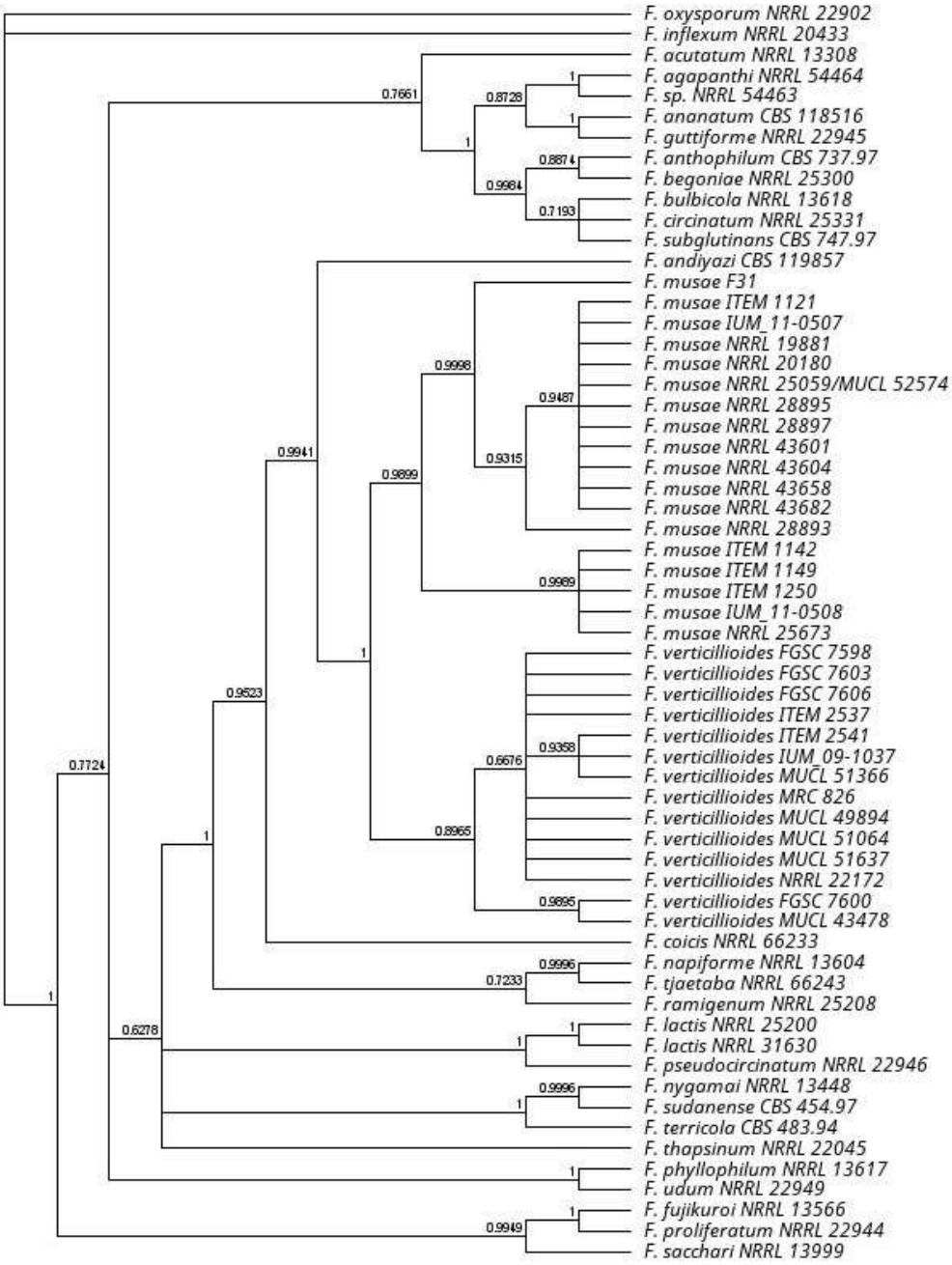

6.4.2 Antifungal Susceptibility

A total of 21 *Fusarium* isolates, namely 19 *F. musae* (8 of human origin and 11 of vegetable origin), two *F. verticillioides* (one of human origin and one of plant origin) were tested for in vitro antifungal susceptibility. All isolates had good growth capacity at 28 °C, while we observed for F. musae a slow growth at 37 °C. For this reason, we chose an incubation at 28 °C for 48 h for all strains tested. The distribution of MIC

values and the geometric mean of the MICs (G-MICs) for the antifungals tested are shown in Table 7.

Table 7. In vitro susceptibility to antifungal drugs of the 21 Fusarium isolates determined by broth microdilution according to the Clinical and Laboratory Standards Institute (CLSI) methodology. a G-MIC, geometric mean MIC. b

MIC50: MIC at which 50% of isolates are inhibited. c MIC90: MIC at which 90% of isolates are inhibited. C= clinical origin. V= vegetable origin.

Fusarium **(no. of Tested Isolates)**	**Antifungal**	**Isolates Origin**	**No. of Isolates with MIC (mg/L) of:**											**[a] G-MIC**	**[b] MIC_{50}**	**[c] MIC_{90}**
			0.03	0.06	0.12	0.25	0.5	1	2	4	8	16	>16			
F. musae (19)	Isavuconazole	total						2	10	7				2.4	2	4
		C (8)						2	4	2				2	2	4
		V (11)							6	5				2.74	2	4
	Itraconazole	total										5	14	16	>16	>16
		C (8)											8	16	>16	>16
		V (11)										5	6	16	>16	>16
	Posaconazole	total				3	11	5						0.54	0.5	1
		C (8)					4	4						0.71	0.5	1
		V (11)				3	7	1						0.44	0.5	1
	Voriconazole	total						14	5					1.2	1	2
		C (8)						6	2					1.19	1	2
		V (11)						8	3					1.21	1	2
	Amphotericin B	total						1	18					1.93	2	2
		C (8)						1	7					1.83	2	2
		V (11)							11					2	2	2
	Difenoconazole	total							5	12	2			3.58	4	4
		C (8)							2	4	2			4	4	8
		V (11)							3	8				3.31	4	4
	Epoxiconazole	total						16	3					1.11	1	2
		C (8)						5	3					1.29	1	2
		V (11)						11						1	1	1
	Fenbuconazole	total										3	16	>16	>16	>16
		C (8)											8	>16	>16	>16
		V (11)										3	8	>16	>16	>16
	Flusilazole	total						7	12					1.55	2	2
		C (8)						1	7					1.83	2	2
		V (11)						6	5					1.37	1	2
	Propiconazole	total							3	16				3.58	4	4
		C (8)							1	7				3.67	4	4
		V (11)							2	9				3.53	4	4
	Tebuconazole	total					5	13	1					0.83	1	1
		C (8)						7	1					1.09	1	1
		V (11)					5	6						0.73	1	1
	Tetraconazole	total											19	>16	>16	>16
		C (8)											8	>16	>16	>16
		V (11)											11	>16	>16	>16
	Prochloraz	total			15	4								0.14	0.12	0.25
		C (8)			5	3								0.16	0.12	0.25
		V (11)			10	1								0.13	0.12	0.12
F. verticillioides (2)	Isavuconazole	total						1	1					1.5	1	2
		C (1)							1							
		V (1)						1								
	Itraconazole	total					1						1	8.25	0.5	>16
		C (1)											1			
		V (1)					1									
	Posaconazole	total					2							0.5	0.5	0.5
		C (1)					1									
		V (1)					1									
	Voriconazole	total						2						1	1	1
		C (1)						1								
		V (1)						1								
	Amphotericin B	total						1	1					1.5	1	2
		C (1)						1								
		V (1)							1							
	Difenoconazole	total							2					2	2	2

High MICs of itraconazole were observed (G-MIC = 16 mg/L) for both human and plant origin strains of *F. musae*. The MICs of the other three medical azoles showed lower

values: the G-MICs ranged from 0.54 mg/L of posaconazole to 1.2 mg/L of voriconazole and to 2.4 mg/L of isavuconazole. No statistically significant differences between the isolates of different origins were observed. The polyene amphotericin B showed a G-MIC of 1.93 mg/L on *F. musae*.

Among the antifungals of agricultural use, the highest activity was shown by the imidazole prochloraz and the triazole tebuconazole (G-MIC of 0.14 mg/L and 0.83 mg/L respectively). The MICs of tebuconazole against the plant origin strains ranged between 0.5 and 1 mg/L (G-MICs = 0.73), slightly lower than those of clinical strains (range 1–2 mg/L). An identical G-MIC (3.58 mg/L) was observed for difenoconazole and propiconazole with a slightly wider range for difenoconazole (2–8 mg/L) than for propiconazole (2–4 mg/L). Tetraconazole and fenbuconazole showed G-MICs > 16 mg/L for all the 19 *F. musae* strains.

The G-MIC of flusilazole for the 19 *F. musae* was 1.55 mg/L, ranging from 1 to 2 mg/L for both human and plant origin isolates. The same range of MIC values was observed for epoxiconazole (G-MIC = 1.11 mg/L), with a MIC value of 1 mg/L for all the 11 isolates of plant origin.

The antifungal susceptibility profile of *F. musae* isolates was different from that of *F. verticillioides* isolates with higher MIC values of epoxiconazole, propiconazole, flusilazole and fenbuconazole (1.11 vs. 0.31, 3.58 vs. 0.31, 1.55 vs. 0.37, >16 vs. 1 mg/L, respectively).

Different MICs of itraconazole were observed between the clinical strain (MIC = 16 mg/L) and the plant strain (MIC = 0.5 mg/L) of *F. verticillioides*. On the contrary, similar MICs of the other medical triazoles were observed between the strains of different origin for isavuconazole, voriconazole and posaconazole. Prochloraz is confirmed to be the agricultural fungicide with lower MIC values, also for *F. verticillioides*.

Origin of the isolate (human or banana) showed a significant difference only for difenoconazole (BF10 3.988) and tebuconazole (BF10 1.911) susceptibility. In both cases strains from banana had higher susceptibility compared to the human strains.

6.5 Discussion

Fungicide susceptibility varies widely in the genus *Fusarium*. Our work is a step towards understanding the patterns of variability within the genus focusing on an

emerging inter-kingdom species such as *F. musae*. These results can be used to infer causes of fungicide resistance relevant to inter-kingdom epidemiology, as well as to provide information to medical practitioners as to which fungicides or medicines are likely to be effective in a given clinical setting. To obtain epidemiological information useful for the clinical practice, fungicide sensitivity studies are coupled to accurate identification of the strains.

In Europe, *F. fujikuroi* species complex, to which *F. verticillioides* and *F. musae* belong, is the predominant cause of human deep infections, and in Italy *F. verticillioides* is the most prevalent species (Tortorano et al., 2014, 2008). This makes its investigation even more significant. The re- identification of one of the strains used in the study, by sequencing the RPB2 gene in addition to the EF, highlights the importance of performing a multilocus molecular identification especially for those species that are morphologically hard to distinguish, such as *F. verticillioides* and *F. musae* (O'Donnell et al., 2010).

Azoles are a widely used category of fungicides employed against human fusariosis as well as plant fungal infections. In this study we focused on the antifungal activity of 13 azoles, chosen among the most used azoles in both clinical and agricultural field, against *F. musae* and *F. verticillioides* isolated from human and plant samples. The results of our work are comparable with data already present in literature (Al-Hatmi et al., 2019, 2018; Espinel-Ingroff et al., 2016; Herkert et al., 2019; O'Donnell et al., 2010). Only MIC values obtained by Triest *et al.* seem to be higher, probably because of a different incubation timing (Triest et al., 2015). As already demonstrated the spectrum and the power of each azole derivative is unique and different from the others, this implies that different drugs have different safety profiles and also antifungal activity as we could observe from the MIC values we obtained. In particular, we observed that voriconazole, isavuconazole and mostly posaconazole may be effective against these two *Fusarium* species studied. On the contrary, itraconazole showed no effect against *F. musae* and *F. verticillioides*, confirming previous studies (Al-Hatmi et al., 2016b; Tortorano et al., 2008; Triest et al., 2015). These data may contribute to improving the decision on the selection of the most appropriate molecule to be used in a clinical setting where a given antifungal might encounter a resistant infecting strain. Our results

contribute to improving the knowledge on the risk of potential resistance occurrence within the *Fusarium* genus.

Little is known about the activity of azoles used in crops, especially against *Fusarium fujikuroi* species complex. According to the European Union for crop protection ("Status - Eurostat," 2021) the imidazole prochloraz is one of the most used in the fields and it appears to be the most effective also in our in vitro study against both *F. verticillioides* and *F. musae*. Tetraconazole and fenbuconazole, instead, showed no in vitro activity against the two species. A poor activity of tetraconazole and fenbuconazole had also been observed in experiments conducted on seeds damaged by fusariosis, on which treatment with the two drugs proved ineffective (Jones, 1999). Among the triazoles for agricultural use, on the other hand, tebuconazole has definitely shown the best in vitro activity against both *F. musae* and *F. verticillioides*.

If we compare sensitivity of the two sister species *F. verticillioides* and *F. musae*, we identified some differences in susceptibility to the azoles. In particular, epoxiconazole, propiconazole, flusilazole and fenbuconazole seemed to need higher concentrations to inhibit the growth of *F. musae* than those needed for its sister species, causing suspicion of some kind of resistance—intrinsic or induced by exposure to these antifungals. Given the small number of strains of *F. verticillioides* these results should suggest future work with a large and diverse population of *F. verticillioides*. Nonetheless our data are largely consistent with previous literature dealing with azole sensitivity in *F. verticillioides*, showing low *F. verticillioides* MIC values have been observed for posaconazole (range 0.25–0.5 mg/L) and voriconazole (0.5–2 mg/L) (Tortorano et al., 2014). One exception is the data obtained by Triest et al. on *F. verticillioides* showing higher MIC for some azoles (Triest et al., 2015). These differences could be partly attributable to Triest's use of the EUCAST method. On the other hand, previous studies conducted with the EUCAST method were consistent with our observation (Tortorano et al., 2014).

Since azoles are the main treatment for both human and agricultural fungal diseases, a major concern could be the predictable emergence of cross-resistance to clinical isolates, driven by the massive use of azole fungicides in agriculture, which have the same mechanism of action as that of those used in humans, as already known for *Aspergillus fumigatus* (Chowdhary et al., 2014; Snelders et al., 2012). As in *A.*

fumigatus and in other fungi, mutations or overexpression of CYP51 gene, encoding 14α-demethylase, is involved in azole resistance, similar mechanisms might be responsible for inducing azole resistance also in *Fusarium* spp..

Pujol I. et al., who compared different *Fusarium* spp. strains of clinical and environmental origin against clinical antifungal drugs, observed a similar activity against both groups of fungi (Pujol et al., 1997). Moreover, in the present study, analyzing the origin of the isolate, human or vegetable (banana), mostly no significant differences were found. The only difference was observed for two agricultural triazoles, difenoconazole and tebuconazole, for which the human *F. musae* isolates showed a reduced susceptibility. In most fungi, clinical isolates are thought to be more resistant to antifungals than environmental isolates, probably due to antifungal exposure during therapy in chronically ill patients (Al-Hatmi et al., 2014). Further studies on larger population are needed to verify the consistency of this finding. Understanding the evolutionary pressure of environmental fungicides also on clinical isolates may allow to better decipher the mechanisms leading to fungicide adaptation (Hartmann et al., 2020). This can lead to set the most appropriate clinical and agricultural fungicide treatments under the “One health” framework applied to *Fusarium* pathogen control strategies (Sáenz et al., 2020).

6.6 Conclusions

Our work defines for the first time a susceptibility level of *F. musae* strains obtained from different hosts and different continents for 12 azoles and amphothericin B, providing the basis for monitoring evolution of the pathogen sensitivity to fungicides both in clinical and agricultural settings.

Chapter 7

Fusarium musae infection in animal and plant hosts confirms its cross-kingdom pathogenicity

The chapter was adapted from:

Manuscript submitted to JoF

Tava V., Reséndiz Sharpe A., Vanhoffelen E., Saracchi M., Cortesi P., Lagrou K., Vande Velde G., Pasquali M. *Fusarium musae* infection in animal and plant hosts confirms its cross-kingdom pathogenicity

Chapter 7

Fusarium musae infection in animal and plant hosts confirms its cross-kingdom pathogenicity

7.1 Abstract

Fusarium musae is a pathogen belonging to the *Fusarium fujikuroi* species complex, isolated from both banana fruits and immunocompromised patients, therefore hypothesized to be a cross-kingdom pathogen. We aimed to characterize *F. musae* infection in plant and animal hosts to prove its cross-kingdom pathogenicity. Therefore, we developed two infection models, one in banana and one in *Galleria mellonella* larvae as a human proxy, for the investigation of cross-kingdom pathogenicity of *F. musae*, along with accurate disease indexes effective to differentiate infection degrees in animal and plant hosts. We tested a worldwide collection of *F. musae* strains isolated both from banana fruit or human patients, and we provided the first experimental proof of the ability of all strains of *F. musae* to cause significant disease in banana fruits as well as in *Galleria mellonella*. Thereby we confirmed that *F. musae* can be considered a cross-kingdom pathogen. We thus provide a solid basis and toolbox for the investigation of the host-pathogen interactions of *F. musae* with its hosts.

7.2 Introduction

Fusarium musae, a pathogenic species within the *Fusarium fujikuroi* species complex, was formally recognized in 2011 as a species closely related to but distinct from *F. verticillioides* (Van Hove et al., 2011). It was first identified as a plant pathogen and recognized as one of the causative agent of crown rot in banana fruits. Cases of infection with *F. musae* have been reported in banana fruits in Hungary (Molnár et al., 2015), Neotropical countries (Hirata et al., 2001; Kamel et al., 2016; Shi et al., 2017) and the Philippines (Van Hove et al., 2011). Later, it was described also as a pathogen in human patients, where it causes keratitis and skin infections as well as systemic

infections in immunocompromised patients (Esposto et al., 2016; Triest, 2016; Triest et al., 2016; Triest and Hendrickx, 2016). Cases of infection with *F. musae* have been reported in Italy, Greece (Esposto et al., 2016), France, Belgium (Triest et al., 2016) and the USA (O'Donnell et al., 2007). Isolation of *F. musae* from different hosts raised suspicion that *F. musae* could be a potential cross-kingdom pathogen, further strengthened by its ability to cause infection in both bananas and humans. Plant fungal pathogens are already known as emerging danger to both food production and ecosystem balance by causing food losses, impacting agricultural productivity, and contaminating food with harmful mycotoxins. But recently, it has become evident that some agricultural fungi may evolve the ability to adapt to infect human hosts, posing direct infection risks and further endangering human health. It is yet unclear if and how *F. musae* transfers from one host to the other: Triest and Hendrickx suggested a role for bananas as carriers of spores leading to diseases in immunocompromised patients in banana consuming countries (Triest and Hendrickx, 2016).

So far, there is no experimental proof of the ability of *F. musae* plant strains to invade an animal (human) host and vice versa, and it has not been shown that *F. musae* possesses the essential virulence factors to cause infection in both a plant and animal host. It is nevertheless essential to prove infection in relevant hosts representing the different kingdoms to confirm the cross-kingdom pathogenicity of a species, thereby complying with Koch's postulates (Bhunjun et al., 2021; Grimes, 2006). Indeed, exploring literature about fungal cross-kingdom pathogens, the classification of a pathogen as cross-kingdom is mainly based on isolation from different hosts and taxonomic criteria that are constantly evolving and need frequent checks and updates. There is a lack of experimentally verified proof of the infection in multiple hosts, only a few papers present experimental evidence of the infection: often populations of strains isolated from different hosts are tested in only one of the hosts (Kim et al., 2020; Van Baarlen et al., 2007). Experimentally demonstrating the ability of a fungal species to cause infection in the host is a crucial step in the characterization and classification of the species as a pathogen.

On the other hand, by setting up relevant experimental model systems, one can investigate the virulence factors that make up a species' ability to infect hosts belonging to different kingdoms. Moreover, applications can be envisaged towards developing

strategies that may prevent infection risks from contaminated food and agricultural losses.

With this work, we provide the first experimental evidence that a collection of *F. musae* strains with different host origins can infect both animals and plants. We aimed to evaluate and compare *F. musae* pathogenicity across kingdoms, demonstrating that strains isolated from different hosts can invade both kingdoms. To reach this goal, we established two infection models: we chose banana fruit as the plant host since it is the only known plant host for *F. musae*, while as the animal host, we used *Galleria mellonella* larvae, a host model for animal infection and a proxy for human infection (Fallon et al., 2012; Pereira et al., 2018; Singkum et al., 2019; Vanhoffelen et al., 2024, 2023).

7.3 Materials and Methods

7.3.1 Fungal strains

For this work we used a collection of nineteen strains of Fusarium musae which included isolates from different organisms and different countries (Table 8).

Table 8 F. musae collection. For each strain we indicated the country, the host from which it was isolated and reference to first description. (a) Five strains isolated from banana and (b) four strains iso-lated from human patients were obtained from the ARS Culture Collection database. (c) Two hu-man strains and (d) one banana strain were obtained from the Belgian coordinated collections of Microorganisms collection. (e) Four banana strains were obtained from the Institute of Food Production Sciences in Bari, Italy. (f) Three strains belonged to the University of Milan.

STRAIN	COUNTRY	HOST (TISSUE)	REFERENCE
F31[f] (DSMZ 112727)	Dominican Republic	Banana (fruit)	(Kamel et al., 2016)
IUM 11-0507[f]	Greece	Human (blood)	(Esposto *et al.* 2016)
IUM 11-0508[f]	Greece	Human (cornea)	(Esposto *et al.* 2016)
NRRL 28893[a]	Mexico	Banana (fruit)	(Van Hove *et al.* 2011)
NRRL 28895[a]	Mexico	Banana	(Hirata et al. 2001)
NRRL 28897[a]	Mexico	Banana	(Hirata et al. 2001)
NRRL 43601[b]	Maryland, USA	Human (skin)	(O'Donnell *et al.* 2007)
NRRL 43604[b]	Ohio, USA	Human (nasal sinus)	(O'Donnell *et al.* 2007)
NRRL 43658[b]	Minnesota, USA	Human (contact lens)	(O'Donnell *et al.* 2007)
NRRL 43682[b]	Minnesota, USA	Human (cornea)	(O'Donnell *et al.* 2007)
NRRL 25673[a] (MUCL 53204)	Guatemala	Banana (fruit)	(Van Hove *et al.* 2011)
NRRL 25059[a]	Honduras	Banana (fruit)	(Van Hove *et al.* 2011)

(CBS 624.87, MUCL 52574)			
IHEM 20180[e]	Brussels, Belgium	Human (sinus biopsy)	(Shi *et al.* 2016)
IHEM 19881[e]	Brest, France	Human (shoulder biopsy)	(Triest *et al.* 2015)
ITEM 1121[e] (MUCL 52573)	Panama	Banana (fruit)	(Triest *et al.* 2015)
ITEM 1142[e] (MUCL 53196)	Ecuador	Banana (fruit)	(Van Hove *et al.* 2011)
ITEM 1149[e] (MUCL 52201)	Panama	Banana (fruit)	(Van Hove *et al.* 2011)
ITEM 1250[e] (MUCL 53203)	Canary Islands	Banana (fruit)	(Van Hove *et al.* 2011)
MUCL 51371[d]	Philippines	Banana (fruit)	(Van Hove *et al.* 2011)

7.3.2 Temperature assay in vitro

To determine the potential ability of *F. musae* strains to grow at different temperatures, we incubated all strains on Petri dishes containing V8 media (200 ml/L V8 juice Campbell, UK; 2 g/L $CaCO_3$ Carlo Erba Reagents S.r.l, Cornaredo, MI, Italy; 15 g/L agar NeoFroxx GmbH, Einhausen, Germany) at 24°C and 37°C for five days. Growing rate was assessed by measuring the diameter of the colony with a ruler on the reverse of the plate, for each colony we calculated the average value of two measurements at 90° angles to each other. We considered the average value of tree replicates.

7.3.3 Banana fruit infection

For the infection in banana fruits we considered 20 infection sites for each strain: 4 banana fruits each infected with 5 sterile toothpicks as previously described (Moretti et al., 2004). Infection was performed with the entire collection of nineteen *F. musae* strains. Control groups with sterile water and *Fusarium oxysporu*m *f.sp. lycopersici* were included.

Strains were recovered from storage on V8 media plates by inoculating few pieces of mycelium into CMC liquid media (15 g/L carboxymethylcellulose sodium (CMC) Sigma-Aldrich; 1 g/L NH_4NO_3 Carlo Erba Reagents S.r.l, Cornaredo, MI, Italy; 1 g/L KH_2PO_4 Sigma-Aldrich; 0,5 g/L $MgSO_4$-$7H_2O$ Sigma-Aldrich; 1 g/L Yeast Extract Thermo Fisher Scientific Inc. (NYSE: TMO)) and incubating at 25°C in the dark while stirring at 150 rpm. After 5 days, spores were harvested by filtering through one-fold Miracloth and

concentrations were estimated using a Burker counting chamber to obtain the concentration of 10^5 spores/ml for infection. Fresh conidia were used for every infection. Healthy, organic bananas with similar maturation levels were used on infection day; sterilized by immersion in 0.7% sodium hypochlorite (3 min), washed in deionized sterile water (3 min) and dried under a sterile laminar flow hood. Sterile toothpicks were immersed for 2 minutes in conidia solution and skewered in bananas for infection. Five toothpicks were evenly positioned per fruit, deep enough to pierce the peel and reach the pulp surface. Subsequently, fruits were covered in plastic bags and incubated at 20°C in the dark for 10 days. After 10 days, levels of infection were estimated by measuring the diameter of the spots grown on the banana fruits as described in (Figure 6).

Figure 6 Scale of browning in banana fruits. Each spot was awarded with a number from 0 to 4 based on halo, browning and mycelium formation in order to assess the level of disease caused by each strain on bananas.

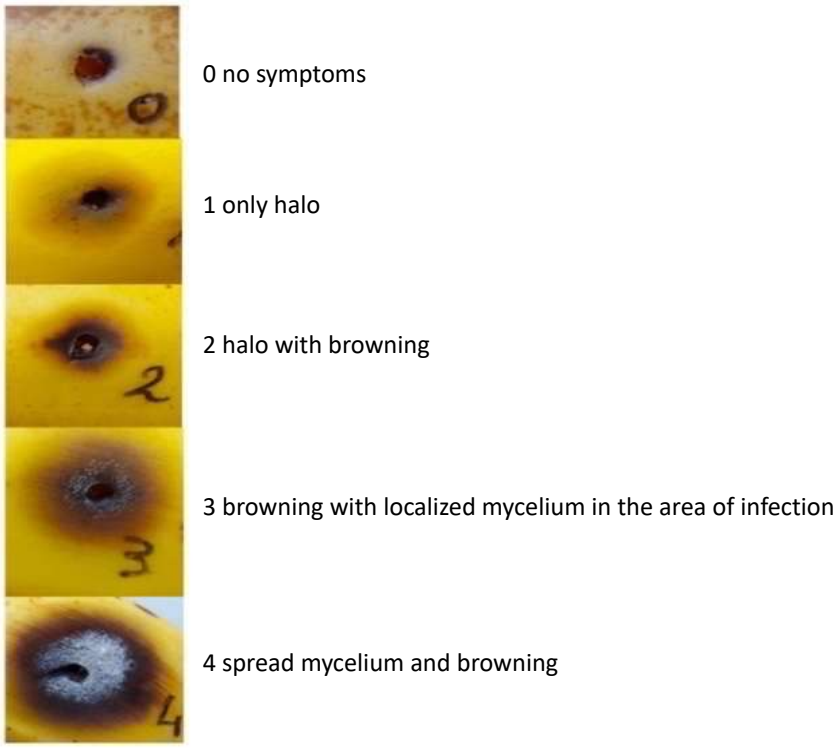

Infections were performed in three independent experimental repeats. In two of the replicates, all five toothpicks positioned per fruit were soaked with conidia from the same strain or water. In the third replicate, each of the five infection points on each fruit

received a different treatment (either conidia suspension or water) to account for any effect the individual fruits might have on infection severity.

We assessed infection in banana fruits by formulating a disease severity index that best represent the disease considering the diameter of the halos as well as browning in each infection point. The index was calculated as follows:

$$disease\ severity\ index = \frac{\left[(S)^2 + \frac{D}{cm}\right]}{2}$$

S = based on the scale of browning; D = diameter of the spot (cm).

7.3.4 Galleria mellonella larvae infection model

For infection in *Galleria mellonella,* we bought specimens of *G. mellonella* at the larval final stage from Biosystems Technology Ltd (Tanners' Yard, 100 High Street, Crediton, Devon, EX17 3LF country). Larvae were maintained at 16°C and infected within 7 days from arrival at our laboratory. Only healthy larvae were selected and used for infection. Fungal strains were recovered from long-term storage at -80°C by inoculating them in Petri dishes containing solid Sabouraud agar (Sigma-Aldrich) and incubating at 24°C for 5 days. On the fifth day, the conidia were harvested directly from the plate by gently flooding the surface with 1 mL of phosphate-buffered saline (PBS) solution (Thermo Fisher Scientific). Concentrations were estimated using a Burker chamber and appropriate dilutions were made to obtain the required concentration of 10^5 conidia/ml for infection. Per strain, groups of 10 larvae were infected with $1x10^5$ conidia/ml in a volume of 10 µl of each inoculum suspension. Infection was performed with a 1 ml insulin syringe into the last left proleg of the larva. Larvae were incubated at the desired temperature (24°C, 28°C or 37°C) in Petri dishes for up to 7 days. PBS and *F. oxysporum* were used as controls.

7.3.5 Temperature assay in Galleria mellonella larvae

Seven representative strains were chosen for temperature assay in *G. mellonella*. We chose as plant strains F31, NRRL 28893, MUCL 51371 and as human strain IUM 11-0508, NRRL 43601, IHEM 20180, NRRL 43658. Infection was performed as described before and larvae were incubated at 24°C, 28°C and 37°C for 7 days.

Twice a day all larvae were observed and each larva was awarded a health score based on the level of activity, pigmentation, cocoon formation and state of life according to the scoring system established by Loh et al. (Table 9) (Loh et al., 2013).

Table 9 Health scoring system for G. mellonella. Representation of the category and scores used to assess the level of disease caused by each strain in G. mellonella (Loh et al., 2013). The disease scoring of each larva at every timepoint is the sum of scores obtained for each category.

CATEGORY	DESCRIPTION	SCORE
Activity	No activity	0
	Minimal activity on stimulation	1
	Active when stimulated	2
	Active without stimulation	3
Cocoon formation	No cocoon	0
	Partial cocoon	0,5
	Full cocoon	1
Melanization	Complete melanization (black)	0
	Dark spots on borwn wax worm	1
	>3 spots on beige wax worm	2
	<3 spots on beige wax worm	3
	No melanization	4
Survival	Dead	0
	Alive	1
	TOTAL	**SUM**

Infections were carried out independently two times. After scoring, dead larvae were removed from the Petri dishes and excluded for the following check points. Dead larvae were placed at -20°C for at least 48h before being disposed of.

7.3.6 Infection assay in Galleria mellonella larvae

Infection in *G. mellonella* was performed with the entire collection of *F. musae* strains using groups of 10 larvae infected with 10 µL of conidia suspension at $1x10^5$ conidia/ml, as described before. Larvae were incubated at 28°C for 7 days and the level of infection was scored daily (Loh et al., 2013).

To be able to compare infection severity in the *G. mellonella* model to the data obtained from the banana model, we transformed the health scores used from evaluating larval health into a measure of disease severity as follows:

$$\textit{Disease severity index} = \frac{[(9 - S) * N]}{10}$$

S (sum)= A + M + C + L; A (activity) = value from 0 to 3; M (melanisation) = value from 0 to 4; C (cocoon formation) = value from 0 to 1; L (survival) = 0 dead, 1 alive.; N= number of dead larvae.

The disease severity index represents the severity of the disease on the final observation day in each infection point, where single infection points are represented by single larvae. Consequently, the disease severity index was assigned to each larva and calculated based on: “S” corresponds to the health score obtained on the 7th day post-infection (Loh et al., 2013), while “N” corresponds to the total number of larvae killed by the strain, and with 10 in the denominator, we account for the standard inclusion of 10 larvae per experimental group.

Specifically, we consider larval death a strong marker of disease severity, thus we gave it greater weight in the formula. The resulting value reflects the overall health status of the larvae at the end of the observation period. If no larval deaths are observed 7 days post-infection, this suggests that the group remains largely healthy and that the infectious strain exhibits low pathogenicity.

7.3.7 Statistical analysis

Statistical analysis of infection of bananas and *G. mellonella* larvae was performed on the disease severity indexes obtained. The values obtained were normalized by dividing them by the average value obtained for strain F31 (used as reference strain) and plotted using the data analysis framework Estimation Stats with H_2O or *F. oxysporum* as shared control under default parameters. Statistical analysis was also performed by data analysis framework Estimation Stats.

For the health score in *G. mellonella*, GraphPad Software (USA, version 8.0.2) was used to plot data obtained from infection at different temperatures, and mixed-effects two-way ANOVA analysis was performed to analyse longitudinal data. Survival analysis was also performed on *G. mellonella* infection using log-rank (Mantel-Cox) test, curve was plotted with the Kaplan-Meier method using SPSS Statistics (version 27).

For quantitative comparison of data from banana and larvae infection, data plot and statistical analysis were performed using Superplotsofdata (Goedhart, 2021).

7.4 Results

7.4.1 F. musae can grow at 24°C as well as at 37°C

To support the hypothesis of *F. musae* as a potential cross-kingdom pathogen, we first tested *in vitro* the ability of *F. musae* strains to survive and spread at 24°C and 37°C. At both temperatures all *F. musae* strains were able to grow, confirming the ability of the species to proliferate at environmental temperature as well as at human body physiological temperature (S1). Strain F31 (banana) and strain IUM 11-0507 (human) showed equal growth rate at both temperatures with no statistically significant difference in diameter of the colony. While all the other strains grew significantly slower at 37°C, observed as a reduction of the diameter of the colonies - compared to the growth at 24°C (table S1). Overall, the host origin of the strains (human or banana) and their geographical origin had no evident effect on the growth of the colonies at the different temperatures. *In vitro* results demonstrated that *F. musae*, regardless of being isolated from plant or human hosts, possesses the ability to grow at 24 as well as 37°C, which supports that *F. musae* is a potential cross-kingdom pathogen.

7.4.2 F. musae is pathogenic to banana fruits

To prove and quantify the capability of *F. musae* to cause infection in a plant pathosystem, we established an infection model with banana fruits.

All nineteen strains presented brown halos surrounding the point of toothpick insertion, with some cases also showing mycelium formation (Figure 7).

Figure 7 Visual representation of the symptoms observed in banana fruits. Formation of brown spots surrounding the point of toothpick insertion in bananas after 10 days of infection with 10^5 conidia/mL of strains F31 (A) and IUM 11-0508 (B). No symptoms are visible in infection with H_2O (C). No symptoms were observed in bananas after 10 days of infection with F. oxysporum (D).

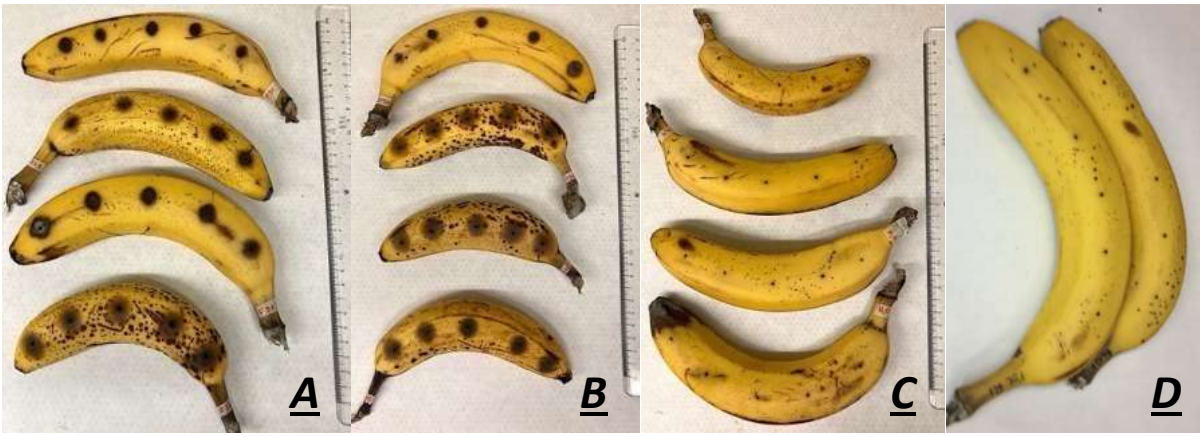

Additionally, disease severity indexes of all strains tested were significantly higher compared to infection with H_2O used as control (Figure 8), demonstrating that they were all able to cause significant disease in banana fruits. Specifically, strain NRRL 19881 (human, France) caused the highest level of infection, followed by NRRL 28897 (banana, Mexico) and NRRL 43604 (human, USA); while the lowest disease was caused by strain IUM 11-0507 (human, Greece) followed by NRRL 20673 (banana, Guatemala).

Figure 8 Disease severity in banana fruits caused by F. musae strains from banana and human isolates. Distribution of disease severity indexes calculated for each infection point in banana fruits. Graphs were made with the data analysis framework Estimation Stats with default parameters, H_2O was used as shared control. N=50 observation points, each mean is depicted as a dot and each 95% confidence interval is indicated by the ends of the vertical error bars. The upper graph represents strains isolated from bananas, the lower graph represents strains isolated from human patients.

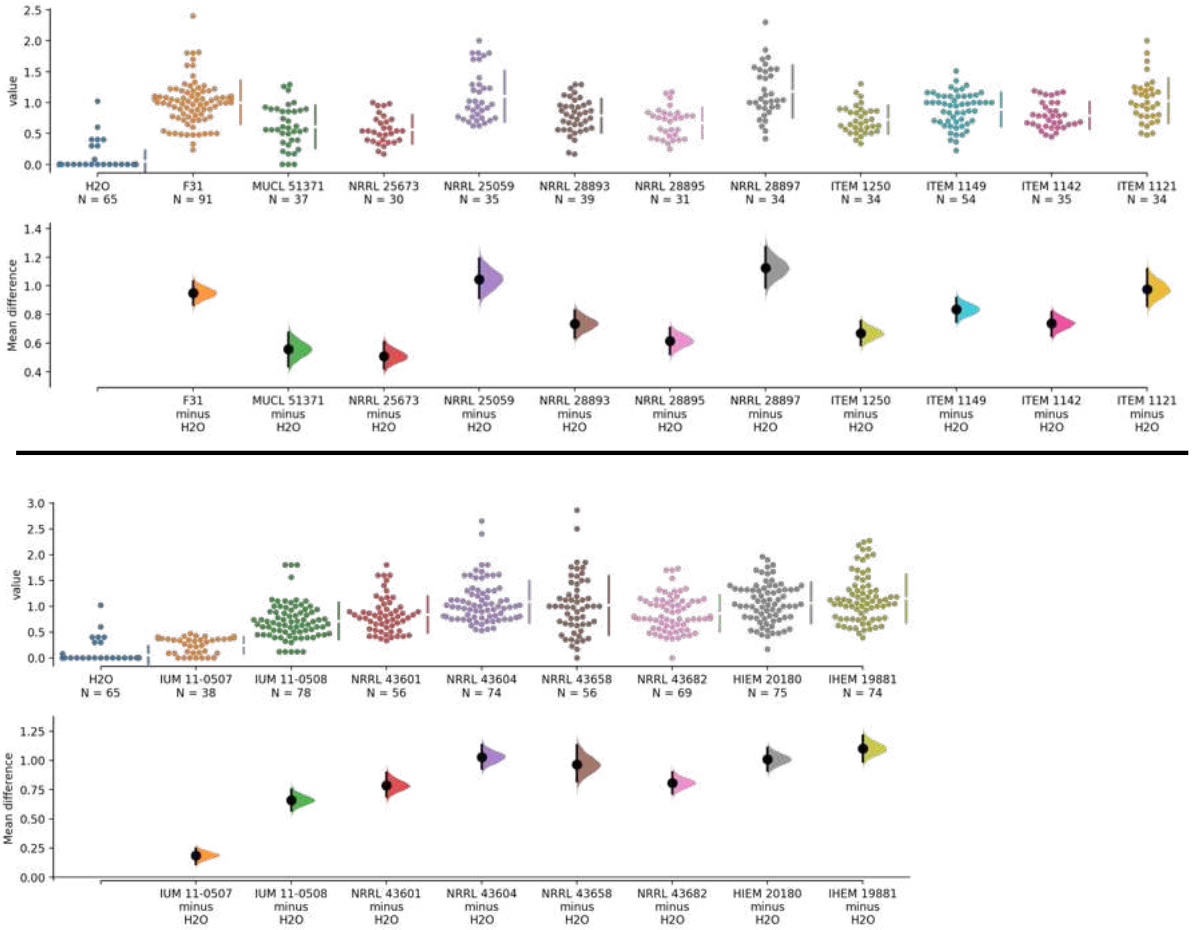

Overall, infection levels were comparable among all strains of our collection, and we did not observe differences in infection severity caused by strains isolated from plants and humans, as all showed similar ability to invade a plant host such as the banana fruit. When comparing the pathogenicity of *F. musae* with the pathogenicity of *F. oxysporum,* as expected, all strains of *F. musae* showed high levels of disease severity compared to *F. oxysporum* that caused no symptoms in fruits with a disease severity score equal to 0 (Figure 9).

Figure 9. Comparison between infection in banana fruits with F. oxysporum and F. musae. Graphs were made with the data analysis framework Estimation Stats with default parameters, Fusarium oxysporum strain f.sp. lycopersici R1 was used as shared control. Each mean difference is depicted as a dot and each 95% confidence interval is indicated by the ends of the vertical error bars. The upper graph represents strains isolated from bananas, the lower graph represents strains isolated from human patients.

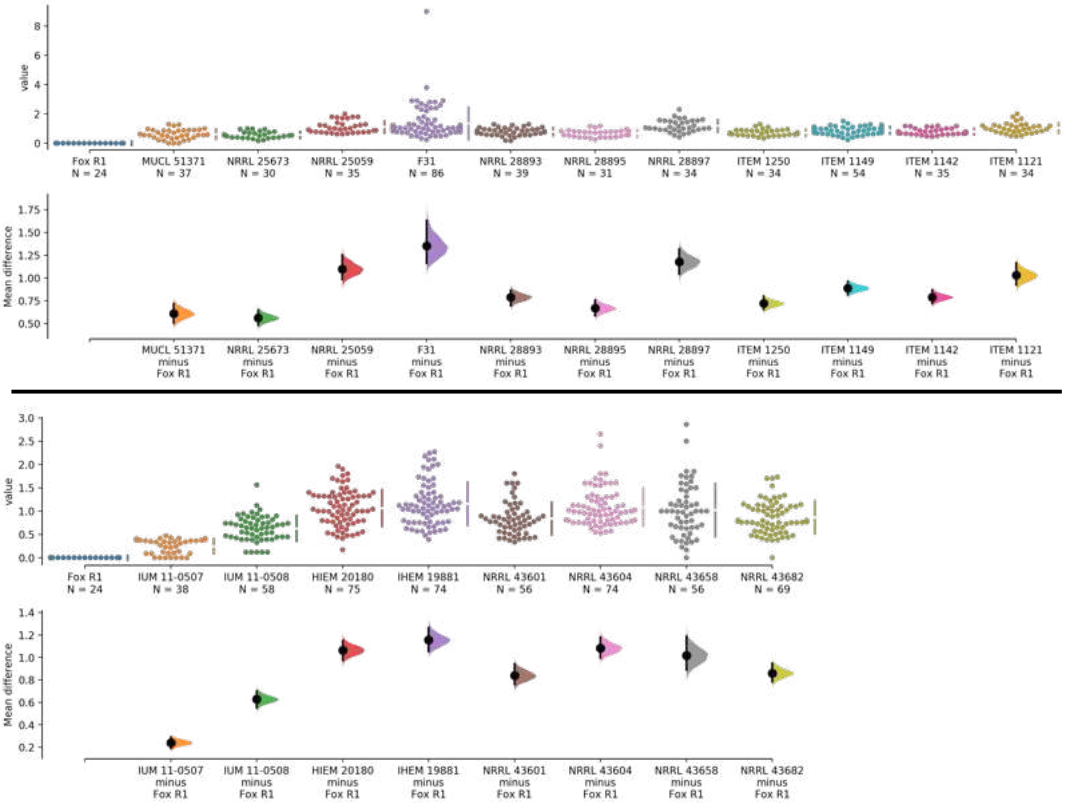

Taken together, we presented the first experimental evidence of *F. musae* pathogenicity in a plant host, establishing a successful model for infection. All tested *F. musae* strains isolated from human patients showed significant infection in a plant pathosystem. In addition, infection levels were comparable between plant and human strains, regardless of geographical origin, suggesting no subgroups are present within the population based on original source.

7.4.3 F. musae causes observable disease in larvae of Galleria mellonella at environmental and mammalian physiological body temperature

To prove the ability of *F. musae* to invade an animal pathosystem, we built an infection model using *Galleria mellonella* larvae and assessed the ability of the species to cause infection at environmental as well as mammalian physiological body temperatures. One of the many advantages of using *G. mellonella* as a host model is that the larvae can tolerate incubation at elevated temperatures (such as 37°C). Furthermore, as we demonstrated, *F. musae* strains grow *in vitro* at both environmental and human body temperatures. Therefore, we tested different incubation temperatures to establish our *F. musae*-*G. mellonella* infection model.

All selected seven strains of *F. musae* were able to cause significant disease in the larvae (Figure 10).

Figure 10. Temperature assay for G. mellonella infection. The virulence of seven representative strains is represented as overall index at 24ºC (A), 28ºC (B) and 37ºC (C). Each colour corresponds to a strain. Infection was done on day 0 and monitored for 7 days, 10 larvae were infected per strain with 1x10^5 conidia/ml and average value for each timepoint are represented. Infection with PBS is used as control.

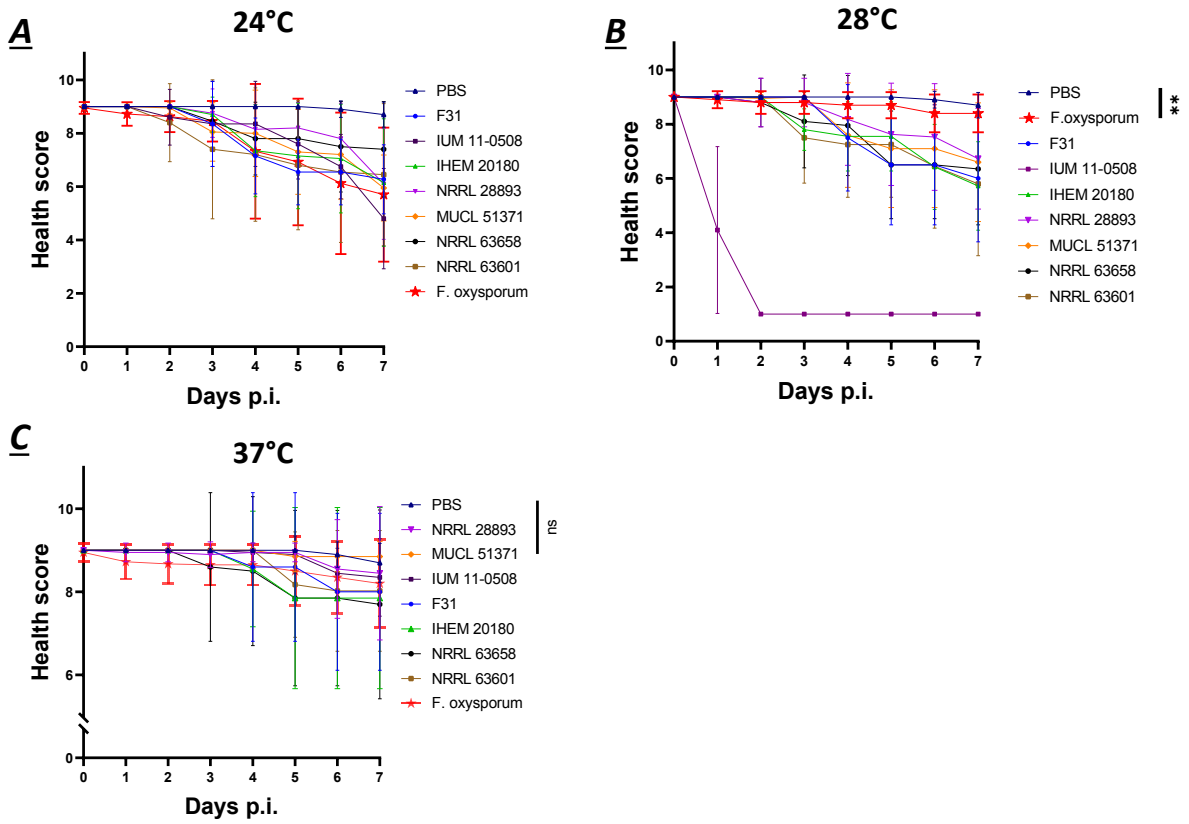

Specifically, strains F31, NRRL 43601, NRRL 43658 and IHEM 20180 showed similar infection levels across the three temperatures. At 24°C and 28°C, we observed the first decline in health scores around 3 days post-infection, decreasing to approximately 7, which reflected reduced larval activity and the appearance of melanized spots. Health continued to decline gradually, reaching values between 5 and 6 by the end of the observation period. At 37°C, larvae began showing symptoms 4 days post-infection, with health scores decreasing to around 7 only by the end of the observation period. Human strain IUM 11-0508 presented significantly different activity at the three temperatures with the highest virulence at 28°C, at this temperature larvae were completely melanized and dead the day after infection. Plant strains MUCL 51371 and

NRRL 28893 showed a significantly reduced activity at 37°C, with no visible symptoms, compared to 24 and 28°C where it exhibited great disease and health score reached values between 5 and 6. Overall, at 37°C the virulence of all strains was reduced compared to lower temperatures, but almost all strains presented visible disease at all temperatures suggesting that they potentially have virulence factors needed for the infection of an animal host at environmental temperature as well as at human body temperature. When compared to infection with *F. oxyxsporum, F. musae* presented significantly higher virulence at 28°C, which we identified as the optimal temperature for infection of *G. mellonella* with *F. musae*. Meanwhile, at 37°C and 24°C the behavior between the two species was comparable.

Altogether, the results provided the first experimental proof of *F. musae* causing infection in an animal pathosystem at different temperatures. All strains responded similarly to the tested temperatures, strains with both plant and human origins cause evident symptoms in *G. mellonella*, making it a relevant model for investigating *F. musae,* which can be extended to other *Fusarium* species as well.

7.4.4 Human and plant strains of F. musae cause comparable levels of infection in G. mellonella larvae

To observe if and how the origin of the strains could be related to a specific disease severity or phenotype in *G. mellonella,* we evaluated the disease severity caused by the entire population of *F. musae* strains.

We observed that all *F. musae* strains were able to cause evident disease, three days after the infection a few melanized spots were already visible on numerous larvae, while larvae injected with PBS remained healthy (Figure 11). Results were consistent and reinforced data obtained at 28°C from temperature assay where only seven representative strains were included.

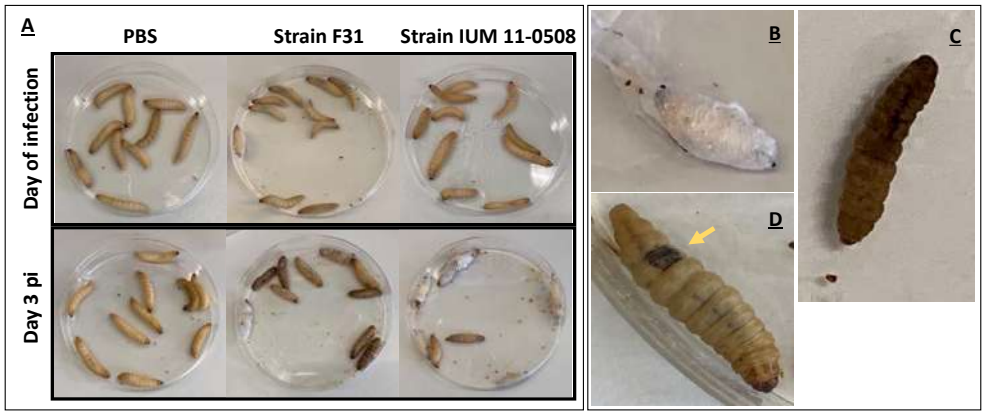

Figure 11. Visual examples of symptoms appearing in larvae of G. mellonella following infection with F. musae strains. Larvae were infected with 1x10^3 conidia/larva, in a volume of 10 µL of strain F31, injection with PBS was used as negative control. Representative pictures of the day of infection and three days after infection are shown here. Symptoms observed during disease progression assessment: cocoon formation (B), complete melanisation and consequent death (C) and appearance of a single dark spot (D).

Of the nineteen *F. musae* strains tested, five (three human IUM 11-0507, NRRL 43601, NRRL 43604 and two plant NRRL 28893, ITEM 1149) showed a level of disease not statistically different from PBS (Figure 12). Strain IUM 11-0508 and NRRL 28895 were the most virulent and they were isolated from human patients and banana fruits, respectively.

At the end of the observation period, in every group infected with *F. musae* strains, we documented the development of significant symptoms that led to larval death across all the groups.

Figure 12. Disease in G. mellonella. Distribution of overall disease severity indexes calculated for each infection point in G. mellonella. Graph was made with the data analysis framework Estimation Stats with default parameters, PBS is used as shared control. N=20 observation points, each mean is depicted as a dot and each 95% confidence interval is indicated by the ends of the vertical error bars. Upper graph represents strains isolated from bananas, lower graph represents strains isolated from human patients

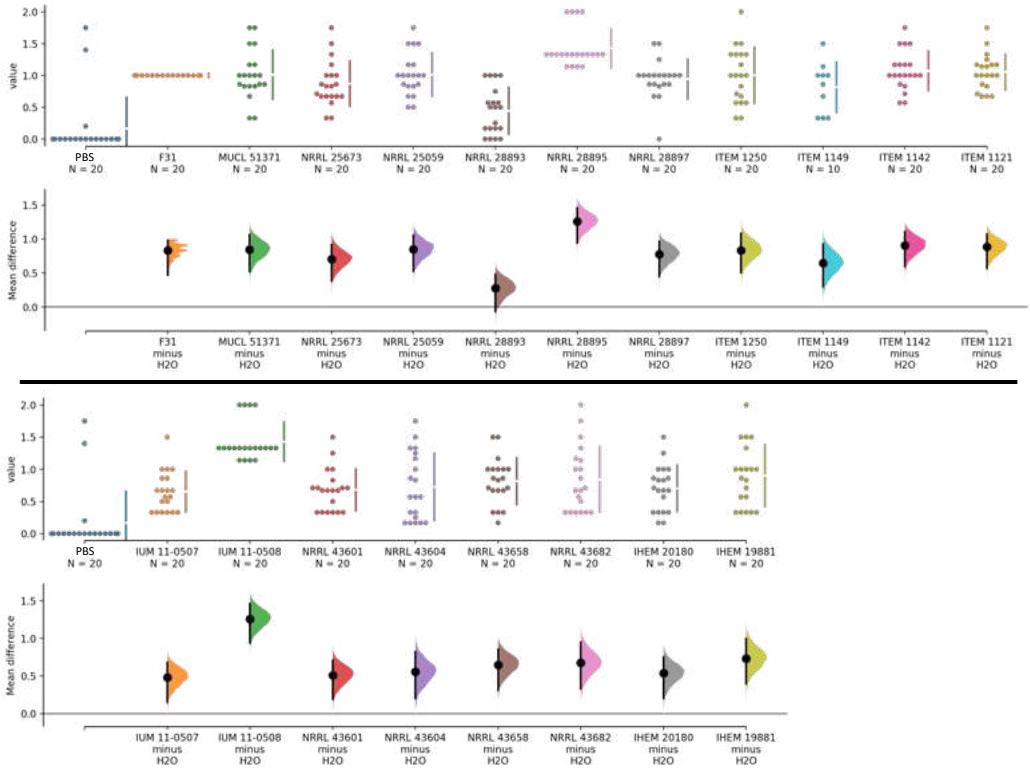

At these conditions, all strains of *F. musae* showed greater levels of disease compared to the *Fusarium oxysporum* strain that presented a disease severity index comparable to sham infected larvae (Figure 13).

Figure 13 Infection in Galleria mellonella larvae with F. musae strains and F. oxysporum. Graph was made with the data analysis framework Estimation Stats with default parameters, Fusarium oxysporum strain f.sp. lycopersici R1 was used as shared control. Each mean difference is depicted as a dot and each 95% confidence interval is indicated by the ends of the vertical error bars. The upper graph represents strains isolated from bananas, the lower graph represents strains isolated from human patients.

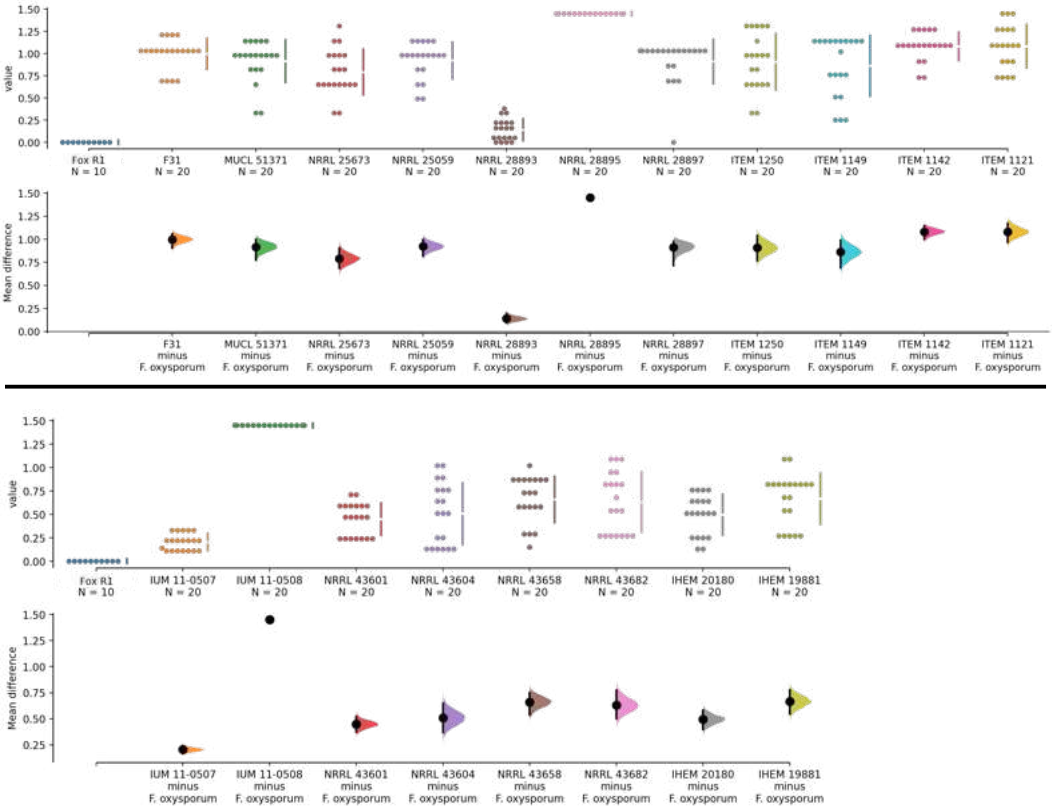

Larvae infected with the *F. oxysporum* strain displayed decreased activity in a few larvae, the appearance of a single melanized spot in two larvae in one of the groups, cocoon formation in half of the larvae and no larvae died within 7 days post-infection. When calculating the disease severity index, infection with *F. oxysporum* resulted in an index equal to zero, comparable to sham-infected larvae. In this case, using larval death as a strong marker of disease severity obscured the representation of other symptoms. However, overall the group remained largely healthy and the infectious strain exhibited low pathogenicity.

Similar to what we found in banana infection, strains with different geographical origins and host isolation sources caused comparable levels of infection in *G. mellonella* suggesting that they all have virulence factors needed for the infection of an animal host.

7.4.5 Survival readouts of G. mellonella larvae infected with human and plant strains of F. musae

Given that survival analysis is still one of the most used readouts in *G. mellonella* studies, and to allow comparison with that body of literature, we decided to include also

survival analysis in the evaluation of our infection model. Survival analysis was done on survival data observed during *G. mellonella* infection assay. *F. musae* infection resulted in significant mortality among the larvae (Figure 14). By 96 hours post-infection, we observed a noticeable increase in the number of dead larvae, which continued to rise over the following days, indicating that both plant and human strains are capable of killing the larvae.

*Figure 14 Survival plot of F. musae infection in G. mellonella larvae. Each colour corresponds to a strain. Infection was done on day 0 and monitored for 7 days, 10 larvae were infected per strain and average value for each timepoint are represented. Infection with PBS is used as negative control. Mean and SD are represented in the graph. The statistics compare all strains against the PBS. ns= nonsignificant; *=p> 0,05; **= p>0,005; ***= p>0,0005; ****= p<0,0001.*

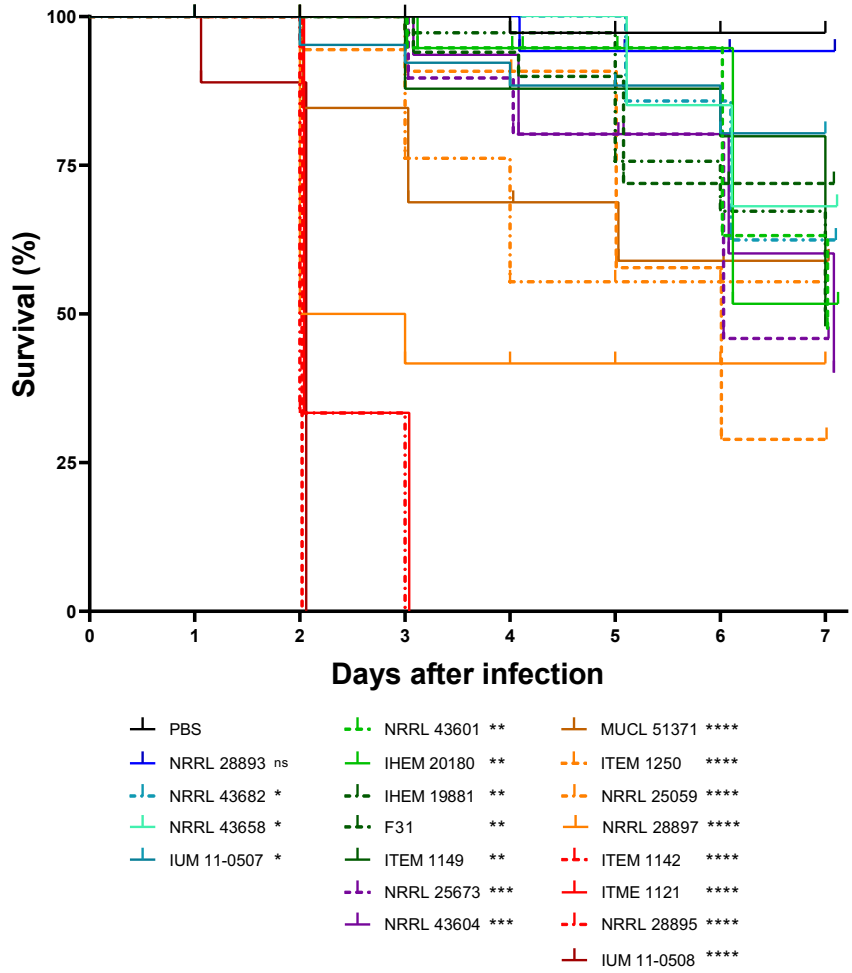

The virulence of the plant strain NRRL 28893 was not statistically different from the negative control. Infection with all other strains was significantly more virulent than sham-infected larvae, with no significant differences observed between strains from different origins. Overall, survival analysis confirmed that infection with *F. musae* led to

a high number of dead larvae, supporting larval death as a strong marker of disease severity.

7.4.6 Quantitative comparison of data from bananas and larvae infection

To study if human and plant strains showed the same behavior in both hosts and if specific trends were observable based on the isolation origin of the strains, we plotted together data obtained from the infection of banana fruits and *G. mellonella* with the entire collection of nineteen strains of *F. musae*. The distribution of data showed that infection severity in banana fruits mostly is comparable with those observed in *G. mellonella* (Fig. 15).

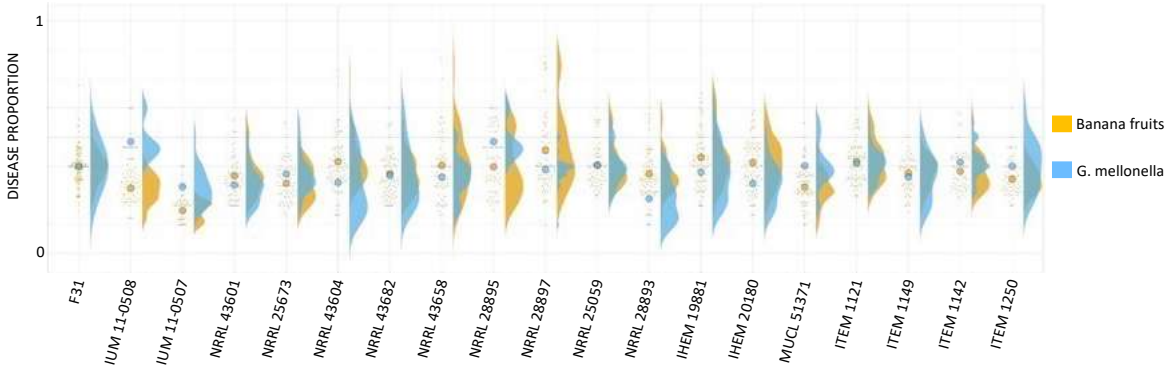

Figure 15 Superplot of virulence of our strains in two hosts. Overall indexes are represented in yellow when related to banana infection and in blue to G. mellonella. Small dots represent single infection points on bananas or single larvae, bigger dots represent mean value. All data are normalized by dividing for average value of F31 of the corresponding replicate.

Only human strain IUM 11-0508 showed a different behavior in the two different hosts as it was highly virulent in *G. mellonella* but less virulent in banana fruits. We did not find any specific interdependence between hosts or geographical origin of the strains and their virulence.

7.5 Discussion

The field of fungal cross-kingdom pathogens is still at its infancy. A conspicuous number of species has been identified as pathogenic to organisms from more than one kingdom (Gauthier and Keller, 2013; Van Baarlen et al., 2007) but, in most of the cases, classification as cross-kingdom pathogen was defined only by isolation from different hosts and identification based on taxonomic criteria that are constantly evolving and

need frequent revision. To qualify as a cross-kingdom pathogen, isolation of a strain from a host needs complementation with evidence of its ability to cause infection in that host. Comprehensive studies including fundamental steps needed for verifying Koch's postulates are limited, especially when pathogens are considered cross-kingdom and the infection must be proven in more than one host.

F. musae is such a putative cross-kingdom pathogen given its appearance as a pathogen in both agricultural and clinical settings. Further supporting its status of a cross-kingdom pathogen are diversity studies that have suggested that strains isolated from humans and bananas are part of a common taxa (Degradi et al., 2022, 2021; Tava et al., 2021; Van Hove et al., 2011). However, the pathogenicity of *F. musae* has not yet been experimentally verified as is required by the Koch's postulates. Therefore, in this work we aimed at proving experimentally if *F. musae* could be confirmed as a cross-kingdom pathogen by validating infection models for the investigation of its pathogenicity in both plant and animal kingdoms.

Our results showed that all *F. musae* strains of our collection, independently of their isolation source, could grow *in vitro* at 25°C as well as at higher temperatures such as 37°C, suggesting that they are all well adapted to occupy different ecological niches and share virulence factors needed to spread at environmental temperature but also at human body temperature.

Indeed, pathogenicity in different host models' environments is an important step to understanding *F. musae* as a cross-kingdom pathogen, therefore our next step was to identify the most suitable hosts for this investigation. Banana fruits are the only known host of *F. musae* in the plant kingdom and the fungus is one of the causative agents of crown rot which is considered one of the most important postharvest diseases of bananas (Kamel et al., 2016). Therefore we established an infection model for the investigation of *F. musae* using banana fruits similar to the model used for the investigation of *F. verticillioides* (Moretti et al., 2004).

For the animal kingdom, we established an infection model with larvae of *Galleria mellonella. G. mellonella* larvae are considered a successful and ethically responsible, relevant host model for the study of host-pathogen interaction. When compared to rodent models of infection, *G. mellonella* larvae offer considerable advantages: they are easily and inexpensively obtained in large numbers, are simple to use, and are

easy to maintain without special laboratory equipment. Additional major benefits are their ability to thrive at 37°C, ease of maintenance and manipulation, few ethical constraints and their size simplifies infection (Capilla et al., 2007; Desalermos et al., 2012; Fuchs et al., 2010; Junqueira and Mylonakis, 2019; Swearengen, 2018). The structural and functional similarities between the innate immune system of mammals and the insect immune response present an additional reason to use it for the study of human fungal pathogens (Kavanagh and Fallon, 2010; Mylonakis, 2005; Slater et al., 2011; Trevijano-Contador and Zaragoza, 2018). Indeed, among the host model alternatives to mice, *Galleria mellonella* larvae present several favourable attributes that make it an optimal model host for the investigation of various fungi, including *Fusarium* spp. as the well-known cross-kingdom pathogens *F. solani* and *F. oxysporum* (Binder et al., 2016; Carvajal et al., 2021; Champion et al., 2018, 2016; Coleman et al., 2011; Fuchs et al., 2010; Gomez-Lopez et al., 2014; Khalaf, 2023; Kryukov et al., 2018; Navarro Velasco et al., 2011; Vanhoffelen et al., 2023). *G. mellonella* larvae were therefore our model of choice to serve as an animal host to experimentally observe for the first time in an animal host *F. musae* strains' pathogenicity.

We hypothesized that temperature would play a crucial role during the infection of *G. mellonella* larvae. Consequently, we tested the ability of our collection of strains to cause infection at environmental as well as mammal physiological body temperatures. We observed that all our strains showed 28°C as the optimum temperature for the infection while at 37°C the growth of our strains was overall reduced. This is consistent with the environments from where they were isolated: bananas usually grow at temperatures ranging from 25°C to 28°C, while the human body temperature is not uniform throughout. While core body temperature is 37°C, extremities and corneal tissues have lower temperatures and are more exposed to injuries, making them more susceptible to fungal infections, including those by *F. musae* (Gauthier and Keller, 2013; Kessel et al., 2010).

We did not only consider the best experimental model for studying *F. musae* pathogenicity, but also the methodology to evaluate the extent of disease caused in host model systems representing plant and animal kingdoms. For evaluating banana fruit infection, we established a semiquantitative scoring system based on halo, browning and mycelium formation. For evaluating disease severity in *G. mellonella*,

survival analysis is the most used readout for the study of virulence of fungi of clinical interest, but it gives a binary result that does not allow us to observe other or milder symptoms of infection. A more sophisticated measure exists, that accounts for not only life or death but several aspects of larval health (Loh et al., 2013). Melanisation is part of *G. mellonella*'s humoral system, it is a complex enzymatic cascade where melanin is synthesized due to wound and pathogen encapsulation and usually it correlates with the death of the wax worm soon after. The degree of melanisation can depend on the infecting pathogen (Champion et al., 2018). Some pathogens cause profound and uniform melanisation, whilst others cause more subtle colour changes which can be difficult to interpret. Higher activity corresponds to a healthier wax worm while cocoon formation and activity of the larvae indicate good health of the individual (Loh et al., 2013; Singkum et al., 2019).

To better represent disease severity in our infection models and enable comparison of the virulence level of single strains, we established disease severity indexes. The banana disease severity index considers the diameter and the level of browning of the spots growing on the fruits. In contrast, the *G. mellonella* severity index considers the importance of larval death as well as other symptoms that can be linked to specific mechanisms involved in pathogen-host interaction. These indexes allowed us to assess and compare the virulence of individual strains in both bananas and *G. mellonella* models, observing possible differences in the interaction with the two different hosts.

Based on this novel experimental model with the disease severity quantification framework we established, we verified that strains of *F. musae* with different hosts and geographical origins could cause a high level of disease and most of the strains did not discriminate between the host tested, as they were able to cause comparable levels of disease in both banana fruits and *G. mellonella* larvae. Interestingly, the human strain IUM 11-0508 showed different infection of the two hosts, causing high disease levels in *G. mellonella* while being a weak pathogen of bananas. Overall, the tested strains of *F. musae* consistently showed comparable infection levels in both our infection models, independently from the isolation source. Nevertheless, subtle variations in symptoms and the degree of infection were observed among *F. musae* strains in both hosts. Our phenotypic tests allowed us to identify strains that have

peculiar behaviour against the different hosts, such as IUM 11-0508, as well as strains that grow with difficulty at the temperature required for human infection, such as NRRL 28897, ITEM 1149. A genomic approach trying to link these characteristics to the genetic background of the strains is warranted as this will guide our comprehension of virulence factors underlying pathogenicity across kingdoms.

7.6 Conclusions

F. musae has been identified as potential cross-kingdom pathogen, as it has been isolated from diseased banana fruits and human patients. This work marks the first experimental demonstration of the ability of this species to actually invade and cause infection in both plant and animal pathosystems. Our findings demonstrate that strains with different isolation source do not exhibit particular trends or behaviors, supporting the hypothesis made on genomic characteristics that strains isolated from humans and bananas are part of a common taxa (Degradi et al., 2022; Tava et al., 2021; Van Hove et al., 2011).

We established two relevant infection models, one involving banana fruits and the other one *G. mellonella* larvae, that resulted successful for the investigation of *Fusarium musae*. These models are valuable tools for further *in vivo* studies on the mechanisms involved in host-pathogen interactions of *F. musae* as well as other relevant *Fusarium* species, as well as antifungal efficacy studies, relevant to the agricultural and clinical context within a One Health concept.

Additionally, considering the similarities in defense systems of plants and humans (Sexton and Howlett, 2006), it is crucial to explore further the strategies evolved by *F. musae* that allow it to invade hosts belonging to different kingdoms, and the underlying genetic determinants of infection.

Supplemental material

*Table S1. In vitro temperature assay of F. musae. The table represents average values of diameters express in cm of the colonies measured five days after incubation at 25°C and 37°C in solid V8 media. Three replicates were done for each strain at each condition. *Two replicates were done for these strains.*

STRAIN	HOST (TISSUE)	24°C	37°C
F31	Banana (fruit)	3,65 ± 0,03	3,4 ± 0,2
IUM 11-0507	Human (blood)	2,6 ± 0,1	2,9 ± 0,14
IUM 11-0508	Human (cornea)	3,4 ± 0,1	2,8 ± 0,5
NRRL 28893	Banana (fruit)	4,52 ± 0,1	1 ± 0,05
NRRL 28895	Banana	4,25 ± 0,7	1,25 ± 0,2
NRRL 28897	Banana	4,57 ± 0,2	0,93 ± 0,02
NRRL 43601	Human (skin)	5,05 ± 0,13	1,7 ± 0,2
NRRL 43604	Human (nasal sinus)	4,6 ± 0,5	1,32 ± 0,7
NRRL 43658	Human (contact lens)	4,85 ± 0,3	1,05 ± 0,4
NRRL 43682	Human (cornea)	4,95 ± 0,3	1,38 ± 0,06
NRRL 25673 (MUCL 53204)	Banana (fruit)	4,6 ± 0,3	1,97 ± 0,6
NRRL 25059 (CBS 624.87, MUCL 52574)	Banana (fruit)	3,86 ± 0,4	1,73 ± 0,2
IHEM 20180	Human (sinus biopsy)	3,97 ± 0,06	1,65 ± 0,3
IHEM 19881	Human (shoulder biopsy)	4,93 ± 0,5	2,12 ± 1,2
ITEM 1121 (MUCL 52573)	Banana (fruit)	4,5 ± 0,7	1,57 ± 0,3
ITEM 1142 (MUCL 53196)	Banana (fruit)	4,6*	1,18 ± 0,2
ITEM 1149 (MUCL 52201)	Banana (fruit)	4,8*	0,87 ± 0,1
ITEM 1250 (MUCL 53203)	Banana (fruit)	4,98 ± 0,6	1,45 ± 0,2
MUCL 51371	Banana (fruit)	3,33 ± 1,3	1,65 ± 1,4

Chapter 8

Bioluminescence imaging, a powerful tool to quantify *F. musae* burden across kingdoms

Chapter 8

Bioluminescence imaging, a powerful tool to quantify *F. musae* burden across kingdoms

8.1 Introduction

As invasive fungal diseases are increasing and the at-risk population continues to expand, it is likely that fungal transkingdom pathogens can become a novel important threat to human and animal health. This makes it imperative that we take immediate action and no longer overlook the threat posed by fungal cross-kingdom pathogens (Fisher and Denning, 2023; Gauthier and Keller, 2013; “One Health - WHO,” 2024).

To acknowledge the significant public health concern associated with fungal pathogens and the need for systematic prioritization, the fungal priority pathogens list (FPPL) was developed (Fisher and Denning, 2023). The list highlight fungal species of global importance, mainly involved in systemic invasive infections and with serious risk of mortality and/or morbidity. Notably, *Fusarium* spp. are categorized within the high-priority group due to their inherently resistance to most antifungal agents and the lack of knowledge about them, their mechanisms of action and treatments, despite the global annual incidence rates of *Fusarium* infection in both medial and agricultural field. Cross-kingdom identification of *Fusarium* pathogens is not uncommon (Moretti, 2009; Summerell, 2019; Van Diepeningen and De Hoog, 2016). They are a major concern in agriculture, where they cause decreases in food production and big food losses. Moreover, several species of *Fusarium* are recognized as opportunistic human pathogens, causing a wide range of diseases. However, knowledge on transkingdom ability of *Fusarium* species is still limited.

The most recently described potential transkingdom species within the *F. fujikuroi* species complex is *F. musae* (Van Hove et al., 2011). *F. musae* is recognized as one of the causative agents of crown rot of banana fruits, one of the most important postharvest diseases worldwide that is source of significant losses in banana fruits and economic damage (Kamel et al., 2016; Triest, 2016). Additionally, *F. musae* has been isolated from human patients, where it can cause superficial infection, such as keratitis

and nail infection, and in few cases systemic disease in immunocompromised individuals (Esposto et al., 2016; Triest, 2016; Triest and Hendrickx, 2016). The ability of *F. musae* to find hosts in both plant and animal kingdom labels it as a potential fungal transkingdom fungal pathogen.

Investigating mechanisms of action behind cross-kingdom pathogens poses unique challenges for both agriculture and medicine due to the difficulty in developing tools and models that are adaptable to diverse host systems and the absence of a common strategy to investigate species considered as or newly defined as cross-kingdom pathogens.

In a previous work, we successfully established infection models for the investigation of *F. musae* using banana fruits and *Galleria mellonella* larvae, a new alternative host model for animal infection and a proxy for human fungal infection (Tava V., et al., Submitted). These models experimentally demonstrated the transkingdom pathogenicity of *F. musae*. Additionally, we developed robust scoring systems to assess infection severity in both hosts, providing a foundation for further research into the mechanisms of *F. musae* pathogenicity.

In this work, we aim to move forward in the investigation of *F. musae* by establishing the first BLI model for studying imaging of the infections and investigate fungal burden. Our objective was to provide insight into of the infection imaging to expand understanding of *F. musae*, as a transkingdom pathogen. We aimed to combine the phenotypic observation of the disease represented by the health score with a quantitative assessments of disease progression with real-time imaging.

Bioluminescence imaging (BLI) has emerged as a powerful strategy for real-time quantitative monitoring of fungal infections in animal models. The technology is based on the sensitive detection of light emission (photons) generated by genetically engineered luciferase-expressing microorganisms secondary to the oxidation of the substrate luciferin (Brock, 2012; Papon et al., 2014). It can provide real-time, non-invasive *in vivo* longitudinal imaging of the infection and possible dissemination by providing quantitative information on the fungal burden.

Papers reporting the use of BLI for fungal infection in animal models underly the versatility of this methodology that can be used for *in vivo* investigation in a wide range of hosts. It's power have been described for traditional models as mouse models, but

also in alternative models such as *G. mellonella* (Delarze et al., 2015; Resendiz-Sharpe et al., 2022; Vanherp et al., 2019; Vanhoffelen et al., 2024, 2023).

At this scope, we built a transformation protocol effective for *F. musae* to develop the first stable reporter BLI strain of *F. musae* expressing firefly luciferase to be used in *in vivo* imaging.

Specifically, we intended to use the BLI strain to track disease progression in *Galleria mellonella* and then apply this method to plant systems, testing its adaptability for studying infections in both animal and plant hosts. Therefore, advancing our existing infection models, we established BLI models using *Galleria mellonella* larvae and banana fruits. These models allowed us to monitor *F. musae* infection and expand our understanding of host-pathogen interactions through *in vivo* imaging and quantification of infection dynamics.

Our final goal was to develop a versatile method that enables quantitative, non-invasive, real-time methodology for monitoring *F. musae* infections, with potential applications to other transkingdom pathogens. This method could be particularly useful for antifungal treatments in both agricultural and clinical settings.

8.2 Material and methods

8.2.1 Bioluminescent Fusarium musae strain engineering

The *F. musae* strain F31 from our collection was transformed for BLI imaging. We integrated in the fungal genome a construct for expression of fusion protein of red-shifted firefly luciferase fused to the far-red fluorescent protein mNEPTUNE. A selection marker for Pyrithiamine hydrobromide was also included.

The resulting BLI *F. musae* strain underwent several rounds of selection, alternating between liquid media to promote sporulation and solid media to allow selection of single conidia, both containing Pyrithiamine as selection marker.

Transformant colonies derived from single conidia were then cultured and imaged to verify stable and strong BLI signal. BLI signal validation was done imaging 10-fold serial dilution of spores *in vitro* with addition of 10% D-luciferin potassium salt using the IVIS Spectrum to ensure a reliable BLI signal. BLI signal was then quantified and compared with BLI signal of a well-characterized BLI *A. fumigatus* strain used as positive control.

For all the following experiments we used the luciferase-expressing *F. musae* strain F31 here described.

Prior to perform *in vivo* experiments, the BLI signal of luciferase-expressing *F. musae* inoculum was verified *in vitro* by imaging 10-fold serial dilutions in a black 96-well plate (Cliniplate; Thermo Scientific, Denmark), with addition of 10% D-luciferin potassium salt (1.25 mg/mL in PBS; Promega, USA).

8.2.2 Inoculum preparation

Spores of BLI strain were stored at -80°C and revived by inoculation onto Petri dishes containing Sabouraud agar (Sigma-Aldrich) with addiction of 0,1 μg/ml Pyrithiamine. Plates were incubated at 24°C for 5 days. Conidia were collected directly from the plates by gently flooding the surface with 1 mL of sterile PBS (Dulbecco's phosphate-buffered saline, Gibco, Paisley, UK). The concentration of conidia was determined using a Burker chamber, and appropriate dilutions were made to achieve the required concentration for infection. When performing in vivo experiments, prior to each infection we ensure a reliable BLI signal by imaging in vitro the inoculum concentration. Cell count was also confirmed by colony forming unit (CFU) plating spore dilutions onto Sabouraud agar plates containing 0,1 μg/ml Pyrithiamine and incubate at 25°C.

8.2.3 Galleria mellonella infection model

We used the *F. musae*-*G. mellonella* larvae model we established in (Tava V., et al., Submitted). We selected healthy *G. mellonella* at the larval final stage in-house bred with weighing 250 ± 50 mg, normal movement, and no melanisation. N = 10 larvae per group were selected and housed individually in 12-well plates without food. Infection was performed by injecting the desired number of spores in each larva in the last right proleg using a Hamilton® syringe (25 µL, 701SN, 31 G, Switzerland). Control group was sham-infected with 10 μL PBS.

The health status of the larvae was assessed daily observing their movement, melanisation and survival, following Loh *et al.* methodology adapted for *F. musae*-*G. mellonella* larvae model we established (Loh et al., 2013; Tava V., et al., Submitted).

8.2.4 In vivo bioluminescence imaging in G. mellonella larvae

BLI signal of infected larvae was detected daily starting from 2h post infection until 9 days post infection. Each day 10 μL of D-luciferin potassium salt (1.25 mg/mL in PBS; Promega, USA) was injected in the last proleg, alternating left and right leg. Larvae were then transferred in black 12-well plates with a transparent bottom (IBL Baustoff 1 Labor GmbH, Austria) and imaged in an IVIS Spectrum imaging system (Revvity, USA).

8.2.5 Ex vivo bioluminescence imaging in G. mellonella larvae

To confirm the relative fungal cell count we performed *ex vivo* BLI on larval homogenates until day 4 post-infection. For each time point, larvae (n=6) were homogenized with a tissue homogenizer in 1 ml of sterile PBS. BLI of homogenate was acquire by in vitro imaging of 10-fold serial dilutions in a black 96-well plate, with addition of 10% D-luciferin potassium salt. Cell count was also confirmed by colony forming unit (CFU) plating spore dilutions onto Sabouraud agar plates containing 0,1 μg/ml Pyrithiamine and incubated at 25°C.

8.2.6 Sensitivity of BLI F. musae to posaconazole

Sensitivity of the BLI strain of *F. musae* to posaconazole was tested *in vivo* in healthy *G. mellonella* larvae at the larval final stage in-house bred with weighing 250 ± 50 mg, normal movement, and no melanisation. N = 10 larvae per group were selected and housed individually in 12-well plates without food. We infected larvae by injecting 10^4 spores/larva in the last right proleg using a Hamilton® syringe (25 µL, 701SN, 31 G, Switzerland). Then larvae were treated daily, starting from 1 hour post-infection, with a dose titration of posaconazole by injecting different dose of posaconazole ranging from 1 to 8 mg/kg in the last left proleg using a syringe. Control groups were sham-infected with 10 μL PBS and sham-treated with 10 μL NaCl.

The health status of the larvae was assessed daily observing their movement, melanisation and survival, following (Loh et al., 2013) methodology adapted for *F. musae-G. mellonella* larvae model we established.

8.2.7 Banana fruits infection model

Organic bananas imported from Ecuador were gifted to us by ©Colruyt Group (Coccinelle, Hoveniersstraat 5, 2860 Sint Katelijne Waver, Belgium). We received healthy, green bananas that had not yet ripened (no gas exposure) and were still grouped in hands of 5 or 6 bananas each.

Prior to infection, banana hands were sterilized by immersion in 0,7% sodium hypochlorite for 3 min, washed with water and dried on a bench on a sheet of paper. Individual bananas were then separated using a clean scalpel, making a cut perpendicular to the crown ensuring the crown remained.

In this work, we infected banana fruits using two different procedures. The first method follows the *F. musae*-banana fruits model we established in our previous infection study (Tava V., et al., Submitted). Here, toothpicks imbued with *F. musae* spores were inserted at a regular distance into the fruits (n= 5 toothpicks per banana), deep enough to break the peel and touch the surface of the pulp. We then included a second method designed to mimic the hypothetical entry route of *F. musae* into banana fruits, as described by (Triest and Hendrickx, 2016). We cut a thin slice from the external part of the pedicel to create a “scar” for the infection. A drop of conidia suspension (approximately 50 µL) was positioned on the exposed scar, making sure it was in contact with the entire surface. Finally, the crown was covered with a piece of sterile aluminum foil (Kamel et al., 2016). The fruits were then placed on trays, covered by plastic bags and incubated at 22°C in the dark for up to 26 days post infection. Three bananas were used per time point and the two infection models were combined on the same fruit when possible. In both procedures we used an inoculum of 10^5 spores/mL. Round sections of bananas stained with methylene blue and observed with stereoscope at magnification 6 days after infection with *F. musae* were included as additional evidence of the presence of the fungus.

8.2.8 Bioluminescence imaging in banana fruits

BLI signals were acquired from different sections and parts of the bananas. First, the entire fruit was imaged to quantify infection levels at the toothpick insertion points. A volume of 10 µL D-luciferin potassium salt (1.25 mg/mL in PBS; Promega, USA) was pipetted on bananas at each toothpick insertion point and spread to the surrounding

area using a cotton stick. The fruits were then sliced at the insertion point of the toothpicks, 10 μL D-luciferin was added, and banana slices were imaged to assess the depth of the infection in the pulp. Banana pedicels were also cut from the fruit, imaged from above, and then cut in halves to observe progression of the disease from the crown. For both sections 10 μL D-luciferin was added and spread across the surface.

8.2.9 BLI signal acquisition

Every time BLI signal was detected using an IVIS Spectrum imaging system (PerkinElmer, USA). Consecutive images (n=5) were acquired with an exposure time of 30 s (open filter or spectral unmixing, F/stop1, subject height of 1.5 cm, and medium binning) per each time point. To quantify the signal, we used Living Image software (version 4.5.4; PerkinElmer, USA) and the total photon flux (photons per second) was measured and used for analysis.

For *G. mellonella* imaging, regions of interest (ROIs) were positioned covering each well and the default emission filter setting (detector without any spectral selectivity) on the IVIS spectrum was selected.

For imaging of banana fruits, was selected spectral unmixing setting on the IVIS spectrum, which uses different single-wavelength emission filters. Different sections were considered and ROIs were positioned as represented in Fig. 16.

Figure 16 Representative images of the banana sections observed and the position of the ROIs. On the left pictures taken with a phone of the different sections and on the right visual representation of BLI signal with IVIS spectrum. We considered: the entire fruit with ROIs surrounding the toothpick insertion points (A), banana slices (B), pedicels imaged from above (C) and cut in halves (D).

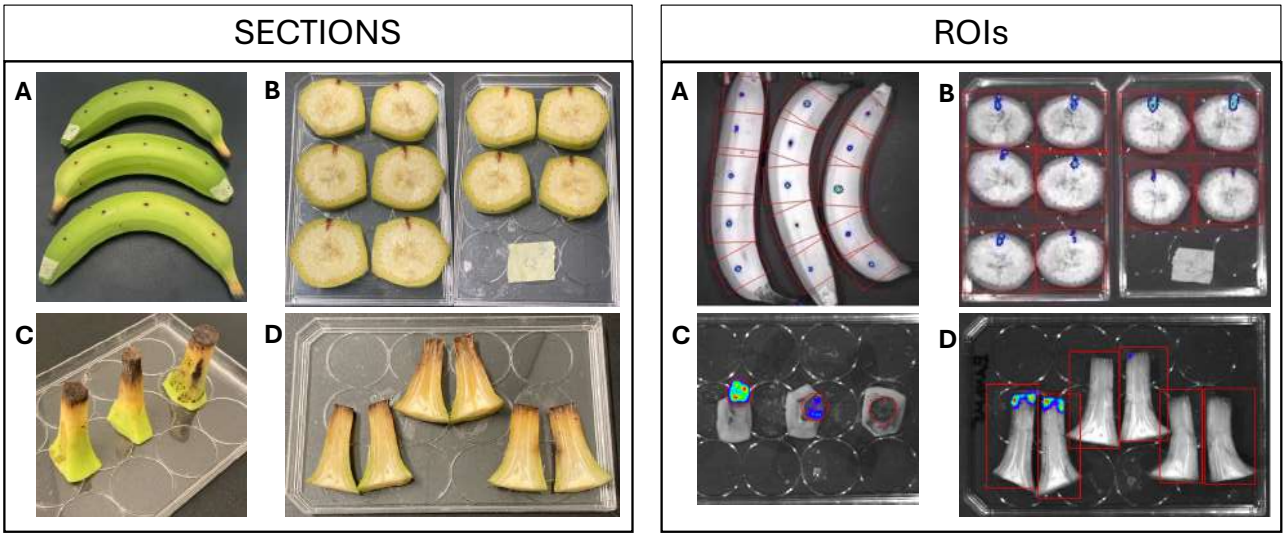

8.2.10 Statistical analysis

Statistical analyses were performed using GraphPad Prism version 8.0.2 (GraphPad Software, USA). In vivo BLI data of both bananas and larvae were log10-transformed and analyzed by mixed-effects two-way analysis of variance (ANOVA) with Tukey's correction for multiple comparisons to detect significant differences between groups and in relation to time. Survival analysis of larvae was analyzed using the log rank (Mantel-Cox) test, while for health score we used the mixed-effects two-way analysis of variance (ANOVA) with Tukey's correction for multiple comparisons. Dead larvae were removed from the plate and not imaged, for them we considered the last BLI quantification before death to plot the graph. The correlation coefficient, r, was computed using Pearson's correlation analysis.

8.3 Results

7.3.1 Bioluminescent Fusarium musae strain engineering

We transformed *F. musae* strain F31 to integrate a construct for the expression of codon-optimized red-shifted firefly luciferase fused to the far red fluorescent protein mNEPTUNE (mNept:luc_red). Transformation resulted in obtaining the first BLI strain of *F. musae* expressing luciferase. This strain was deeply characterized and then used for BLI of *F. musae* in both *G. mellonella* larvae and banana fruits.

8.3.2 In vitro validation of red-shifted emission of light of the bioluminescent F. musae strain

BLI signal of luciferase-expressing *F. musae* strain was quantified and compared with BLI signal of a well-characterized luciferase-expressing *A. fumigatus* strain used as positive control. Results demonstrated that the BLI signal of *F. musae* is clear, stable and even higher than luciferase-expressing *A. fumigatus* (Fig. 17A), allowing us to proceed with *in vivo* experiments. Quantification of the signal showed emission of bioluminescence highly comparable to the inoculum concentration determined using a Burker chamber and then used for the infection (Fig. 17B, 17C).

Figure 17. In vitro validation of luciferase-expressing F. musae. A, visual representation of BLI signal of 10-fold serial dilution of spores of F. musae BLI strain and luciferase-expressing A. fumigatus strain used as positive control, three replicates were considered. B, correlation graph of the quantification of the bioluminescence signal of F. musae and its inoculum concentration determined using a Burker chamber. C, visual representation of the inoculum validation performed for each group prior to infection, data were used to build the correlation graph.

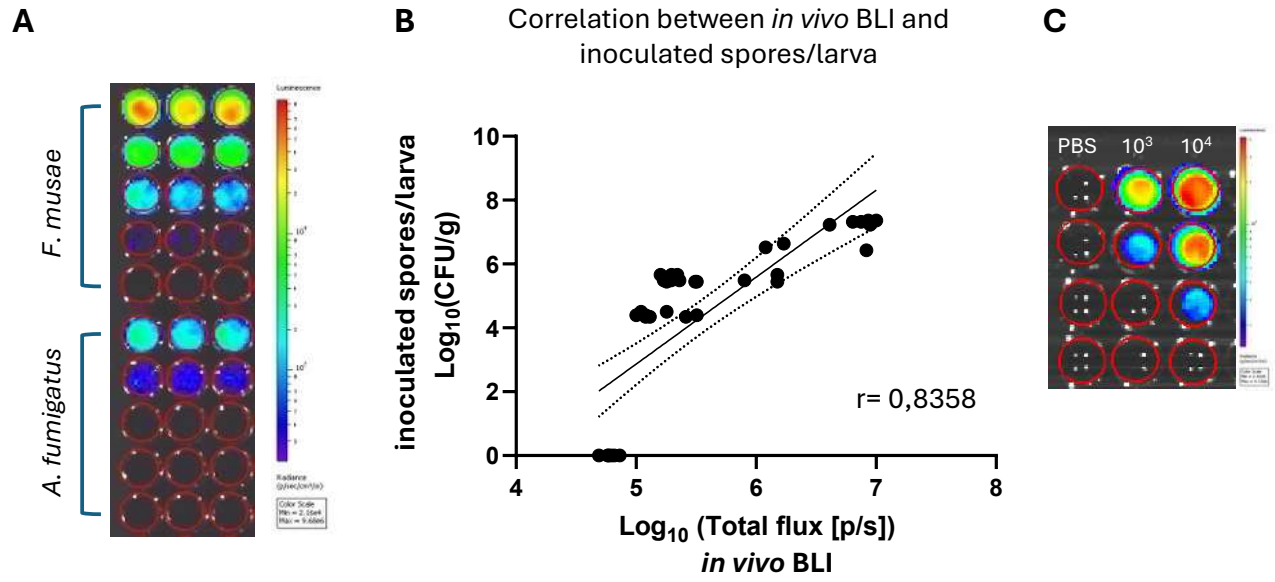

8.3.3 BLI allows for in vivo monitoring of F. musae fungal burden in Galleria mellonella larvae

To validate our *F. musae-G. mellonella* model for bioluminescence imaging detection and track disease progression, we infected the larvae with different concentrations of spores. The goal was to assess the sensitivity of our newly transformed BLI strain in an *in vivo* model. We started by testing inoculum concentrations ranging from 10^3 to 10^6 spores per larva to determine whether the inoculum size previously used to establish the model could also be detected using BLI. Larvae infected with inoculum sizes ranging from 10^3 to 10^6 spores per larva were imaged with BLI 2h post infection. We observed that increasing inocula corresponded with increased BLI signal (Fig. 18A). Larvae infected with 10^3 spores exhibited a low signal, while larvae infected with higher inoculum concentrations presented strong and clearly distinguishable BLI signals. Overall, we were able to differentiate fungal loads. Quantification of the signal confirmed our observation (Fig. 18B). Larvae infected with 10^3 spores/larva showed a BLI signal significantly higher than sham-infected larvae already from 2h post infection.

The bioluminescence signal intensity, then, increased with the concentration of the inoculum, with larvae infected with 10^6 spores each presenting the strongest BLI signal. We next determined the detection threshold, i.e. the lowest *F. musae* inoculum that could be detected in *G. mellonella* with BLI, by infecting larvae with 10 and 100 spores per larva and imaging them with BLI 2h post infection. Results showed that the BLI signal of larvae infected with 10 spores of luciferase-expressing *F. musae* was significantly higher from larvae sham-infected (Fig. 18A e B), reflecting the possibility to detect the presence even few spores of our luciferase-expressing *F. musae* strain. However, the detection threshold at 2h post infection does not allow quantification of different fungal loads when the number of spores present is lower than 10^3 spores/larvae, indeed infection with 10 and 100 spores/larvae resulted not significantly different from those infected with 10^3 spores/larvae.

*Figure 18. Imaging of G. mellonella larvae 2h post infection with luciferase-expressing F. musae. A, visual representation of the signal acquired with IVIS spectrum of larvae (n=12) infected with: PBS (sham-infected), 10 spores/larva, 102 spores/larva, 103 spores/larva, 104 spores/larva, 105 spores/larva, 106 spores/larva. B, quantification of the signal 2h post infection, each dot represents a single larva. Mean and SD are represented in the graph. For statistics: ns= nonsignificant; * p> 0,01; **= p>0,001; ***= p>0,0001; ****= p<0,0001.*

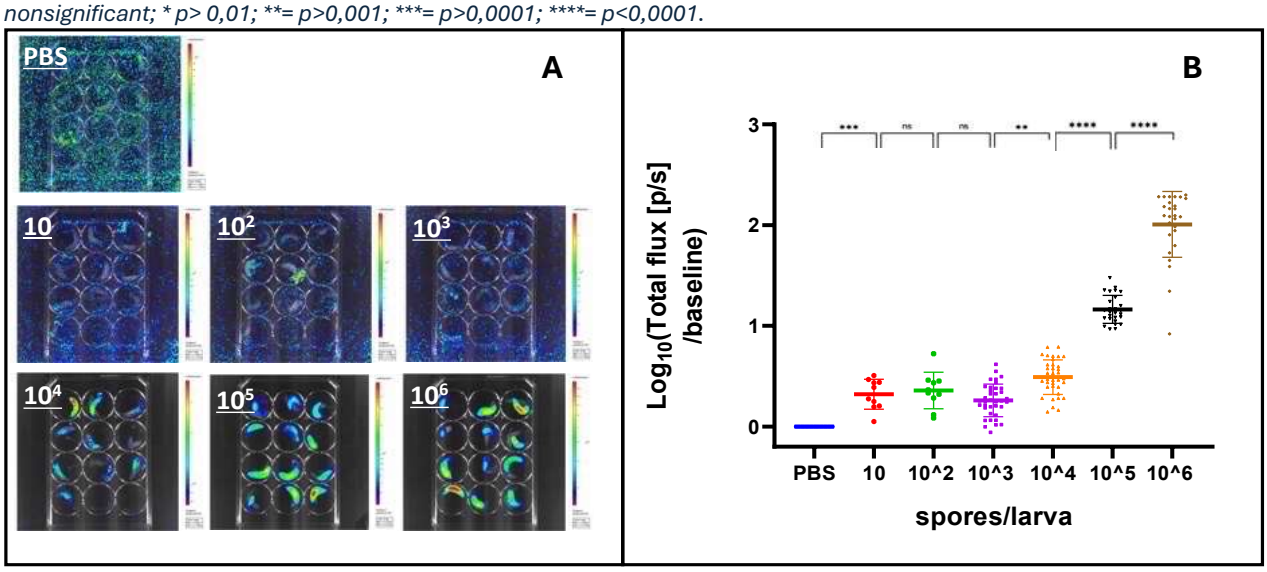

We then observed the longitudinal evolution of BLI signal in *G. mellonella* after infection with *F. musae* (Fig. 19).

Larvae infected with 10^5 and 10^6 spores/larvae gave high and clear signal 2 hours post-infection, however the inoculum was too high for the larvae, leading to illness and death within a few days after infection. On the other hand, groups infected with 10 and 100 spores/larvae exhibited a higher fungal load compared to the sham-infected group at

2 hours post-infection, but the signal did not significantly differ from the sham group over time. Most larvae in these groups remained healthy, showing little to no infection symptoms. Overall, the group of larvae infected with 10^4 spores/larva provided the strongest BLI signal intensity but with the highest number of healthy larvae.

Our results confirm that the bioluminescent reporter strain of *F. musae* is highly stable, producing a strong *in vivo* BLI signal that is effectively detected and quantified using BLI. The sustained strength of the BLI signal over time indicates that even a small number of spores can be detected with this method, although precise quantification may be limited to higher spore concentrations.

These findings overall validate our approach and provide a robust, non-invasive methodology for monitoring *F. musae* infections in *Galleria mellonella* larvae with BLI.

*Figure 19. In vivo longitudinal monitoring of G. mellonella larvae infected with F. musae reporter strain. The graphs represent: A, in vivo BLI; B, health score, C, in vivo BLI of single larvae, D, survival. Data were acquired daily and for each group were considered n=10 larvae, average value and SD are represented. For statistics: ns= nonsignificant; * p> 0,01; **= p>0,001; ***= p>0,0001; ****= p<0,0001.*

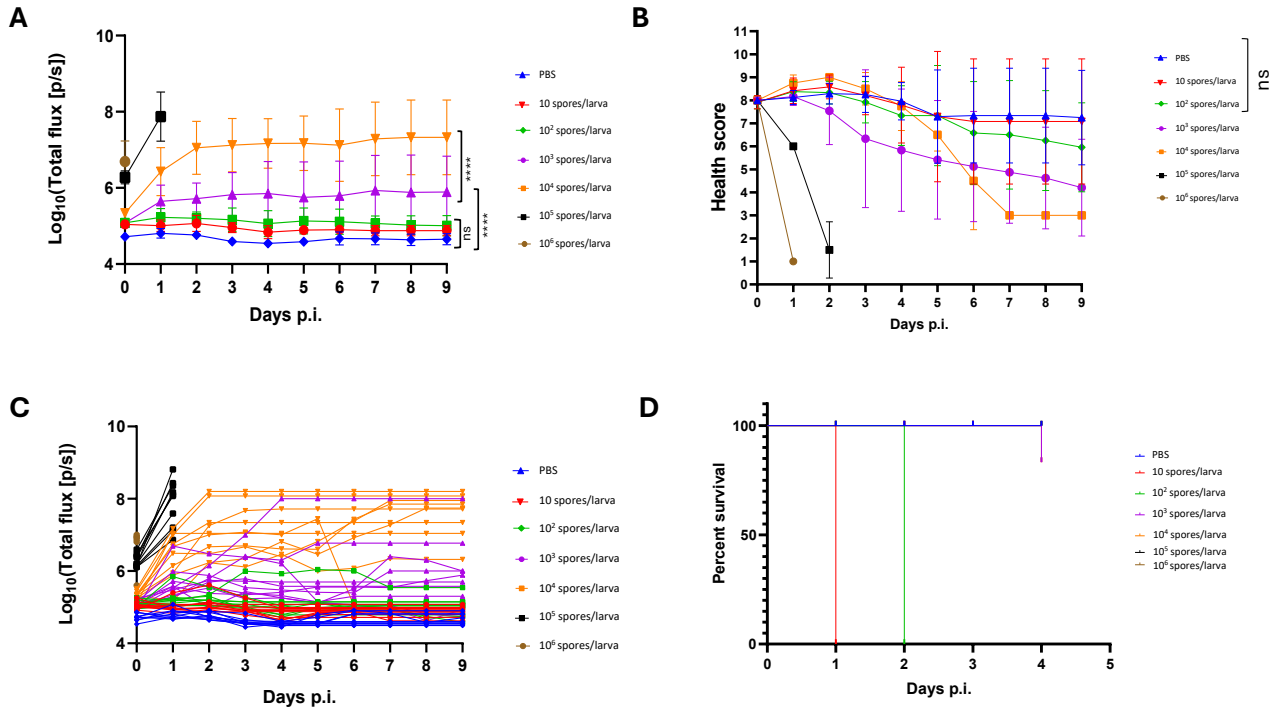

8.3.4 Ex vivo correlates with in vivo bioluminescence in G. mellonella

CFU counting still represent the gold standard for quantifying fungal infections. To support our *in vivo* longitudinal results, we checked relative cell count by colony forming

unit (CFU) plating spore dilutions and *ex vivo* BLI on larval homogenates. The goal was to evaluate whether our newly established BLI, which we have already validated for longitudinal monitoring of fungal burden, could replace endpoint CFU counting.

Daily, following health score assessment and BLI *in vivo* imaging, larvae (n=6) were homogenized. A portion of the homogenate was incubated onto Sabouraud agar plates containing 0,1 mg/ml Pyrithiamine for CFU counts, while the remaining portion was imaged for *ex vivo* quantification.

Results showed that *in vivo* BLI signal increased until day 2 post-infection, after which it slightly decreases. In contrast, the corresponding CFU count initially decreased, followed by an increase after 3 days pi, ultimately returning to the initial range (Fig. 20A). The CFU counts confirmed the presence of *F. musae* each day post infection, indicating that the infection persisted and the larvae did not clear the inoculated spores. However, the correlation between the two methodology was low.

When then comparing data from *in vivo* and *ex vivo* BLI, a clear correlation over time was observed (Fig 20B), suggesting that the difference between in vivo BLI and CFU is not due to differences between *in vivo* and *ex vivo* samples but has a methodological origin.

Overall, with our results we validated the use of in vivo BLI over time for fungal burden quantification, establishing it as an effective alternative to endpoint CFU counting.

Figure 20. In vivo, ex vivo and CFU comparison. A, comparison between in vivo BLI signal and CFU counts after larval halogenation?. B, correlation graph of BLI signal quantification of in vivo larvae and homogenized larvae. Infection was performed with 10^4 spores/larva and monitored daily over 5 days. The Pearson correlation coefficient (r) is shown.

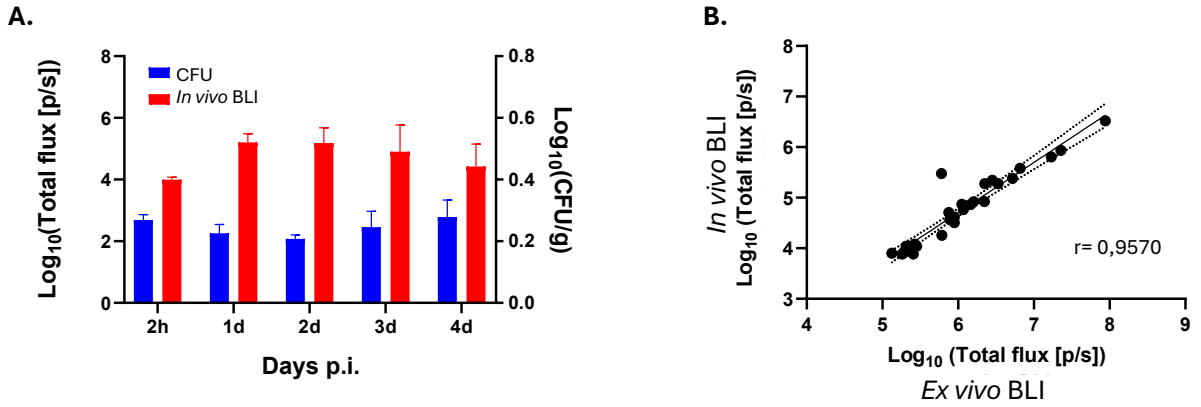

8.3.5 1BLI allows to monitor fungal growth in vivo even when symptoms are not visible

Next, we investigated whether BLI could detect differences host-pathogen interactions during fungal infection in larvae incubated at different temperatures. Larvae infected with the bioluminescent *F. musae* strain were incubated at room temperature (22°C), 30°C and 37°C, and their BLI signals were measured. Once again, larval health was assessed daily by monitoring movement, melanisation, and survival as described before. Afterward, we injected the larvae with 10 µL of D-luciferin potassium salt and detected the BLI signal. Health score and survival data were compared with previous observations noted in the infection study on *F. musae* at different temperatures.

As expected, larvae incubated at 22°C exhibited the highest BLI signal over time, consistent with their lower health scores. Interestingly, larvae incubated at 37°C also showed relatively high BLI signals, despite their health scores indicating that they were largely unaffected by the infection at this temperature showing little to no infection symptoms (Fig. 21).

Overall, our results suggest that BLI can detect infection variations that health scores and survival rates do not capture. Common metric in infection studies, such as health scores and survival rates, failed to reflect certain host-pathogen interactions that are not indicated by the disease symptoms. The use of BLI highlight its power in identifying infection at early stage and when symptoms are not yet visible.

*Figure 21. In vivo BLI in larvae incubated at different temperatures. The graphs represent: A, in vivo BLI; B, health score, C, in vivo BLI of single larvae, D, survival. Data were acquired daily and for each group were considered n=10 larvae, average value and SD are represented. For statistics: ns= nonsignificant; * p> 0,01; **= p>0,001; ***= p>0,0001; ****= p<0,0001.*

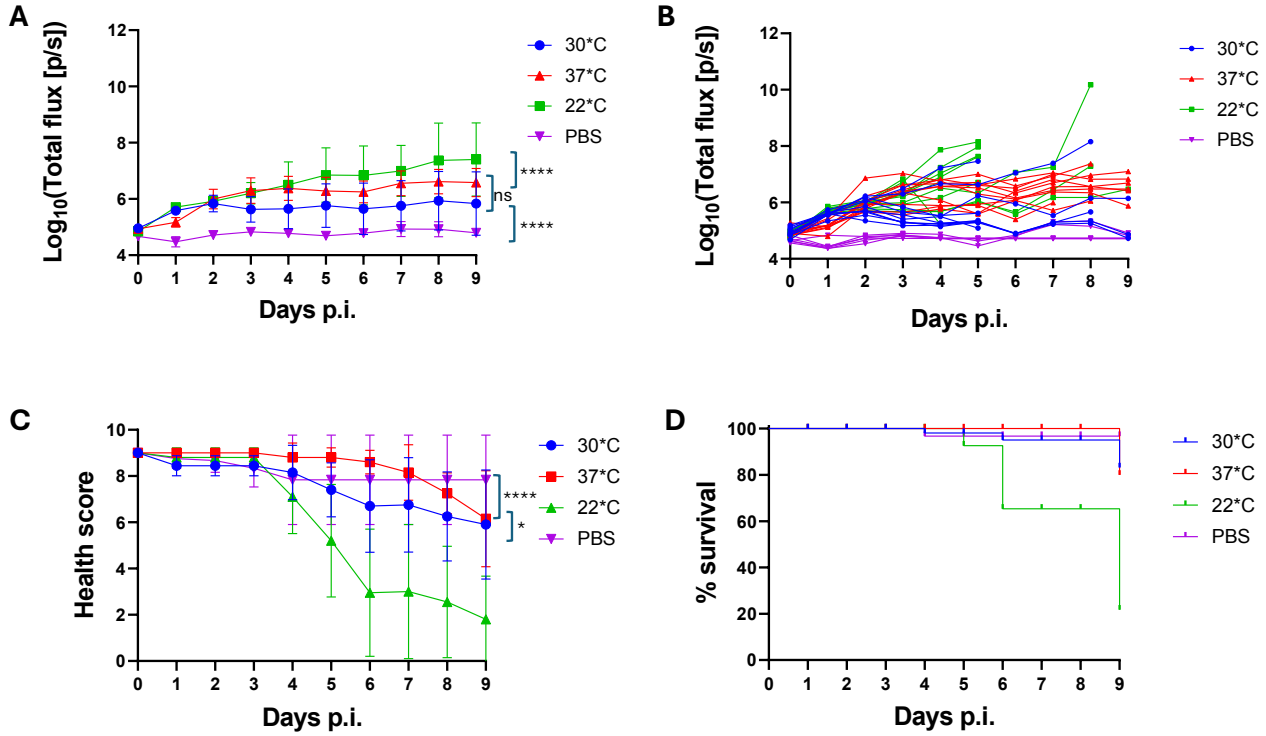

8.3.6 BLI can be a tool for screening antifungal treatments

To assess the potential applications of BLI for screening antifungal treatments against F. *musae*, we tested in vivo in *G. mellonella* four different antifungal doses ranging from 1 to 8 mg/kg. The goal was to validate BLI as a readout for dose-response studies using posaconazole, whose effectiveness against *F. musae* has already been established, with G-MIC value of 0,54 mg/L (Tava et al., 2021).

Treatment with different doses of posaconazole resulted in observation of dose-response to posaconazole that was reflected in decrease of BLI signal observed with the increase of the posaconazole dose administered. Specifically, as expected the lowest BLI signal was observed in larvae treated with dose of posaconazole of 4 mg/kg, while decreasing the dose of posaconazole the BLI signal tended to increased, validating BLI as a readout for dose-response studies (Figure 22). Surprisingly larvae treated with the highest posaconazole dose (8 mg/kg) presented values higher than sham-treated larvae. No statistical significances were observed between treated and sham-treated larvae in terms of in vivo BLI, health score or survival. However, the overall trend showed that increasing posaconazole concentrations corresponded to decreased BLI signals, confirming a dose response of *F. musae* to the treatment.

These results suggest that BLI has potential as a method for screening of antifungal treatments against *F. musae*. However, further experiments are necessary to increase the number of repetitions, the larval sample size or testing different antifungal compounds.

*Figure 22 Dose response of posaconazole in G. mellonella against azole-susceptible F. musae strain. A, in vivo BLI flux; B, AUC; C, health scoring; and D, survival readouts in G. mellonella larvae treated with 8, 4, 2 and 1 mg/kg, and two controls, followed longitudinally for four days post-infection (pi). Statistics refer to longitudinal differences over four days where * P < 0.05, ns = non-significant (P >0.05), data are means ± SD, n = 10.*

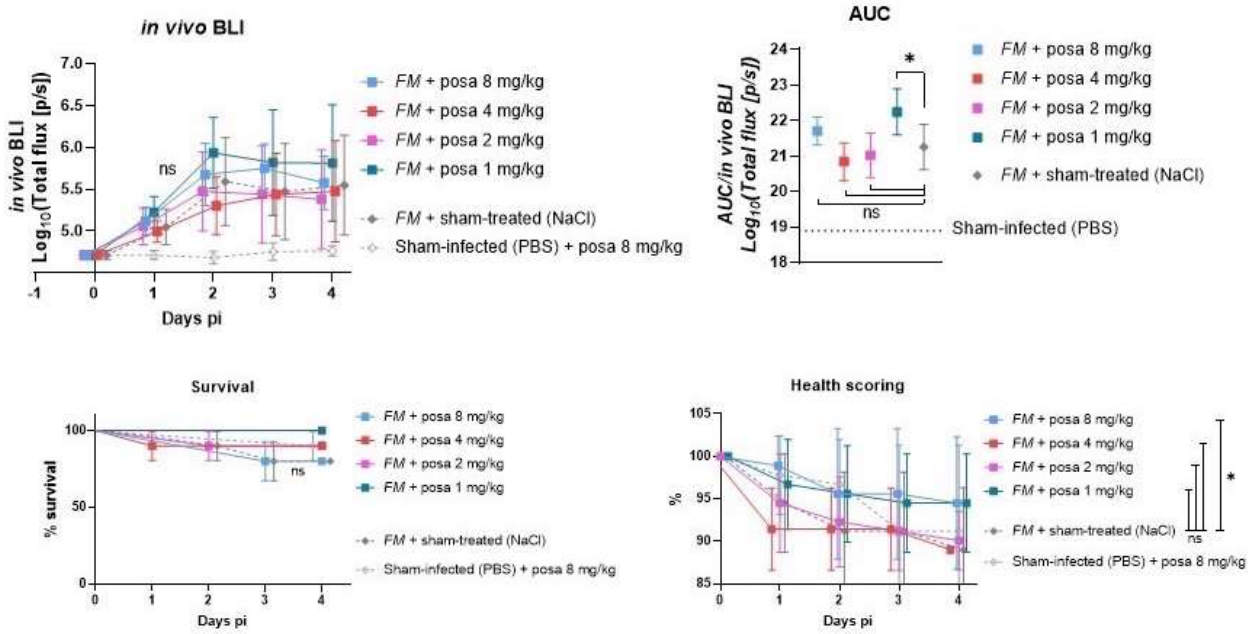

8.3.7 BLI allows disease progression in banana fruits infected with F. musae

To test the adaptability of BLI imaging to a plant system, we validate our *F. musae*-banana fruit model for bioluminescence imaging detection. The goal was to quantify *F. musae* infection in banana fruits while avoiding interference from lignin and other compounds in the peel, which can affect imaging techniques (Tiessen, 2018). In addition, we wanted to determine whether different ripeness stages affect the BLI signal acquisition.

Initial imaging using the default emission filter setting (detector without any spectral selectivity) on the IVIS spectrum, commonly selected by our group for *in vivo* imaging, resulted in high background BLI signal this was due to phosphorescent properties of banana peel, which masked the fungal signal and hindered infection detection. To

address this issue, we employed spectral unmixing setting, which uses different single-wavelength emission filters, aiming to minimize background interference.

As shown in Fig. 23A, when bananas are infected with luciferase-expressing *F. musae,* we observed a distinct BLI intensity profile across discrete emission filters, while non-infected bananas resulted in giving the same signal at different wavelengths. In particular, the more we utilized emission filters specifically tuned to the luciferase-associated wavelength (620 nm), the more we observed a distinct and intensified signal, suggesting that the fungus is successfully detected at this wavelength. Additional evidence of the presence of the fungus was obtained by adding few drops of methylene blue dye to the infected area to localize *F. musae* (Fig. 23B), observations were made using a stereoscope.

As non-infected control fruits, we included both pale green and brown bananas. The goal was to assess whether the browning of the fruits, due to the ripeness stage of the fruits, would affect the acquisition of the BLI signal. As observed in Fig. 23, pale green and brown bananas presented a comparable intensity in the BLI signal, suggesting that the ripeness stage of the fruits does not affect the BLI signal.

Figure 23. BLI signal detected from bananas when using spectral unmixing modality. A, the graph represents in blue, fruits infected with F. musae (26 days p.i.); in red, pale green fruits in the first stages of ripening; in green, brown fruits in late ripening stage. Each dot corresponds to a single fruit. B, visual representation of infection progression observed 6 days post-infection in ripe bananas with naked eye, after addition of methylene blue and at BLI.

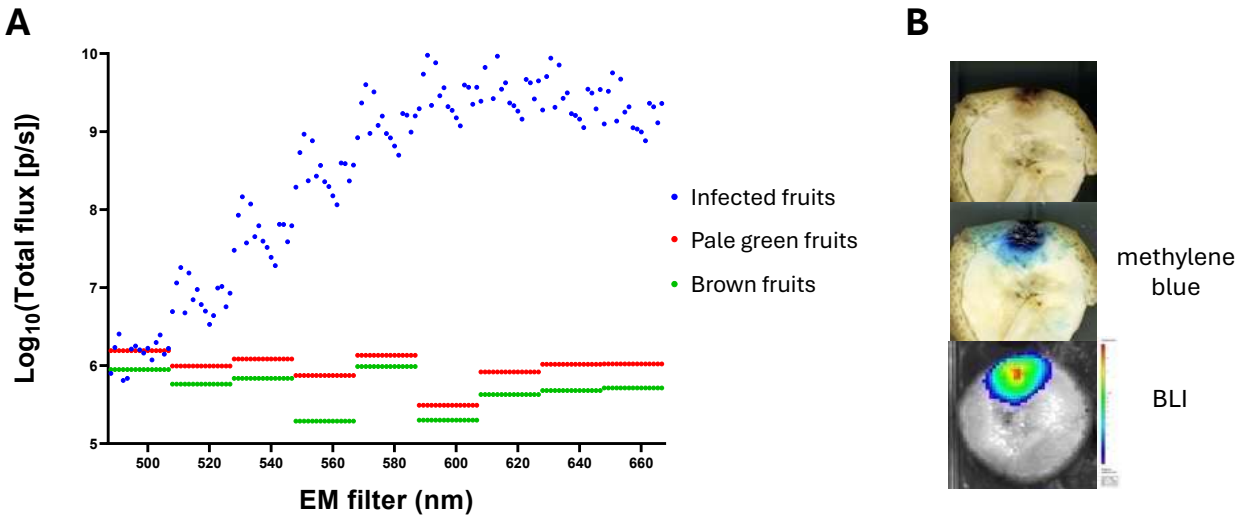

8.3.8 BLI enable in vivo disease progression banana fruits infected with F. musae

Once the optimal imaging parameters for monitoring the disease in bananas were established and verified, we tracked the progression of the infection over a period of 26 days. This extended timeframe was selected because unripe bananas provide fewer accessible nutrients for fungal growth, leading to a slower disease progression. Additionally, prior experiments showed that infections initiated at the crown level take longer to manifest symptoms and spread.

Bananas were infected and incubated for up to 26 days post-infection. Day 1, 2, 7, 9, 13, 16, 19, 23, 26 post infection were selected as timepoints for imaging. At each time point, images of the designated sections (as described in the methods) were captured using both a phone camera and the IVIS Spectrum to measure luminescent signals.

BLI signal was observed from the earliest days post-infection, suggesting the presence of the fungal spores and that the infection was successfully performed. For whole fruit analysis, regions of interest (ROIs) were delineated around the infection points, and the data were plotted. Initially, the luminescent signal remained low and similar to water-infected controls until day 16. From day 16 onwards, there was a marked exponential increase in the signal, indicating significant fungal progression (Fig. 24). This pattern was consistent with earlier observations where fruits incubated for 10 days showed minimal signs of infection until day 7, followed by a rapid escalation in disease severity (as described in (Tava V., et al., Submitted)). BLI signal closely correlated with visual assessments and the browning formation. However, in the later stages of infection, IVIS imaging revealed diffuse patterns that were no longer distinguishable by the naked eye. This might reflect the advantage in sensitivity of BLI, which can detect fungal presence before visible mycelium formation.

Observations from round-sections of infected bananas indicated that *F. musae* began spreading from the infection point early on, penetrating deeply into the pulp and moving toward the fruit's center before reemerging at the peel (Fig. 24). This may explain the delayed appearance of symptoms observed on the peel of the fruits.

Infection at the pedicel provided a clear representation of disease progression. The luminescent signal initially localized at the inoculation site in the upper region, then spread through the vascular system of the fruit (Fig. 24). BLI could offer the greatest advantages for monitoring disease progression in the pedicel. In this area of the fruit

infection is not visually clear without imaging techniques, making it challenging to assess infection levels based solely on external symptoms and to establish a scale of disease severity as we did previously in (Tava V., et al., Submitted).

Overall, longitudinal monitoring demonstrated that the spread of BLI *F. musae* could be effectively tracked in the banana fruit system. BLI promises to be reliable tool for monitoring *F. musae* infection in banana fruits, allowing for the detection and quantification of disease progression in real-time with high sensitivity.

Figure 24. In vivo longitudinal BLI monitoring of banana fruits infected with the F. musae reporter strain over a 26-day period. Three distinct fruit sections were analyzed: whole fruit, round cross-sections, and pedicel. Representative images of the infected banana sections were captured at days 2, 16, and 19 post-infection. The graphs display BLI signals acquired at days 1, 2, 7, 9, 13, 16, 19, 23, and 26 post-infection for each fruit section. Data are presented as mean ± SD in the upper graph and as individual data points in the lower graph.

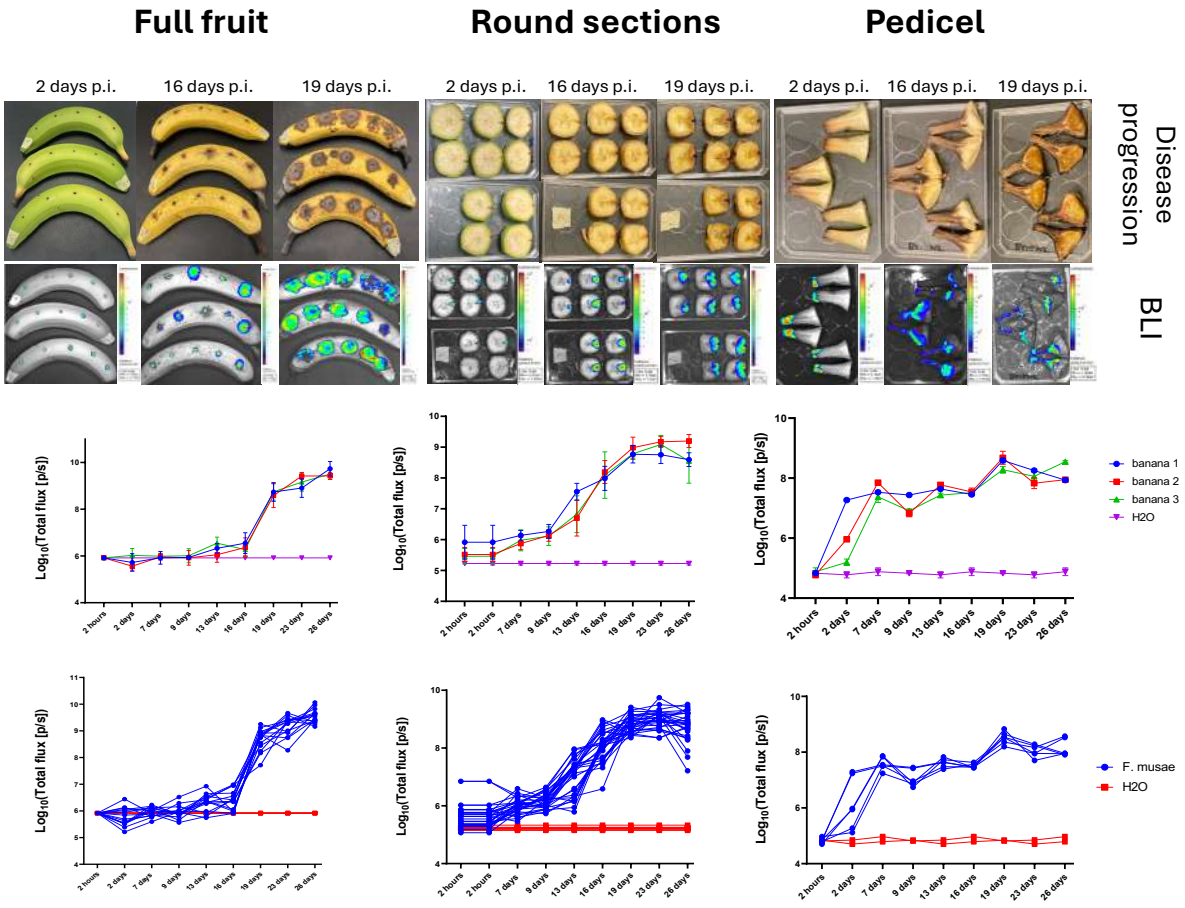

8.4 Discussion

In recent years, the threat posed by fungal cross-kingdom pathogens to public health has gained significant attention. The number of invasive fungal infections has

increased, with many diseases attributed to fungal species already known for their impact in agriculture (Gauthier and Keller, 2013; Sharma et al., 2014; Yasir Rehman, 2015; Zhai et al., 2020). In addition, the continued expansion of the at risk-population makes it clear the urgent need for more research on cross-kingdom fungal pathogens (Fisher and Denning, 2023; Misra and Chaturvedi, 2015; “One Health - WHO,” 2024; Van Baarlen et al., 2007). Despite this, the field of cross-kingdom pathogens is still at its infancy. Several species are known to cross kingdom boundaries, but there is currently no common strategy followed for their investigation. Among the challenges present, there is the difficulty in developing tools and models that are adaptable to diverse host systems and can be exploited in both agriculture and medical fields.

Among the potential cross-kingdom fungal pathogens, our research focuses on *Fusarium musae*, a species pathogenic to both banana fruits and human patients (Esposto et al., 2016; Kamel et al., 2016; Triest, 2016; Triest et al., 2016). Knowledge about *F. musae* is still limited, in a previous work we demonstrated experimentally the cross-kingdom ability of *F. musae* (Tava V., et al., Submitted). We developed representative infection models using banana fruits and *G. mellonella* larvae, and we demonstrated the ability of a collection of *F. musae* strains to cause significant infection in both host models.

Here, we developed the first bioluminescence readout to quantify *F. musae* fungal burden and to track disease progression adapting the infection models previously established with banana fruits and *G. mellonella* for BLI imaging.

BLI is a powerful method that allows non-invasive *in vivo* imaging in real-time and over time. It has proven especially effective for monitoring and quantifying fungal infection (Papon et al., 2014; Resendiz-Sharpe et al., 2022; Vanherp et al., 2019; Vanhoffelen et al., 2024, 2023). The technology relies on detecting light emission (photons) generated by genetically engineered luciferase-expressing microorganisms through the oxidation of luciferin (Brock, 2012).

At first, we developed the first BLI *F. musae* strain expressing firefly luciferase in the fusion protein mNept:luc_red transforming the strain F31 belonging to our *F. musae* collection. *In vitro* results demonstrated the successful of the transformation. The BLI signal of our reporter strains resulted stable and higher than the well-established

luciferase-expressing *A. fumigatus* strain we used as positive control making us move forward toward *in vivo* investigation.

Next, we used the newly transformed BLI strain to image and monitor *F. musae* infection *in vivo* in *G. mellonella* larvae and banana fruits over time, adapting existing infection models for BLI fungal detection and quantification. Our goal was to establish a real-time method to track disease progression, with potential in both agricultural and medical field.

The *G. mellonella* larvae model, already established for BLI investigations of (other species such as) *A. fumigatus*, was successfully validated for *F. musae* in this study (Resendiz-Sharpe et al., 2022; Vanhoffelen et al., 2023).

Results demonstrated that BLI is a highly sensitive tool, capable of detecting even low *F. musae* loads with stable and strong signal *in vivo*. Using IVIS Spectrum system we achieved effective detection and quantification of *F. musae*, allowing at very early stages of infection quantification of different fungal loads. The strength and consistency of the BLI signal over time indicates that, indeed, even a small number of spores as few as 10 spores/larva can be detected with this method producing a statistically higher signal compared to sham infected controls, although precise quantification may be limited when spore concentrations is lower that 10^3 spores/larva. In addition, consistency of the BLI signal across individual larvae further confirmed the method's robustness.

Importantly, BLI proved to detect variations in infection progression that were not captured by traditional health scores or survival rates, offering a more sensitive means of identifying early symptoms, potentially due to host responses to infection. In addition, while CFU is considered the gold standard for quantifying viable cells in microbiology, it lacks the ability to provide the dynamic insights that BLI offers by capturing not only fungal growth but also the presence of fungal filaments, offering a more comprehensive view of fungal activity as observed also by (Vanhoffelen et al., 2023).

These findings validate our approach as a non-invasive, effective technique for monitoring *F. musae* infections *in vivo* and underscore the advantages of BLI over conventional infection assessment methods, validating imaging of *G. mellonella* larvae with BLI as a successful model also for the investigation of fungal burden of *F. musae*.

Given the positive results, we aim to take advantage of this technology to explore whether a similar approach could also be applied to banana fruit, the plant model established for *F. musae*, in order to directly compare the two models.

Quantification of fungal infection in banana fruits has long been challenging due to the banana peel composition, which is rich in chlorophyll and other compounds, that can interfere with imaging techniques (Tiessen, 2018). BLI proved to be a valuable tool in overcoming this challenge by selecting a specific wavelength for firefly luciferase (EM filter 620), that allowed us to distinguish signals related to disease progression from background signals produced by banana peel, enabling us to track infection marks over time.

For banana fruits BLI model, we employed two distinct infection models: toothpick model to monitor disease progression and validate our imaging methodology, and crown model to simulate natural infection scenarios in fruits. BLI successfully supported both these models, delivering detailed insights into disease evolution in banana fruits. Using the IVIS Spectrum system, we could monitor disease progression, providing valuable real-time data on its evolution. Our findings suggest that *F. musae* is relatively less aggressive compared to other known *Fusarium* species involved in crown rot disease, exhibiting slower progression and less aggressive behavior (Kamel et al., 2016).

To summarize, with our work we evaluated for the first time the use of BLI to investigate *F. musae* in *in vivo* host models such as *G. mellonella* and banana fruits. We provide a methodology that could be applied to observe the same pathogen in models representing two different biological kingdoms. In both, BLI demonstrated its strength in detecting fungal infections with high sensitivity, surpassing traditional methods that can be insufficient. In *G. mellonella*, BLI made it possible to monitor fungal burden at 37°C despite their health scores indicating that they were largely unaffected by the infection at this temperature showing little to no infection symptoms. In addition, results from our preliminary screening for antifungal treatments in *G. mellonella* showed that BLI is a highly sensitive tool for evaluating therapeutical options against *F. musae*, providing a non-invasive approach to assess treatment efficacy over time. While, in banana fruits, BLI offered the greatest advantages for monitoring disease progression in the pedicel. In this area of the fruit infection is not visually clear without imaging

techniques, making it challenging to assess infection levels based solely on external symptoms and to establish a scale of disease severity. However, additional experiments are needed to validate results in banana fruit. It is crucial to prove that with BLI we observe specifically assess the presence of the pathogen on the host and not merely the host's symptomatic response. Including a negative control in the imaging protocol, where bananas are infected with a non-luminescent strain, could help differentiate whether the signal is emitted directly from the BLI strain or is a result of tissue degradation.

Moreover, BLI allows detection of early-stage symptoms that are not immediately visible, allowing us to study infections even before the host shows any noticeable reactions. This capability is crucial for understanding the timing and stages of fungal infection, offering insights that are critical for disease progression studies.

8.5 Conclusions

To conclude, our work establishes the first bioluminescence readout to quantify *F. musae* fungal burden and to track disease progression in different hosts. Our preliminary results demonstrated that BLI could be a useful tool in disease progression studies allowing identification of crucial time points and stages of fungal infection, specifically at early-stages where symptoms are not immediately visible.

Furthermore, future research could extend the use of BLI to other crops or animal models to examine potential treatments or control measures for *F. musae*.

Chapter 9

Discussion and future perspectives

Chapter 9

Discussion and future perspectives

F. musae is the most recently described species within the *F. fujikuroi* species complex (Van Hove et al., 2011). It has been identified as one of the causative agents of crown rot disease in banana fruits, the only known host in the plant kingdom, and, few years later, it was isolated from human immunocompromised patients as an opportunistic pathogen causing typical fusariosis symptoms (Esposto et al., 2016; Kamel et al., 2016; Triest, 2016). Cases reporting infection with *F. musae* are very few in both agricultural and medical fields, and when we began our investigation in 2020, there were only a few papers available in literature on the topic.

Our curiosity about exploring this novel potential cross-kingdom pathogen, together with the increasing public concern over fungal infections, drove us to explore *F. musae* considering it as a model species for studying cross-kingdom pathogens.

We built a worldwide collection of *F. musae* strains including a set of 19 strains, of which 3 strains were obtained at the University of Milan and 16 strains obtained from public databases. Research in databases as ARS Culture Collection Database (USA), Institute of Science of Food Production (Bari, Italy) and Belgian coordinated collections of Microorganisms Collection immediately revealed that the number of deposited strains is limited, reflecting the low incidence of the infection. Analyzing strains records, we observed that plant strains were isolated from bananas harvested in big banana-producing countries while infection in human patients was mostly recorded in countries where bananas are primarily consumed. In addition, the isolation timeline indicated that the majority of the strains were isolated between the 1990s and the early 2010s, with no further reports of this pathogen publicly deposited out of this period. This raised the question of whether infection with *F. musae* represents a historical concern or remain a relevant threat today.

To determine the contemporaneity of infection with *F. musae*, we carried out a survey on banana fruits around Milan (Italy), sampling symptomatic bananas with the aim of isolating potential pathogens and verifying the presence of *F. musae*. Our work confirmed *F. musae* as one of the most relevant *Fusarium* species found on the banana

fruits that reach our markets highlighting its contemporary significance. However, symptomatic bananas (as the one we obtained) are typically excluded from distribution because they do not meet the standards of food safety and food security and therefore, they do not reach consumers' tables. Reasons behind their disease manifestation are not investigated and this might explain the discrepancy between the small number of reported cases and the diffusion that this pathogen still has.

The exact origin and initial emergence of *F. musae* remain not documented. Similarly, its mode of transmission from one host to the other remains unknown. The main hypothesis is the one explored by Triest and Hendrickx, that states that bananas acquire the infection with *F. musae* when harvested from the plant and subsequently act as carriers of spores, which reach human patients in consumer countries after banana shipments (Triest and Hendrickx, 2016). However, this hypothesis has not yet been proven.

To confirm banana fruits as the primary host of *F. musae*, it is necessary to verify its presence at the site of banana plantation, demonstrating indeed that the fungus infects bananas at harvest at the site of production rather than during transport or distribution. This means that additional sampling studies should be conducted in banana-producing countries to detect the presence of *F. musae* in bananas, but also in soil and over plantation environment, to trace the origin of this pathogen within these regions. In addition, it would be valuable to research for *F. musae* in hospitals within banana-producing countries, particularly by monitoring patients presenting possible fusariosis symptoms and assessing their medical history. Given the hypothesized presence of *F. musae* in these countries and its cross-kingdom transmission potential, it would be unlikely for *F. musae* to not appear in local hospital cases. Detecting its presence in these regions could also help clarify whether human infection occurs from contact with infected bananas or through other sources in the environment.

Our survey in Milan area has established the presence of *F. musae* on bananas sold in Italy. Previously, a similar study was conducted by Molnar et al. performed on bananas marketed in Hungary (Molnár et al., 2015). Together these studies demonstrated that this pathogen is indeed capable of moving from banana-producing regions to consumer markets in Europe.

Recently, da Silva Santos et al. further confirmed the presence of *F. musae* in Brazil by reevaluating the species identity of *Fusarium* cultures stored in URM collection (da Silva Santos et al., 2023). Collectively, these findings highlight the spread of *F. musae* across multiple countries, reinforcing the emerging threat posed by this pathogen. They emphasize the critical importance of ongoing sampling to monitor *F. musae* distribution and consequently its evolution and biological diversity. In addition, these studies underline the necessity of accurate identification through advanced molecular-based approach and advocate for the reidentification of isolates present in culture collections to trace the pathogen's current and historical distribution. This approach should not be limited to *F. musae* but could also serve as a valuable model for tracking and understanding other pathogenic species.

Indeed, a crucial factor to consider in *F. musae* investigation is that this species has not been fully investigated yet, resulting in very few available tools for its identification, and these are known to only a limited number of experts.

The fist molecular characterization of *F. musae* dates to 2011, when Van Hove at al. described it as a unique lineage in the *Gibberella fujikuroi* species complex related to but distinct from *F. verticillioides*, underlighting the impossibility to morphologically distinguish between the two species (Van Hove et al., 2011). During our investigation, we encountered strains originally identified as *F. musae*, which we reclassified as *F. verticillioides* (and *vice versa*) after deep characterization with specific informative genes (Esposto et al., 2016; Tava et al., 2021). This highlights the limited knowledge surrounding *F. musae* and the challenges of precise species-level identification, especially in the medical field, where the priority is to quickly identify the most effective treatment for patients, and a deeper classification of the pathogen is secondary.

We characterized *F. musae* strains isolated from different hosts and locations using multilocus phylogenetic analyses based on informative genes, including elongation factor (EF-1a), β-tubulin, RNA polymerase second largest subunit (RPB2), calmodulin and fumonisin gene cluster excision (DFGC).

Consistent with the literature, *F. musae* strains of our collection proved to be part of the same clade within the *F. fujikuroi* species complex, related to but distinct from *F. verticillioides*. Looking at the position of the strains within the phylogenetic tree, we observed that the strains are interspersed within the group, suggesting a close

taxonomic origin of strains isolated from different host origin, or location. All strains amplified for fumonisin gene cluster excision, confirming it as a distinctive feature of *F. musae* (Tava et al., 2021).

With the use of informative genes, we showed that it is possible to clearly distinguish *F. musae*, even from a closely related species as *F. verticillioides*. The presence of fumonisin gene cluster excision (DFGC) serves as a unique characteristics of *F. musae* that we demonstrated enable rapid and accurate identification immediately after isolation. Typically, the fumonisin gene cluster (FGC) is a conserved trait of *Fusarium* species and it is responsible for production of fumonisin, a mycotoxin secreted by the fungi to invade hosts and cause infection (Van Hove et al., 2008). The excision of FGC in *F. musae* suggests that this species may use other alternative strategies and produce other toxins for hosts invasion. The identification of additional genes unique of *F. musae* would not only facilitate faster and more accurate identification of this emerging pathogen, but also unravel specific genes that could explain its mechanisms of action and the competitive advantages of this species over other *Fusarium* species. In addition, investigation of *F. musae* specific genes could shift toward to genomic and comparative genomics studies, aiming at understanding variations within the population *F. musae* that may have let to invasion of one host over another and comparing them with other *Fusarium* (and non-*Fusarium*) species.

It is known that coding genes but also genomic features that could be linked to adaptation, evolution as well as pathogenic traits of the species (Plissonneau et al., 2017; Waalwijk et al., 2017). Population genomics studies on *F. asiaticum* genomes (Yang et al., 2024) and *F. pseudograminearum* (Li et al., 2023) already demonstrated the use of genome analysis to investigate the mechanisms of geographical distribution differences and the species' pathogenic evolution. A similar approach could be explored to understand the origin and evolution of *F. musae* across different hosts and regions. However, these analyses require a large number of strains, emphasizing once again the importance of sampling new strains from various regions as a starting point. Obtaining a high-quality genome assembly is the most crucial step for these studies. In this work, we obtained chromosome-level genome assembly of *F. musae* F31 combining Nanopore long reads and Illumina paired-end reads (Degradi et al., 2021). This genome represented the first sequenced genome completed at chromosome level

of *F. musae* published in literature providing important information on *F. musae* genome and a reference in the FFSC. This also validates an efficient protocol for the extraction and sequencing of *F. musae*, that will be useful for obtaining a broader collection of high-quality genomes of *F. musae* strains for further comparative genomic studies.

To move forward population studies and verify the taxonomic identity of *F. musae,* as well as to address the question regarding its transmissibility in different hosts, we investigated the population homogeneity infecting human and plant hosts by exploring mitogenomes diversity. Mitochondrial genomes evolve independently of and faster than the nuclear genome. They have a higher DNA copy number and the presence of highly conserved mobile genetic elements (MGEs) along with their distribution can help discriminate species and subgroups, tracking the spread of fungal populations. All *F. musae* strains presented identical mitogenomes at coding level. However, different mitochondrial haplotype groups can be distinguished based on non-coding regions. Particularly, three strains from different geographical and host origins fell under the same haplotype, indirectly indicating a transfer event from food to humans (Degradi et al., 2022).

One of the peculiarities of *Fusarium spp*. is its inherent resistance to most antifungal agents. Their susceptibility to azoles is higher than to other antifungal treatments but a real effective treatment strategy against infection with *Fusarium* has not been established yet (Al-Hatmi et al., 2018, 2016a). Previous studies already evaluated the sensitivity of *F. musae* to different antifungal compounds, verifying azoles as the most effective treatment also against this novel *Fusarium* species (Baria and Rakholiya, 2021, 2020; Verbeke et al., 2020).

Therefore, we tested the sensitivity *in vitro* of our *F. musae* collection to different azole treatments used in both agricultural and clinical settings. Selection of antifungals for the sensitivity study was not based on common usage. Instead, we explored a diverse range of treatments with different chemical structure to have a wider spectrum of their clinical/agricultural applications and resistance profiles. Most of the antifungals selected are no longer available on the market due to the hazard they pose on the environment and human health. Still, their use in the past may have contributed to the rising of resistances, leading to increased virulence, and enabling the pathogen to

overcome defensive strategies of multiple hosts (Fisher and Denning, 2023; Rosa et al., 2019; Zhao et al., 2021).

Our aim was to compare the sensitivity of our collection of strains to data reported in literature, with a specific focus in differences between strains isolated from different hosts and their geographical origin. Secondly, we examined the fitness of this novel species by observing strain behavior under treatment pressure to identify specific traits, such as azole resistance. These traits may have provided advantages that contributed to the emergence of the species and its competition with other species, such as *F. verticillioides*. Results could not prove any type of resistance of *F. musae* or differences between strains. However, we proved that *F. musae* is significantly less sensitive than *F. verticillioides* to most of the fungicides tested suggesting that this species could have carried some advantages over its “sister species” that made it differentiate or evolve (Tava et al., 2021).

Azole compounds have been introduced and used as medical and agricultural agents against fungal infections over the past few decades (Lamb et al., 1999). The increase of fungal infections, coupled with the consequent extended use of azole compounds for treatment, has contributed to the emergence of resistance to these therapies in both agricultural and medical settings. Azole-resistances have been observed not only in *Fusarium* spp*.,* but also in other species considered of critical and high importance in FPPL. Literature also reports cases of azole resistance of *Aspergillus fumigatus* and *Candida albicans*, underling once again the emergence of existing and new resistance, as well as treatability issues related to the increasing threat of fungal infections (Assress, 2021; Chowdhary et al., 2013; Rogers, 2017; World Health Organization, 2022).

A key step in the investigation of a transkingdom fungal pathogen is the proof of its ability to cause infection in different hosts. Literature about transkingdom fungal pathogens very often lacks experimental infection proofs. Indeed, identification of the pathogenic species is done following taxonomic criteria avoiding the full completion of Koch’s postulates, essential for claiming the role of an organism as a pathogen of a specific host. It is essential to demonstrate the ability of the fungi to cause infection in all hosts from which the microorganism has been isolated, confirming that the observed disease remains unchanged. Demonstrating infection across various hosts presents a

significant challenge given that the specialized ability and designated laboratories needed for manipulating different hosts are uncommon. Works in literature reporting proof of infection of fungal pathogens in multiple hosts are very limited. In literature is present a total of 17 papers that experimentally demonstrate infection of different fungal species in plant or animal hosts. Of these, only two studies have proven infection in both types of hosts. Specifically St. Lever et al. observed *Aspergillus flavus* in *G. mellonella* larvae, bean leaves and corn kernels, while Fornari et al. studied fungal genus *Fonsecaea* in mouse models and *M. pudica* seeds (Fornari et al., 2018; St. Leger et al., 2000).

Infection proof of *F. musae* was still missing. To fill the gap and confirm *F. musae* as a transkingdom pathogen, we established infection models together with a real-time method to track disease progression in different hosts. Our goal was to advance research on *F. musae* by establishing a quantitative, non-invasive, real-time methodology for monitoring fungal burden and host-pathogen interactions.

Bioluminescence imaging (BLI) has emerged as a powerful strategy to serve this scope (Papon et al., 2014; Resendiz-Sharpe et al., 2023; Vanherp et al., 2019). At first, we transformed strain F31 of our collection to express a red-shifted firefly luciferase in order to generate a reporter strain of *F. musae* stable enough to be used for *in vivo* imaging.

Infection studies in animals require following a set of strict and precise procedures and measures. Obtaining ethical approval is a big part of the experimental plan, and work with animal models requires the acquisition of specific training and skills. Recently research has been exploring and proposing alternative model organisms to complement the traditional mammalian models and in accordance with the 3R policy of replacement, reduction, and refinement of animal utilization in research (Junqueira and Mylonakis, 2019). Larvae of the wax moth, *Galleria mellonella*, have been validated as a great alternative model for bacterial and fungal infections (Binder et al., 2016; Champion et al., 2016; Curtis et al., 2022; Loh et al., 2013; Trevijano-Contador and Zaragoza, 2018). The insect can survive at 37°C and its immune response is structurally and functionally similar to the innate immune system of mammals. In addition, they are easy to maintain and to manipulate, their cost is low, and they don't need ethical approval. *G. mellonella* larvae are also a well-established model for the

use of BLI and potential applications for this model are already in use (Vanhoffelen et al., 2024, 2023). Therefore, we adapted this model for *F. musae* investigation to evaluate whether it had the same potential. The *F. musae-G. mellonella* model resulted successful in the representation of the disease and BLI imaging showed high sensitivity in detection and quantification of *F. musae* fungal burden, allowing observation of very early stages of infection even with low fungal loads, as well as of strong and consistent signal over time.

On the other hand, in the plant kingdom the only known host of *F. musae* is the banana. Fruits are easy to obtain and manipulate and relatively their price is relatively low. However, imaging techniques are not very diffused in plant field due to the highly fluorescent and phosphorescent properties of fruits peel and wooden structures, which complicate proper investigation (Tiessen, 2018). Tissue staining is also one of the most adopted technique for imaging, but it requires disruption of tissue, making it impossible to examine the same sample over time. For these reasons when we explored BLI as a readout of the fungal infection also in banana fruits, we encounter significant challenges doe to the high signal coming from the fruit peels. Adapting IVIS Spectrum settings specifically for imaging in this model, we could demonstrate that BLI could be a powerful tool also for the investigation of fungal infection in plant models. Following and adapting banana infection models already in use as the one described by Kamel et al. and Moretti et al., we obtained a successful representation of *F. musae* virulence in a plant system (Kamel et al., 2016; Moretti et al., 2004). The observation of a clear and stable BLI signal from our luciferase-expressing strain in both models demonstrated that it is well-suited for in vivo studies. This opens up possibilities for using this strain in other infection models, such as murine models, thereby advancing research in infection.

Overall, we were able to establish comparable infection models for both kingdoms with banana fruits and *G. mellonella* larvae to prove transkingdom ability of *F. musae.* Both models successfully represented the disease progression and our customized indexes, together with imaging quantification made the models comparable. All the strains proved to have the ability to cause infection and visible symptoms in both hosts demonstrating that this species is, indeed, capable of causing disease in both plant

and human kingdoms and suggesting it does not discriminate between an animal or a plant host.

We provided the first experimental proof of *F. musae* infection in both animal and plant kingdoms, offering addiction demonstration of its transkingdom infectious capacity. The infection models we developed not only served this purpose but can also be adapted for studying infection of other pathogens, advising the versatility of the methodology. This approach requires engineered strains for BLI imaging, which may present a disadvantage and limit its application. However, the advantages in providing in vivo, real-time and non-disruptive observations during host-pathogen interactions over time, make it highly valuable.

For *F. musae* research, these models provide a foundation for identifying specific behavior, interaction or stages during the infection of both plant and animal that could guide transcriptomic and comparative transcriptomic analysis. Transcriptomics may then reveal genomic determinants for *F. musae* infection across multiple hosts, identifying factors that influence its discrimination for one host over another. Additionally, this approach could clarify the dynamics behind host-pathogen interactions relevant to the mechanisms of action of *F. musae,* while allowing for comparison with other transkingdom pathogens as *F. oxysporum,* for which transcriptomics is being conducted (Guo et al., 2014; Huang et al., 2019).

Bacterial infections have long been a primary concern in both the clinical field and public health. In 2017, WHO developed its first bacterial priority pathogens list (BPPL) in order to address the emergency related to the increasing antibacterial resistance.

In recent years, however, the number of reported fungal infections have been increasing significantly motivating experts to acknowledge for the first time invasive fungal diseases as major concern for public health (World Health Organization, 2022). In line with BPPL, a fungal priority pathogens list (FPPL) was written in 2022 (Fisher and Denning, 2023). The list includes fungal species that impact the global population, mainly involved in systemic invasive infections and with serious risk of mortality and/or morbidity. Overall, the species included addressed in FPPL are considered as global threats due to the limited therapeutic options available and the difficulties in their diagnostic, which often lead to late detection and therapeutic intervention. In the critical priority group are mentioned *Criptococcus neoformans* and *Candida auris* and *C.*

albicans. These are responsible for acute and subacute systemic fungal infections for which no specific treatment has yet been established. *Aspergillus fumigatus* is also mentioned, as it presents increased mortality and morbidity in patients with other underlying conditions, and it has also been linked to azole-resistance due to extensive use of azoles in agriculture.

In the high priority group we can find *Fusarium spp*., which seem to be inherently resistant to most antifungal agents and global annual incidence rates of fusariosis cannot be assessed due to the lack of studies.

Examining the species on this list and the factors behind their global impact highlights that the rising threat posed by fungal infections is largely due to the lack of knowledge about their biology, their mechanisms of action and effective treatments.

The rising of fungal infections has roots across the full One Heath spectrum. Climate change, population growth, globalization, deforestation and intensive farming have been altering the balance between interactions between animal, human and environment, making pathogens evolving new strategies to survive and invade in a different way. Application of fungicides to minimize agricultural losses contributes to induce resistance in fungi, while the rise of new advanced medical treatments further complicates the complexity of patient populations with immunodeficiency disorders increasing the at-risk population. Consequently, fungal pathogens evolve new survival strategies and develop resistance that limits therapeutic options for treating new diseases (Fisher and Denning, 2023; Gauthier and Keller, 2013). In addition, multiple fungi recently identified as human opportunistic pathogens were originally known as plant pathogens, posing a concern that was primary for agriculture a direct threat to human health.

In spite of their increasing diffusion, transkingdom pathogens are still so far underestimated by funding and international research activities (Almeida et al., 2019). Fungal infections emergency extends across multiple disciplines, rising challenges for healthcare, agriculture and new food safety standards. Therefore, there is the need to address this urgency through a united effort between authorities, researchers, and public awareness.

Fusarium species are among the primary fungal genus addressed for investigation and monitoring with high priority as stated by FPPL. In my thesis we aimed to respond to

the call from WHO and One Health by contributing to the understanding of fungal infection and by exploring *F. musae* within the banana-human pathosystem as a model organism for *Fusarium* genus and transkingdom pathogens. With this project, we provided a comprehensive study on transkingdom pathogens, incorporating various fields and aspects that must be considered when researching *F. musae* specifically and transkingdom pathogens more broadly.

Our research on *F. musae* has highlighted the importance of approaching the issue from multiple perspectives, examining areas such as morphology, phenotypic analysis, genetics, taxonomy, molecular biology, infection biology, and evolutionary fitness of the species to develop an exhaustive understanding and effectively address fungal investigation. The study also underscores the necessity of mobilizing collaborations across various sectors, disciplines, and communities to tackle this priority threat.

Overall, we built a set of procedures that propose a protocol for investigating fungal infections and an outline to address future emerging fungal species as they arise. This research will contribute to establish novel standards of food safety and awareness in medical and agricultural field about the importance of fungal infection within the One Health concept and the risk posed by fungal transkingdom pathogens.

Chapter 10

References

Chapter 10

10.1 References

Al-Hatmi, A.M.S., Bonifaz, A., Ranque, S., Sybren de Hoog, G., Verweij, P.E., Meis, J.F., 2018. Current antifungal treatment of fusariosis. International Journal of Antimicrobial Agents 51, 326–332. https://doi.org/10.1016/j.ijantimicag.2017.06.017

Al-Hatmi, A.M.S., Meis, J.F., de Hoog, G.S., 2016a. Fusarium: Molecular Diversity and Intrinsic Drug Resistance. PLoS Pathog 12. https://doi.org/10.1371/journal.ppat.1005464

Al-Hatmi, A.M.S., Sandoval-Denis, M., Nabet, C., Ahmed, S.A., Demar, M., Normand, A.-C., de Hoog, G.S., 2019. Fusarium volatile, a new potential pathogen from a human respiratory sample. Fungal Syst Evol 4, 171–181. https://doi.org/10.3114/fuse.2019.04.09

Al-Hatmi, A.M.S., Van Den Ende, A.H.G.G., Stielow, J.B., Van Diepeningen, A.D., Seifert, K.A., McCormick, W., Assabgui, R., Gräfenhan, T., De Hoog, G.S., Levesque, C.A., 2016b. Evaluation of two novel barcodes for species recognition of opportunistic pathogens in Fusarium. Fungal Biology, Barcoding - Species Concepts and Species Recognition in Medical Mycology 120, 231–245. https://doi.org/10.1016/j.funbio.2015.08.006

Al-Hatmi, A.M.S., Van Diepeningen, A.D., Curfs-Breuker, I., De Hoog, G.S., Meis, J.F., 2014. Specific antifungal susceptibility profiles of opportunists in the Fusarium fujikuroi complex. Journal of Antimicrobial Chemotherapy dku505. https://doi.org/10.1093/jac/dku505

Almeida, J.R. de, Pachón, D.M.R., Franceschini, L.M., Santos, I.B. dos, Ferrarezi, J.A., Andrade, P.A.M. de, Monteiro-Vitorello, C.B., Labate, C.A., Quecine, M.C., 2021. Revealing the high variability on nonconserved core and mobile elements of Austropuccinia psidii and other rust mitochondrial genomes. PLOS ONE 16, e0248054. https://doi.org/10.1371/journal.pone.0248054

Almeida, F., Rodrigues, M.L., Coelho, C., 2019. The Still Underestimated Problem of Fungal Diseases Worldwide. Front. Microbiol. 10, 214. https://doi.org/10.3389/fmicb.2019.00214

Al-Reedy, R.M., Malireddy, R., Dillman, C.B., Kennell, J.C., 2012. Comparative analysis of *Fusarium* mitochondrial genomes reveals a highly variable region that encodes an exceptionally large open reading frame. Fungal Genetics and Biology 49, 2–14. https://doi.org/10.1016/j.fgb.2011.11.008

Alzate Acevedo, S., Díaz Carrillo, Á.J., Flórez-López, E., Grande-Tovar, C.D., 2021. Recovery of Banana Waste-Loss from Production and Processing: A Contribution to a Circular Economy. Molecules 26, 5282. https://doi.org/10.3390/molecules26175282

Aoki, T., O'Donnell, K., Geiser, D.M., 2014. Systematics of key phytopathogenic Fusarium species: current status and future challenges. J Gen Plant Pathol 80, 189–201. https://doi.org/10.1007/s10327-014-0509-3

Assress, H.A., 2021. Antifungal azoles and azole resistance in the environment: current status and future perspectives—a review. Rev Environ Sci Biotechnol.

Bandelt, H.J., Forster, P., Rohl, A., 1999. Median-joining networks for inferring intraspecific phylogenies. Molecular Biology and Evolution 16, 37–48. https://doi.org/10.1093/oxfordjournals.molbev.a026036

Baria, T.T., Rakholiya, K.B., 2021. Effect of *Fusarium musae* on cell wall degrading enzymes, total soluble sugar and total phenol content of infected banana fruits. ELSR 07, 21–27. https://doi.org/10.31783/elsr.2021.712127

Baria, T.T., Rakholiya, K.B., 2020. Evaluation of the Efficacy of Different Fungicides against Fusarium musae, a Fruit Rot Disease of Banana. ARRB 212–219.

https://doi.org/10.9734/arrb/2020/v35i1230326

Batista, B.G., Chaves, M.A. de, Reginatto, P., Saraiva, O.J., Fuentefria, A.M., 2020. Human fusariosis: An emerging infection that is difficult to treat. Rev. Soc. Bras. Med. Trop. 53, e20200013. https://doi.org/10.1590/0037-8682-0013-2020

Berg, G., Krause, R., Mendes, R., 2015. Cross-kingdom similarities in microbiome ecology and biocontrol of pathogens. Frontiers in Microbiology 6. https://doi.org/10.3389/fmicb.2015.01311

Bhunjun, C.S., Phillips, A.J.L., Jayawardena, R.S., Promputtha, I., Hyde, K.D., 2021. Importance of Molecular Data to Identify Fungal Plant Pathogens and Guidelines for Pathogenicity Testing Based on Koch's Postulates. Pathogens 10, 1096. https://doi.org/10.3390/pathogens10091096

Binder, U., Maurer, E., Lass-Flörl, C., 2016. Galleria mellonella: An invertebrate model to study pathogenicity in correctly defined fungal species. Fungal Biology, Barcoding - Species Concepts and Species Recognition in Medical Mycology 120, 288–295. https://doi.org/10.1016/j.funbio.2015.06.002

Bonavita, G. (EST), 2024. Banana Market Review.

Brankovics, B., van Diepeningen, A.D., de Hoog, G.S., van der Lee, T.A.J., Waalwijk, C., 2020. Detecting Introgression Between Members of the *Fusarium fujikuroi* and *F. oxysporum* Species Complexes by Comparative Mitogenomics. Front. Microbiol. 11, 1092. https://doi.org/10.3389/fmicb.2020.01092

Brock, M., 2012. Application of Bioluminescence Imaging for *In Vivo* Monitoring of Fungal Infections. International Journal of Microbiology 2012, 1–9. https://doi.org/10.1155/2012/956794

Capilla, J., Clemons, K.V., Stevens, D.A., 2007. Animal models: an important tool in mycology. Med Mycol 45, 657–684. https://doi.org/10.1080/13693780701644140

Carvajal, S.K., Alvarado, M., Rodríguez, Y.M., Parra-Giraldo, C.M., Varón, C., Morales-López, S.E., Rodríguez, J.Y., Gómez, B.L., Escandón, P., 2021. Pathogenicity Assessment of Colombian Strains of Candida auris in the Galleria mellonella Invertebrate Model 10.

Casadevall, A., 2023. Global warming could drive the emergence of new fungal pathogens. Nat Microbiol 8, 2217–2219. https://doi.org/10.1038/s41564-023-01512-w

Champion, O., Titball, R., Bates, S., 2018. Standardization of G. mellonella Larvae to Provide Reliable and Reproducible Results in the Study of Fungal Pathogens. JoF 4, 108. https://doi.org/10.3390/jof4030108

Champion, O.L., Wagley, S., Titball, R.W., 2016. *Galleria mellonella* as a model host for microbiological and toxin research. Virulence 7, 840–845. https://doi.org/10.1080/21505594.2016.1203486

Chowdhary, A., Kathuria, S., Xu, J., Meis, J.F., 2013. Emergence of Azole-Resistant Aspergillus fumigatus Strains due to Agricultural Azole Use Creates an Increasing Threat to Human Health. PLOS Pathogens 9, e1003633. https://doi.org/10.1371/journal.ppat.1003633

Chowdhary, A., Sharma, C., van den Boom, M., Yntema, J.B., Hagen, F., Verweij, P.E., Meis, J.F., 2014. Multi-azole-resistant *Aspergillus fumigatus* in the environment in Tanzania. Journal of Antimicrobial Chemotherapy 69, 2979–2983. https://doi.org/10.1093/jac/dku259

Coleman, J.J., Muhammed, M., Kasperkovitz, P.V., Vyas, J.M., Mylonakis, E., 2011. Fusarium pathogenesis investigated using *Galleria mellonella* as a heterologous host. Fungal Biology 115, 1279–1289. https://doi.org/10.1016/j.funbio.2011.09.005

Curtis, A., Binder, U., Kavanagh, K., 2022. *Galleria mellonella* Larvae as a Model for Investigating Fungal—Host Interactions. Frontiers in Fungal Biology 3.

da Silva Santos, A.C., do Nascimento Barbosa, R., Cavalcanti, A.D., de Souza-Motta, C.M., de Oliveira, N.T., Tiago, P.V., Moreira, K.A., 2023. Molecular identification of Brazilian Fusarium strains: sources of proteases with milk-clotting properties. Braz J Microbiol 54, 1665–1674. https://doi.org/10.1007/s42770-023-01016-z

de Hoog, G.S., Nishikaku, A.S., Fernandez-Zeppenfeldt, G., Padín-González, C., Burger, E., Badali, H., Richard-Yegres, N., van den Ende, A.H.G.G., 2007. Molecular analysis and pathogenicity of the *Cladophialophora carrionii* complex, with the description of a novel species. Studies in Mycology 58, 219–234. https://doi.org/10.3114/sim.2007.58.08

Dean, R., Van Kan, J. a. L., Pretorius, Z.A., Hammond-Kosack, K.E., Di Pietro, A., Spanu, P.D., Rudd, J.J., Dickman, M., Kahmann, R., Ellis, J., Foster, G.D., 2012. The Top 10 fungal pathogens in molecular plant pathology. Molecular Plant Pathology 13, 414–430. https://doi.org/10.1111/j.1364-3703.2011.00783.x

Degradi, L., Tava, V., Kunova, A., Cortesi, P., Saracchi, M., Pasquali, M., 2021. Telomere to Telomere Genome Assembly of *Fusarium musae* F31, Causal Agent of Crown Rot Disease of Banana. Mol Plant Microbe Interact 34, 1455–1457. https://doi.org/10.1094/MPMI-05-21-0127-A

Degradi, L., Tava, V., Prigitano, A., Esposto, M.C., Tortorano, A.M., Saracchi, M., Kunova, A., Cortesi, P., Pasquali, M., 2022. Exploring Mitogenomes Diversity of *Fusarium musae* from Banana Fruits and Human Patients. Microorganisms 10, 1115. https://doi.org/10.3390/microorganisms10061115

Delarze, E., Ischer, F., Sanglard, D., Coste, A.T., 2015. Adaptation of a *Gaussia princeps* Luciferase reporter system in *Candida albicans* for *in vivo* detection in the *Galleria mellonella* infection model. Virulence 6, 684–693. https://doi.org/10.1080/21505594.2015.1081330

Demerutis, C., Quirós, L., Martinuz, A., Alvarado, E., Williams, R.N., Ellis, M.A., 2008. Evaluation of an organic treatment for post-harvest control of crown rot of banana. Ecological Engineering 34, 324–327. https://doi.org/10.1016/j.ecoleng.2007.02.004

Desalermos, A., Fuchs, B.B., Mylonakis, E., 2012. Selecting an Invertebrate Model Host for the Study of Fungal Pathogenesis. PLoS Pathog 8, e1002451. https://doi.org/10.1371/journal.ppat.1002451

Dierckxsens, N., Mardulyn, P., Smits, G., 2020. Unraveling heteroplasmy patterns with NOVOPlasty. NAR Genomics and Bioinformatics 2, lqz011. https://doi.org/10.1093/nargab/lqz011

Espinel-Ingroff, A., Colombo, A.L., Cordoba, S., Dufresne, P.J., Fuller, J., Ghannoum, M., Gonzalez, G.M., Guarro, J., Kidd, S.E., Meis, J.F., Melhem, T.M.S.C., Pelaez, T., Pfaller, M.A., Szeszs, M.W., Takahaschi, J.P., Tortorano, A.M., Wiederhold, N.P., Turnidge, J., 2016. International Evaluation of MIC Distributions and Epidemiological Cutoff Value (ECV) Definitions for *Fusarium* Species Identified by Molecular Methods for the CLSI Broth Microdilution Method. Antimicrob. Agents Chemother. 60, 1079–1084. https://doi.org/10.1128/AAC.02456-15

Esposto, M.C., Prigitano, A., Tortorano, A.M., 2016. *Fusarium musae* as cause of superficial and deep-seated human infections. J Mycol Med 26, 403–405. https://doi.org/10.1016/j.mycmed.2016.02.021

Evans, E.A., Ballen, F.H., Siddiq, M., 2020. Banana Production, Global Trade, Consumption Trends, Postharvest Handling, and Processing, in: Handbook of Banana Production, Postharvest Science, Processing Technology, and Nutrition. John Wiley & Sons, Ltd, pp. 1–18. https://doi.org/10.1002/9781119528265.ch1

Ewané, C.A., Lepoivre, P., Lassois, L., 2012. Involvement of phenolic compounds in

the susceptibility of bananas to crown rot. A review. Biotechnol. Agron. Soc. Environ. 12.
Fallon, J., Kelly, J., Kavanagh, K., 2012. Galleria mellonella as a Model for Fungal Pathogenicity Testing, in: Brand, A.C., MacCallum, D.M. (Eds.), Host-Fungus Interactions, Methods in Molecular Biology. Humana Press, Totowa, NJ, pp. 469–485. https://doi.org/10.1007/978-1-61779-539-8_33

Fisher, M.C., Denning, D.W., 2023. The WHO fungal priority pathogens list as a game-changer. Nat Rev Microbiol 21, 211–212. https://doi.org/10.1038/s41579-023-00861-x

Fonseca, P.L.C., De-Paula, R.B., Araújo, D.S., Tomé, L.M.R., Mendes-Pereira, T., Rodrigues, W.F.C., Del-Bem, L.-E., Aguiar, E.R.G.R., Góes-Neto, A., 2021. Global Characterization of Fungal Mitogenomes: New Insights on Genomic Diversity and Dynamism of Coding Genes and Accessory Elements. Front. Microbiol. 12. https://doi.org/10.3389/fmicb.2021.787283

Fornari, G., Gomes, R.R., Degenhardt-Goldbach, J., Santos, S.S. dos, Almeida, S.R. de, Santos, G.D. dos, Muro, M.D., Bona, C., Scola, R.H., Trindade, E.S., Bini, I.H., Ferreira-Maba, L.S., Kestring, D.R., Nascimento, M.M.F. do, Lima, B.J.F. de S., Voidaleski, M.F., Steinmacher, D.A., Soley, B. da S., Deng, S., Bocca, A.L., da Silva, M.B., Salgado, C.G., de Azevedo, C.M.P. e S., Vicente, V.A., de Hoog, S., 2018. A Model for Trans-Kingdom Pathogenicity in *Fonsecaea* Agents of Human Chromoblastomycosis. Front. Microbiol. 9. https://doi.org/10.3389/fmicb.2018.02211

Fourie, G., Van der Merwe, N.A., Wingfield, B.D., Bogale, M., Wingfield, M.J., Steenkamp, E.T., 2018. Mitochondrial introgression and interspecies recombination in the Fusarium fujikuroi species complex. IMA Fungus 9, 37–48. https://doi.org/10.5598/imafungus.2018.09.01.04

Fuchs, B.B., O'Brien, E., El Khoury, J.B., Mylonakis, E., 2010. Methods for using *Galleria mellonella* as a model host to study fungal pathogenesis. Virulence 1, 475–482. https://doi.org/10.4161/viru.1.6.12985

Gauthier, G.M., Keller, N.P., 2013. Crossover fungal pathogens: The biology and pathogenesis of fungi capable of crossing kingdoms to infect plants and humans. Fungal Genetics and Biology 61, 146–157. https://doi.org/10.1016/j.fgb.2013.08.016

Ghosh, S.K., 2022. An in-sight analysis of molecular evolution of *Trichoderma* as emerging human pathogen (preprint). In Review. https://doi.org/10.21203/rs.3.rs-1421986/v1

Goedhart, J., 2021. SuperPlotsOfData—a web app for the transparent display and quantitative comparison of continuous data from different conditions. MBoC 32, 470–474. https://doi.org/10.1091/mbc.E20-09-0583

Gomez-Lopez, A., Forastiero, A., Cendejas-Bueno, E., Gregson, L., Mellado, E., Howard, S.J., Livermore, J.L., Hope, W.W., Cuenca-Estrella, M., 2014. An invertebrate model to evaluate virulence in *Aspergillus fumigatus*: The role of azole resistance. Medical Mycology 52, 311–319. https://doi.org/10.1093/mmy/myt022

Grimes, D.J., 2006. Koch's Postulates — Then and Now. Microbe Magazine 1, 223–228. https://doi.org/10.1128/microbe.1.223.1

Guarro, J., 2013. Fusariosis, a complex infection caused by a high diversity of fungal species refractory to treatment. Eur J Clin Microbiol Infect Dis 32, 1491–1500. https://doi.org/10.1007/s10096-013-1924-7

Guo, L., Han, L., Yang, L., Zeng, H., Fan, D., Zhu, Y., Feng, Y., Wang, G., Peng, C., Jiang, X., Zhou, D., Ni, P., Liang, C., Liu, L., Wang, J., Mao, C., Fang, X., Peng, M., Huang, J., 2014. Genome and Transcriptome Analysis of the Fungal Pathogen *Fusarium oxysporum f. sp. cubense* Causing Banana Vascular Wilt Disease. PLoS ONE 9, e95543. https://doi.org/10.1371/journal.pone.0095543

Hamari, Z., Juhász, Á., Kevei, F., 2005. Role of mobile introns in mitochondrial genome diversity of fungi. Acta Microbiologica et Immunologica Hungarica 49, 331–335. https://doi.org/10.1556/amicr.49.2002.2-3.22

Hartmann, F.E., Snirc, A., Cornille, A., Godé, C., Touzet, P., Van Rossum, F., Fournier, E., Le Prieur, S., Shykoff, J., Giraud, T., 2020. Congruent population genetic structures and divergence histories in anther-smut fungi and their host plants Silene italica and the S*ilene nutans* species complex. Molecular Ecology 29, 1154–1172. https://doi.org/10.1111/mec.15387

Herkert, P.F., Al-Hatmi, A.M.S., de Oliveira Salvador, G.L., Muro, M.D., Pinheiro, R.L., Nucci, M., Queiroz-Telles, F., de Hoog, G.S., Meis, J.F., 2019. Molecular Characterization and Antifungal Susceptibility of Clinical *Fusarium* Species From Brazil. Front. Microbiol. 10, 737. https://doi.org/10.3389/fmicb.2019.00737

Heslop-Harrison, J.S., Schwarzacher, T., 2007. Domestication, Genomics and the Future for Banana. Annals of Botany 100, 1073–1084. https://doi.org/10.1093/aob/mcm191

Hirata, T., Kimishima, E., Aoki, T., Nirenberg, H.I., O'Donnell, K., 2001. Morphological and molecular characterization of *Fusarium verticillioides* from rotten banana imported into Japan. Mycoscience 42, 155–166. https://doi.org/10.1007/BF02464132

Hof, H., 2006. A new, broad-spectrum azole antifungal: posaconazole ? mechanisms of action and resistance, spectrum of activity. Mycoses 49, 2–6. https://doi.org/10.1111/j.1439-0507.2006.01295.x

Huang, C.-Y., Wang, H., Hu, P., Hamby, R., Jin, H., 2019. Small RNAs – Big Players in Plant-Microbe Interactions. Cell Host and Microbe 26, 173–182. https://doi.org/10.1016/j.chom.2019.07.021

Jelen, V., Jonge, R. de, Peer, Y.V. de, Javornik, B., Jakše, J., 2016. Complete mitochondrial genome of the Verticillium-wilt causing plant pathogen *Verticillium nonalfalfae*. PLOS ONE 11, e0148525. https://doi.org/10.1371/journal.pone.0148525

Jones, R.K., 1999. Seedling Blight Development and Control in Spring Wheat Damaged by *Fusarium graminearum* Group 2. Plant Disease 83, 1013–1018. https://doi.org/10.1094/PDIS.1999.83.11.1013

Junqueira, J., Mylonakis, E., 2019. Current Status and Trends in Alternative Models to Study Fungal Pathogens. JoF 5, 12. https://doi.org/10.3390/jof5010012

Kamel, M.A.M., Cortesi, P., Saracchi, M., 2016. Etiological agents of crown rot of organic bananas in Dominican Republic. Postharvest Biology and Technology 120, 112–120. https://doi.org/10.1016/j.postharvbio.2016.06.002

Kavanagh, K., Fallon, J.P., 2010. *Galleria mellonella* larvae as models for studying fungal virulence. Fungal Biology Reviews 24, 79–83. https://doi.org/10.1016/j.fbr.2010.04.001

Kessel, L., Johnson, L., Arvidsson, H., Larsen, M., 2010. The Relationship between Body and Ambient Temperature and Corneal Temperature. Investigative Ophthalmology & Visual Science 51, 6593–6597. https://doi.org/10.1167/iovs.10-5659

Khalaf, M., 2023. Screening of *Fusarium* isolates pathogenicity in vitro by using the larvae of *Galleria Mellonella* L. Decision Sciences 38, 19–28.

Kim, J.-S., Yoon, S.-J., Park, Y.-J., Kim, S.-Y., Ryu, C.-M., 2020. Crossing the kingdom border: Human diseases caused by plant pathogens. Environmental Microbiology 22, 2485–2495. https://doi.org/10.1111/1462-2920.15028

Kryukov, V.Y., Yaroslavtseva, O.N., Whitten, M.M.A., Tyurin, M.V., Ficken, K.J., Greig, C., Melo, N.R., Glupov, V.V., Dubovskiy, I.M., Butt, T.M., 2018. Fungal infection dynamics in response to temperature in the lepidopteran insect *Galleria mellonella*. Insect Science 25, 454–466. https://doi.org/10.1111/1744-7917.12426

Kulik, T., Bilska, K., Żelechowski, M., 2020. Promising Perspectives for Detection, Identification, and Quantification of Plant Pathogenic Fungi and Oomycetes through Targeting Mitochondrial DNA. International Journal of Molecular Sciences 21, 2645. https://doi.org/10.3390/ijms21072645

Lamb, D., Kelly, D., Kelly, S., 1999. Molecular aspects of azole antifungal action and resistance. Drug Resistance Updates 2, 390–402. https://doi.org/10.1054/drup.1999.0112

Lamessa, K., 2021. Performance Evaluation of Banana Varieties, through Farmer's Participatory Selection. International Journal of Fruit Science 21, 768–778. https://doi.org/10.1080/15538362.2021.1930628

Laraba, I., Kim, H.-S., Proctor, R.H., Busman, M., O'Donnell, K., Felker, F.C., Aime, M.C., Koch, R.A., Wurdack, K.J., 2020. *Fusarium xyrophilum, sp. nov.*, a member of the *Fusarium fujikuroi* species complex recovered from pseudoflowers on yellow-eyed grass (Xyris spp.) from Guyana. Mycologia 112, 39–51. https://doi.org/10.1080/00275514.2019.1668991

Leslie, J.F., Summerell, B.A., 2006. The fusarium laboratory manual. Blackwell publ, Ames (Iowa).

Li, H., Durbin, R., 2010. Fast and accurate long-read alignment with Burrows–Wheeler transform. Bioinformatics 26, 589–595. https://doi.org/10.1093/bioinformatics/btp698

Li, W., Cao, S., Sun, H., Yang, X., Xu, L., Zhang, X., Deng, Y., Pavlov, I.N., Litovka, Y.A., Chen, H., 2023. Genome analyses reveal the secondary metabolites potentially influence the geographical distribution of *Fusarium pseudograminearum* populations. https://doi.org/10.1101/2023.08.25.554839

Loh, J.M., Adenwalla, N., Wiles, S., Proft, T., 2013. *Galleria mellonella* larvae as an infection model for group A streptococcus. Virulence 4, 419–428. https://doi.org/10.4161/viru.24930

López-Berges, M.S., Hera, C., Sulyok, M., Schäfer, K., Capilla, J., Guarro, J., Di Pietro, A., 2013. The velvet complex governs mycotoxin production and virulence of *Fusarium oxysporum* on plant and mammalian hosts: Velvet governs mycotoxins and virulence in *Fusarium*. Molecular Microbiology 87, 49–65. https://doi.org/10.1111/mmi.12082

Lowe, T.M., Chan, P.P., 2016. tRNAscan-SE On-line: integrating search and context for analysis of transfer RNA genes. Nucleic Acids Res 44, W54–W57. https://doi.org/10.1093/nar/gkw413

Lücking, R., Aime, M.C., Robbertse, B., Miller, A.N., Aoki, T., Ariyawansa, H.A., Cardinali, G., Crous, P.W., Druzhinina, I.S., Geiser, D.M., Hawksworth, D.L., Hyde, K.D., Irinyi, L., Jeewon, R., Johnston, P.R., Kirk, P.M., Malosso, E., May, T.W., Meyer, W., Nilsson, H.R., Öpik, M., Robert, V., Stadler, M., Thines, M., Vu, D., Yurkov, A.M., Zhang, N., Schoch, C.L., 2021. Fungal taxonomy and sequence-based nomenclature. Nat Microbiol 6, 540–548. https://doi.org/10.1038/s41564-021-00888-x

Ma, Q., Wu, H., Geng, Y., Li, Q., Zang, R., Guo, Y., Xu, C., Zhang, M., 2021. Mitogenome-wide comparison and phylogeny reveal group I intron dynamics and intraspecific diversification within the phytopathogen *Corynespora cassiicola*. Computational and Structural Biotechnology Journal 19, 5987–5999. https://doi.org/10.1016/j.csbj.2021.11.002

Mackenzie, J.S., Jeggo, M., 2019. The One Health Approach—Why Is It So Important? TropicalMed 4, 88. https://doi.org/10.3390/tropicalmed4020088

Mehl, H.L., Epstein, L., 2007. *Fusarium solani* species complex isolates conspecific with *Fusarium solani* f. sp. *cucurbitae* race 2 from naturally infected human and plant tissue and environmental sources are equally virulent on plants, grow at 37°C and are interfertile: FSSC 1, a human and plant pathogen. Environmental Microbiology 9, 2189–2199.

https://doi.org/10.1111/j.1462-2920.2007.01333.x

Meza-Menchaca, T., Singh, R.K., Quiroz-Chávez, J., García-Pérez, L.M., Rodríguez-Mora, N., Soto-Luna, M., Gastélum-Contreras, G., Vanzzini-Zago, V., Sharma, L., Quiroz-Figueroa, F.R., 2020. First Demonstration of Clinical Fusarium Strains Causing Cross-Kingdom Infections from Humans to Plants. Microorganisms 8, 947. https://doi.org/10.3390/microorganisms8060947

Migheli, Q., Balmas, V., Harak, H., Sanna, S., Scherm, B., Aoki, T., O'Donnell, K., 2010. Molecular Phylogenetic Diversity of Dermatologic and Other Human Pathogenic Fusarial Isolates from Hospitals in Northern and Central Italy. J. Clin. Microbiol. 48, 1076. https://doi.org/10.1128/JCM.01765-09

Mikheenko, A., Prjibelski, A., Saveliev, V., Antipov, D., Gurevich, A., 2018. Versatile genome assembly evaluation with QUAST-LG. Bioinformatics 34, i142–i150. https://doi.org/10.1093/bioinformatics/bty266

Misas, E., Chow, N.A., Gómez, O.M., Muñoz, J.F., McEwen, J.G., Litvintseva, A.P., Clay, O.K., 2020. Mitochondrial Genome Sequences of the Emerging Fungal Pathogen Candida auris. Front. Microbiol. 11. https://doi.org/10.3389/fmicb.2020.560332

Misra, B.B., Chaturvedi, R., 2015. When plants brace for the emerging pathogens. Physiological and Molecular Plant Pathology 92, 181–185. https://doi.org/10.1016/j.pmpp.2015.03.004

Molnár, O., Bartók, T., Szécsi, Á., 2015. Occurrence of *Fusarium verticillioides* and *Fusarium musae* on banana fruits marketed in Hungary. Acta Microbiologica et Immunologica Hungarica 62, 109–119. https://doi.org/10.1556/030.62.2015.2.2

Moretti, A., 2009. Taxonomy of Fusarium genus: A continuous fight between lumpers and splitters. Zb Mat srp prir nauk 7–13. https://doi.org/10.2298/ZMSPN0917007M

Moretti, A., Mule, G., Susca, A., González-Jaén, M., Logrieco, A., 2004. Toxin Profile, Fertility and AFLP Analysis of Fusarium verticillioides from Banana Fruits. European Journal of Plant Pathology 110, 601–609. https://doi.org/10.1023/B:EJPP.0000032399.83330.d7

Moussa, T.A.A., Al-Zahrani, H.S., Kadasa, N.M.S., Ahmed, S.A., de Hoog, G.S., Al-Hatmi, A.M.S., 2017. Two new species of the *Fusarium fujikuroi* species complex isolated from the natural environment. Antonie van Leeuwenhoek 110, 819–832. https://doi.org/10.1007/s10482-017-0855-1

Munkvold, G., 2017. *Fusarium* Species and Their Associated Mycotoxins, in: Methods in Molecular Biology (Clifton, N.J.). pp. 51–106. https://doi.org/10.1007/978-1-4939-6707-0_4

Mylonakis, 2005. *Galleria mellonella* as a Model System To Study *Cryptococcus neoformans* Pathogenesis [WWW Document]. https://doi.org/10.1128/iai.73.7.3842-3850.2005

Navarro Velasco, G., Prados-Rosales, R., Ortiz-Urquiza, A., Quesada-Moraga, E., Pietro, A., 2011. Galleria mellonella as model host for the trans-kingdom pathogen Fusarium oxysporum. Fungal genetics and biology : FG & B 48, 1124–9. https://doi.org/10.1016/j.fgb.2011.08.004

Nnadi, N.E., Carter, D.A., 2021. Climate change and the emergence of fungal pathogens. PLOS Pathogens 17, e1009503. https://doi.org/10.1371/journal.ppat.1009503

O'Donnell, K., Cigelnik, E., 1997. Two Divergent Intragenomic rDNA ITS2 Types within a Monophyletic Lineage of the Fungus *Fusarium* Are Nonorthologous. Molecular Phylogenetics and Evolution 7, 103–116. https://doi.org/10.1006/mpev.1996.0376

O'Donnell, K., Cigelnik, E., Nirenberg, H.I., 1998. Molecular systematics and phylogeography of the *Gibberella fujikuroi* species complex. Mycologia 90, 465–493.

https://doi.org/10.1080/00275514.1998.12026933

O'Donnell, K., Sarver, B.A.J., Brandt, M., Chang, D.C., Noble-Wang, J., Park, B.J., Sutton, D.A., Benjamin, L., Lindsley, M., Padhye, A., Geiser, D.M., Ward, T.J., 2007. Phylogenetic Diversity and Microsphere Array-Based Genotyping of Human Pathogenic Fusaria, Including Isolates from the Multistate Contact Lens-Associated U.S. Keratitis Outbreaks of 2005 and 2006. Journal of Clinical Microbiology 45, 2235–2248. https://doi.org/10.1128/JCM.00533-07

O'Donnell, K., Sutton, D.A., Rinaldi, M.G., Sarver, B.A.J., Balajee, S.A., Schroers, H.-J., Summerbell, R.C., Robert, V.A.R.G., Crous, P.W., Zhang, N., Aoki, T., Jung, K., Park, J., Lee, Y.-H., Kang, S., Park, B., Geiser, D.M., 2010. Internet-Accessible DNA Sequence Database for Identifying *Fusaria* from Human and Animal Infections. Journal of Clinical Microbiology 48, 3708–3718. https://doi.org/10.1128/JCM.00989-10

One Health - European Commission [WWW Document], 2023. URL https://health.ec.europa.eu/one-health/overview_en (accessed 10.9.24).

One Health - WHO [WWW Document], 2024. . WHO - World Health Organization. URL https://www.who.int/europe/initiatives/one-health (accessed 10.9.24).

One Health - WOAH [WWW Document], 2024. . WOAH - World Organisation for Animal Health. URL https://www.woah.org/en/what-we-do/global-initiatives/one-health/ (accessed 10.9.24).

Ortoneda, M., Guarro, J., Madrid, M.P., Caracuel, Z., Roncero, M.I.G., Mayayo, E., Di Pietro, A., 2004. *Fusarium oxysporum* as a Multihost Model for the Genetic Dissection of Fungal Virulence in Plants and Mammals. IAI 72, 1760–1766. https://doi.org/10.1128/IAI.72.3.1760-1766.2004

Papon, N., Courdavault, V., Lanoue, A., Clastre, M., Brock, M., 2014. Illuminating Fungal Infections with Bioluminescence. PLoS Pathog 10, e1004179. https://doi.org/10.1371/journal.ppat.1004179

Pasquali, M., Acquadro, A., Balmas, V., Migheli, Q., Lodovica Gullino, M., Garibaldi, A., 2004. Development of PCR Primers for a New F*usarium oxysporum* Pathogenic on Paris Daisy (Argyranthemum frutescens L.). European Journal of Plant Pathology 110, 7–11. https://doi.org/10.1023/B:EJPP.0000010141.37327.d0

Pasquali, M., Pallez-Barthel, M., Beyer, M., 2020. Searching molecular determinants of sensitivity differences towards four demethylase inhibitors in *Fusarium graminearum* field strains. Pesticide Biochemistry and Physiology 164, 209–220. https://doi.org/10.1016/j.pestbp.2020.02.006

Peeran, M.F., Muthalagu, A., Sarathambal, C., 2019. Morphological and Molecular Characterization of *Fusarium oxysporum f.sp.* Vanilla Inciting Root and Stem Rot Disaease in Vanilla. Int.J.Curr.Microbiol.App.Sci 8, 1578–1590. https://doi.org/10.20546/ijcmas.2019.804.183

Pereira, T.C., Rossoni, R.D., Ribeiro, F. de C., de Menezes, R.T., Junqueira, J.C., Scorzoni, L., 2018. Recent Advances in the Use of *Galleria mellonella* Model to Study Immune Responses against Human Pathogens 19.

Pitt, S.J., Gunn, A., 2024. The One Health Concept. Br J Biomed Sci 81, 12366. https://doi.org/10.3389/bjbs.2024.12366

Plissonneau, C., Benevenuto, J., Mohd-Assaad, N., Fouché, S., Hartmann, F.E., Croll, D., 2017. Using Population and Comparative Genomics to Understand the Genetic Basis of Effector-Driven Fungal Pathogen Evolution. Front. Plant Sci. 8. https://doi.org/10.3389/fpls.2017.00119

Pujol, I., Guarro, J., Gene, J., Sala, J., 1997. In-vitro antifungal susceptibility of clinical

and environmental Fusarium spp. strains. Journal of Antimicrobial Chemotherapy 39, 163–167. https://doi.org/10.1093/jac/39.2.163

Ra, M.S.L., Cavalcanti, M.A.S., Trilles, L., Nishikawa, M.M., Wanke, B., 1998. *Cryptococcus neoformans var. gattii* – evidence for a natural habitat related to decaying wood in a pottery tree hollow. Medical Mycology 4.

Reeb, V., Lutzoni, F., Roux, C., 2004. Contribution of RPB2 to multilocus phylogenetic studies of the euascomycetes (*Pezizomycotina*, Fungi) with special emphasis on the lichen-forming Acarosporaceae and evolution of polyspory. Molecular Phylogenetics and Evolution 32, 1036–1060. https://doi.org/10.1016/j.ympev.2004.04.012

Resendiz Sharpe, A., Lagrou, K., Meis, J.F., Chowdhary, A., Lockhart, S.R., Verweij, P.E., ISHAM/ECMM *Aspergillus* Resistance Surveillance working group, 2018. Triazole resistance surveillance in Aspergillus fumigatus. Med Mycol 56, 83–92. https://doi.org/10.1093/mmy/myx144

Resendiz-Sharpe, A., Da Silva, R.P., Geib, E., Vanderbeke, L., Seldeslachts, L., Hupko, C., Brock, M., Lagrou, K., Vande Velde, G., 2022. Longitudinal multimodal imaging-compatible mouse model of triazole-sensitive and -resistant invasive pulmonary aspergillosis. Disease Models & Mechanisms 15, dmm049165. https://doi.org/10.1242/dmm.049165

Resendiz-Sharpe, A., Vanhoffelen, E., Velde, G.V., 2023. Bioluminescence Imaging, a Powerful Tool to Assess Fungal Burden in Live Mouse Models of Infection. Methods Mol Biol 2667, 197–210. https://doi.org/10.1007/978-1-0716-3199-7_15

Rogers, P.D., 2017. Azole Antifungal Resistance in Candida albicans and Emerging Non-albicans Candida Species. Frontiers in Microbiology 7.

Rosa, P.D.D., Ramirez-Castrillon, M., Borges, R., Aquino, V., Meneghello Fuentefria, A., Zubaran Goldani, L., 2019. Epidemiological aspects and characterization of the resistance profile of *Fusarium* spp. in patients with invasive fusariosis. Journal of Medical Microbiology 68, 1489–1496. https://doi.org/10.1099/jmm.0.001059

Sáenz, V., Alvarez-Moreno, C., Pape, P.L., Restrepo, S., Guarro, J., Ramírez, A.M.C., 2020. A One Health Perspective to Recognize *Fusarium* as Important in Clinical Practice. JoF 6, 235. https://doi.org/10.3390/jof6040235

Santamaria, M., Vicario, S., Pappadà, G., Scioscia, G., Scazzocchio, C., Saccone, C., 2009. Towards barcode markers in Fungi: an intron map of Ascomycota mitochondria. BMC Bioinformatics 10, S15. https://doi.org/10.1186/1471-2105-10-S6-S15

Sarmiento-Ramírez, J.M., Abella, E., Martín, M.P., Tellería, M.T., López-Jurado, L.F., Marco, A., Diéguez-Uribeondo, J., 2010. *Fusarium solan*i is responsible for mass mortalities in nests of loggerhead sea turtle, *Caretta caretta,* in Boavista, Cape Verde. FEMS Microbiol Lett 312, 192–200. https://doi.org/10.1111/j.1574-6968.2010.02116.x

Schäfer, K., Di Pietro, A., Gow, N.A.R., MacCallum, D., 2014. Murine Model for Fusarium oxysporum Invasive Fusariosis Reveals Organ-Specific Structures for Dissemination and Long-Term Persistence. PLoS ONE 9, e89920. https://doi.org/10.1371/journal.pone.0089920

Sexton, A.C., Howlett, B.J., 2006. Parallels in Fungal Pathogenesis on Plant and Animal Hosts. Eukaryot Cell 5, 1941–1949. https://doi.org/10.1128/EC.00277-06

Sharma, K., Goss, E.M., Dickstein, E.R., Smith, M.E., Johnson, J.A., Southwick, F.S., Bruggen, A.H.C. van, 2014. *Exserohilum rostratum*: Characterization of a Cross-Kingdom Pathogen of Plants and Humans. PLOS ONE 9, e108691. https://doi.org/10.1371/journal.pone.0108691

Shi, W., Tan, Y., Wang, S., Gardiner, D.M., Saeger, S.D., Liao, Y., Wang, C., Fan, Y., Wang, Z., Wu, A., 2017. Mycotoxigenic Potentials of *Fusarium* Species in Various Culture

Matrices Revealed by Mycotoxin Profiling 16.

Singkum, P., Suwanmanee, S., Pumeesat, P., Luplertlop, N., 2019. A powerful in vivo alternative model in scientific research: *Galleria mellonella*. Acta Microbiologica et Immunologica Hungarica 28.

Slater, J.L., Gregson, L., Denning, D.W., Warn, P.A., 2011. Pathogenicity of *Aspergillus fumigatus* mutants assessed in *Galleria mellonella* matches that in mice. Med Mycol 49, S107–S113. https://doi.org/10.3109/13693786.2010.523852

Snelders, E., Camps, S.M.T., Karawajczyk, A., Schaftenaar, G., Kema, G.H.J., van der Lee, H.A., Klaassen, C.H., Melchers, W.J.G., Verweij, P.E., 2012. Triazole Fungicides Can Induce Cross-Resistance to Medical Triazoles in *Aspergillus fumigatus*. PLoS ONE 7, e31801. https://doi.org/10.1371/journal.pone.0031801

Sommerhalder, R.J., McDonald, B.A., Zhan, J., 2007. Concordant evolution of mitochondrial and nuclear genomes in the wheat pathogen *Phaeosphaeria nodorum*. Fungal Genetics and Biology 44, 764–772. https://doi.org/10.1016/j.fgb.2007.01.003

Springer, D.J., Mohan, R., Heitman, J., 2017. Plants promote mating and dispersal of the human pathogenic fungus *Cryptococcus*. PLoS ONE 12, e0171695. https://doi.org/10.1371/journal.pone.0171695

St. Leger, R.J., Screen, S.E., Shams-Pirzadeh, B., 2000. Lack of Host Specialization in *Aspergillus flavus*. Appl. Environ. Microbiol. 66, 320–324. https://doi.org/10.1128/AEM.66.1.320-324.2000

Status - Eurostat [WWW Document], 2021. URL https://ec.europa.eu/eurostat/portal/page/portal/product_details/publication?p_product_code=KS-76-06-669 (accessed 4.22.21).

Summerell, B.A., 2019. Resolving *Fusarium* : Current Status of the Genus. Annu. Rev. Phytopathol. 57, 323–339. https://doi.org/10.1146/annurev-phyto-082718-100204

Swearengen, J.R., 2018. Choosing the right animal model for infectious disease research. Animal Model Exp Med 1, 100–108. https://doi.org/10.1002/ame2.12020

Tava, V., Prigitano, A., Cortesi, P., Esposto, M.C., Pasquali, M., 2021. Fusarium musae from Diseased Bananas and Human Patients: Susceptibility to Fungicides Used in Clinical and Agricultural Settings. JoF 7, 784. https://doi.org/10.3390/jof7090784

Tava V., Reséndiz Sharpe A., Vanhoffelen E., Saracchi M., Cortesi P., Lagrou K., Vande Velde G.,, Pasquali M., Submitted. *Fusarium musae* infection in animal and plant hosts confirms its cross-kingdom pathogenicity.

The Manhattan Principles [WWW Document], 2005. URL https://oneworldonehealth.wcs.org/About-Us/Mission/The-Manhattan-Principles.aspx#:%7E:text=Recognize%20the%20essential%20link%20between,functioning%20ecosystems%20we%20all%20require (accessed 10.10.24).

Theelen, B., Christinaki, A.C., Dawson, T.L., Boekhout, T., Kouvelis, V.N., 2021. Comparative analysis of *Malassezia furfur* mitogenomes and the development of a mitochondria-based typing approach. FEMS Yeast Research 21, foab051. https://doi.org/10.1093/femsyr/foab051

Tiessen, A., 2018. The fluorescent blue glow of banana fruits is not due to symplasmic plastidial catabolism but arises from insoluble phenols estherified to the cell wall. Plant Science 275, 75–83. https://doi.org/10.1016/j.plantsci.2018.07.006

Tortorano, A.M., Prigitano, A., Dho, G., Esposto, M.C., Gianni, C., Grancini, A., Ossi, C., Viviani, M.A., 2008. Species Distribution and In Vitro Antifungal Susceptibility Patterns of 75 Clinical Isolates of *Fusarium* spp. from Northern Italy. AAC 52, 2683–2685. https://doi.org/10.1128/AAC.00272-08

Tortorano, A.M., Prigitano, A., Esposto, M.C., Arsenijevic, V.A., Kolarovic, J., Ivanovic, D., Paripovic, L., Klingspor, L., Nordøy, I., Hamal, P., Akdagli, S.A., Ossi, C., Grancini, A., Cavanna, C., Cascio, G.L., Scarparo, C., Candoni, A., Caira, M., Drogari, M., 2014. European Confederation of Medical Mycology (ECMM) epidemiological survey on invasive infections due to *Fusarium* species in Europe. Eur J Clin Microbiol Infect Dis 8.

Trevijano-Contador, N., Zaragoza, O., 2018. Immune Response of Galleria mellonella against Human Fungal Pathogens. JoF 5, 3. https://doi.org/10.3390/jof5010003

Triest, D., 2016. Banana fruits affected by *Fusarium* post-harvest disease as source of human fusariosis. Acta Microbiologica et Immunologica Hungarica 63, 359–360. https://doi.org/10.1556/030.63.2016.008

Triest, D., Hendrickx, M., 2016. Postharvest Disease of Banana Caused by *Fusarium musae*: A Public Health Concern? PLoS Pathog 12, e1005940. https://doi.org/10.1371/journal.ppat.1005940

Triest, D., Piérard, D., De Cremer, K., Hendrickx, M., 2016. *Fusarium musae* infected banana fruits as potential source of human fusariosis: May occur more frequently than we might think and hypotheses about infection. Communicative & Integrative Biology 9, e1162934. https://doi.org/10.1080/19420889.2016.1162934

Triest, D., Stubbe, D., De Cremer, K., Piérard, D., Detandt, M., Hendrickx, M., 2015. Banana infecting fungus, *Fusarium musae* , is also an opportunistic human pathogen: Are bananas potential carriers and source of fusariosis? Mycologia 107, 46–53. https://doi.org/10.3852/14-174

Valenti, I., Degradi, L., Kunova, A., Cortesi, P., Pasquali, M., Saracchi, M., 2022. The First Mitochondrial Genome of *Ciborinia camelliae* and Its Position in the *Sclerotiniaceae* Family. Front. Fungal Biol. 2. https://doi.org/10.3389/ffunb.2021.802511

Van Baarlen, P., Van Belkum, A., Summerbell, R.C., Crous, P.W., Thomma, B.P.H.J., 2007. Molecular mechanisms of pathogenicity: how do pathogenic microorganisms develop cross-kingdom host jumps? FEMS Microbiology Reviews 31, 239–277. https://doi.org/10.1111/j.1574-6976.2007.00065.x

Van Diepeningen, A.D., De Hoog, G.S., 2016. Challenges in *Fusarium*, a Trans-Kingdom Pathogen. Mycopathologia 181, 161–163. https://doi.org/10.1007/s11046-016-9993-7

Van Hove, F., Waalwijk, C., González-Jaén, M.-T., Moretti, A., Munaut, F., 2008. A *Fusarium* population from banana missing the fumonisin gene cluster: a new species closely related to *F. verticillioides*, in: Journal of Plant Pathology. Presented at the 10th International *Fusarium* Workshop and Fusarium Genomics Workshop 2008, p. 22.

Van Hove, F., Waalwijk, C., Logrieco, A., Munaut, F., Moretti, A., 2011. *Gibberella musae (Fusarium musae) sp. nov.,* a recently discovered species from banana is sister to F. verticillioides. Mycologia 103, 570–585. https://doi.org/10.3852/10-038

Vanherp, L., Ristani, A., Poelmans, J., Hillen, A., Lagrou, K., Janbon, G., Brock, M., Himmelreich, U., Vande Velde, G., 2019. Sensitive bioluminescence imaging of fungal dissemination to the brain in mouse models of cryptococcosis. Disease Models & Mechanisms 12, dmm039123. https://doi.org/10.1242/dmm.039123

Vanhoffelen, E., Michiels, L., Brock, M., Lagrou, K., Reséndiz-Sharpe, A., Vande Velde, G., 2023. Powerful and Real-Time Quantification of Antifungal Efficacy against Triazole-Resistant and -Susceptible *Aspergillus fumigatus* Infections in *Galleria mellonella* by Longitudinal Bioluminescence Imaging. Microbiology Spectrum 0, e00825-23. https://doi.org/10.1128/spectrum.00825-23

Vanhoffelen, E., Vermoesen, L., Michiels, L., Lagrou, K., Reséndiz-Sharpe, A., Vande

Velde, G., 2024. Sensitive bioluminescence imaging of cryptococcosis in *Galleria mellonella* improves antifungal screening under *in vivo* conditions. Virulence 15, 2327883. https://doi.org/10.1080/21505594.2024.2327883

Verbeke, V., Bourgeois, T., Lodewyck, T., Van Praet, J., Lagrou, K., Reynders, M., Nulens, E., 2020. Successful Outcome of Disseminated *Fusarium musae* Fungemia with Skin Localization Treated with Liposomal Amphotericin B and Voriconazole in a Patient with Acute Myeloid Leukemia. Mycopathologia 185, 1085–1089. https://doi.org/10.1007/s11046-020-00499-w

Waalwijk, C., Vanheule, A., Audenaert, K., Zhang, H., Warris, S., Van De Geest, H., Van Der Lee, T., 2017. *Fusarium* in the age of genomics. Trop. plant pathol. 42, 184–189. https://doi.org/10.1007/s40858-017-0128-6

Walker, B.J., Abeel, T., Shea, T., Priest, M., Abouelliel, A., Sakthikumar, S., Cuomo, C.A., Zeng, Q., Wortman, J., Young, S.K., Earl, A.M., 2014. Pilon: An Integrated Tool for Comprehensive Microbial Variant Detection and Genome Assembly Improvement. PLoS ONE 9, e112963. https://doi.org/10.1371/journal.pone.0112963

Wang, C.-J., Thanarut, C., Sun, P.-L., Chung, W.-H., 2020. Colonization of human opportunistic *Fusarium oxysporum* (HOFo) isolates in tomato and cucumber tissues assessed by a specific molecular marker. PLoS ONE 15, e0234517. https://doi.org/10.1371/journal.pone.0234517

Warpeha, K.M., Park, Y.-D., Williamson, P.R., 2013. Susceptibility of Intact Germinating Arabidopsis thaliana to Human Fungal Pathogens *Cryptococcus neoformans* and C. gattii. Appl. Environ. Microbiol. 79, 2979–2988. https://doi.org/10.1128/AEM.03697-12

World Health Organization, 2022. WHO fungal priority pathogens list to guide research, development and public health action [WWW Document]. URL https://www.who.int/publications-detail-redirect/9789240060241 (accessed 7.13.23).

Wyrębek, J., Molcan, T., Myszczyński, K., van Diepeningen, A.D., Stakheev, A.A., Żelechowski, M., Bilska, K., Kulik, T., 2021. Uncovering Diagnostic Value of Mitogenome for Identification of Cryptic Species *Fusarium graminearum* Sensu Stricto. Front. Microbiol. 12. https://doi.org/10.3389/fmicb.2021.714651

Xue, C., Tada, Y., Dong, X., Heitman, J., 2007. The Human Fungal Pathogen *Cryptococcus* Can Complete Its Sexual Cycle during a Pathogenic Association with Plants. Cell Host & Microbe 1, 263–273. https://doi.org/10.1016/j.chom.2007.05.005

Yang, M., Smit, S., De Ridder, D., Feng, J., Liu, T., Xu, J., Van Der Lee, T.A.J., Zhang, H., Chen, W., 2024. Adaptation of Fusarium Head Blight Pathogens to Changes in Agricultural Practices and Human Migration. Advanced Science 2401899. https://doi.org/10.1002/advs.202401899

Yang, M., Zhang, H., van der Lee, T.A.J., Waalwijk, C., van Diepeningen, A.D., Feng, J., Brankovics, B., Chen, W., 2020. Population Genomic Analysis Reveals a Highly Conserved Mitochondrial Genome in *Fusarium asiaticum*. Front. Microbiol. 11. https://doi.org/10.3389/fmicb.2020.00839

Yasir Rehman, S.M., 2015. Cross-Kingdom Pathogenicity across Plants and Human Beings. J Bacteriol Parasitol 06. https://doi.org/10.4172/2155-9597.1000e124

Yilmaz, N., Sandoval-Denis, M., Lombard, L., Visagie, C.M., Wingfield, B.D., Crous, P.W., 2021. Redefining species limits in the *Fusarium fujikuroi* species complex. Persoonia 46, 129–162. https://doi.org/10.3767/persoonia.2021.46.05

Zhai, B., Ola, M., Rolling, T., Tosini, N.L., Joshowitz, S., Littmann, E.R., Amoretti, L.A., Fontana, E., Wright, R.J., Miranda, E., Taur, Y., Hohl, T.M., 2020. High-resolution mycobiota analysis reveals dynamic intestinal translocation preceding invasive candidiasis.

Nature Medicine 26, 59–64. https://doi.org/10.1038/s41591-019-0709-7

Zhao, B., He, D., Wang, L., 2021. Advances in *Fusarium* drug resistance research. Journal of Global Antimicrobial Resistance 24, 215–219. https://doi.org/10.1016/j.jgar.2020.12.016